

CONFIGURABLE ROBOT BASE DESIGN
FOR
MIXED TERRAIN APPLICATIONS

A THESIS SUBMITTED TO
THE GRADUATE SCHOOL OF NATURAL AND APPLIED SCIENCES
OF
MIDDLE EAST TECHNICAL UNIVERSITY

BY

GÖKHAN BAYAR

IN PARTIAL FULFILLMENT OF THE REQUIREMENTS FOR THE DEGREE
OF
MASTER OF SCIENCE
IN
MECHANICAL ENGINEERING DEPARTMENT

AUGUST 2005

Approval of the Graduate School of Natural and Applied Sciences

Prof Dr. Canan ÖZGEN

Director

I certify that this thesis satisfies all the requirements as a thesis for the degree of Master of Science.

Prof. Dr. Kemal İDER

Head of Department

This is to certify that we have read this thesis and that in our opinion it is fully adequate, in scope and quality, as a thesis for the degree of Master of Science .

Assoc. Prof. Dr. İlhan KONUKSEVEN

Co-Supervisor

Assoc. Prof. Dr. Buğra KOKU

Supervisor

Examining Committee Members

Prof Dr. Reşit SOYLU

(METU, ME)

Asst. Prof. Dr. Buğra KOKU

(METU, ME)

Prof. Dr. Kemal İDER

(METU, ME)

Asst. Prof. Dr. İlhan KONUKSEVEN

(METU, ME)

Asst. Prof. Dr. Erol ŞAHİN

(METU, CENG)

I hereby declare that all information in this document has been obtained and presented in accordance with academic rules and ethical conduct. I also declare that, as required by these rules and conduct, I have fully cited and referenced all material and results that are not original to this work.

Name, Last name : Gökhan BAYAR

Signature :

ABSTRACT

CONFIGURABLE ROBOT BASE DESIGN FOR MIXED TERRAIN APPLICATIONS

BAYAR, Gökhan

MS., Department of Mechanical Engineering

Supervisor : Asst. Prof. Dr. Buğra KOKU

Co-Supervisor : Asst. Prof. Dr. İlhan KONUKSEVEN

August 2005, 124 pages

Mobile robotics has become a rapidly developing field of interdisciplinary research within robotics. This promising field has attracted the attention of academia, industry, several government agencies. Currently from security to personal service mobile robots are being used in a variety of tasks. The use of such robots is expected to only increase in the near future.

In this study, it is aimed to design and manufacture a versatile robot base. This base is aimed to be the main driving unit for various applications performed both indoors and outdoors ranging from personal service and assistance to military applications. The study does not attempt to individually address any specific application, indeed it is aimed to shape up a robotic module that can be used in a wide range of application on different terrain with proper modification. The robot base is specifically designed for mixed terrain applications, yet this study attempts to provide some guidelines to help robot designers. The manufactured robot base is tested with tracks, wheels, and

with both tracks and wheels, results are provided as guidelines to robot designers. Last but no the least, this study aims to obtain the know-how of building functional and flexible robots in Turkey by facilitating local resources as much as possible.

Keywords : Robotic platform, mobile robot, modular robot structure.

ÖZ

DEĞİŞİK ARAZİ KOŞULLARI İÇİN AYARLANABİLİR ROBOT PLATFORMU TASARIMI

BAYAR, Gökhan

Yüksek Lisans, Makina Mühendisliği Bölümü

Tez Yöneticisi : Yrd. Doç. Dr. Buğra KOKU

Yardımcı Tez Yöneticisi : Yrd. Doç. Dr. İlhan KONUKSEVEN

Ağustos 2005, 124 sayfa

Robotik çalışmalarda, disiplinler arası yapısı ile hareketli robot çalışmaları hızla gelişen bir araştırma alanı oluşturmaktadır. Gelecek vaat eden bu alan, eğitim kurumlarının, sanayinin, devlet kurumlarının ve güvenlik şirketlerinin ilgisini çekmeye başlamıştır. Bugün, hareketli robotlar bir çok alanda değişik görevleri üstlenmişlerdir. Yakın gelecekte bu robotların yoğun bir şekilde kullanılması beklenmektedir.

Bu tez çalışmasında, değişik amaçlar için kullanılabilir bir robot platformunun tasarımı ve üretimi hedeflenmiştir. Bir çok amaca hizmet edebilecek şekilde tasarlanan robot platformu, kapalı alanların yanı sıra açık alanda arazi şartlarında da çalışabilmesi amaçlanmış ve kişisel hizmet verebileceği gibi askeri uygulamalarda da görev alabilmesi düşünülmüştür. Bu çalışmada, özel bir uygulama alanında çalışabilecek tek bir robot platformundan çok uygun ayarlamalarla değişik yüzeylerde kullanılabilir, geniş uygulama alanına sahip bir robot modülün

tasarlanıp üretilmesi ana amaçtır. Robot platformu her türlü arazi koşullarında çalışabilecek şekilde tasarlanmıştır. Bu çalışmanın robot tasarımcılarına tasarım sürecinde nasıl bir yol izleyebilecekleri hakkında ışık tutması da hedeflenmiştir. Üretimi yapılan robot platformu paletli, tekerli ve hem teker hem de paletli olarak test edilmiş ve sonuçları hareketli robot tasarımcılarına ışık tutacak şekilde sunulmuştur. Ayrıca bu çalışma ile Türkiye'de kendi imkanlarımızla esnek ve modüler robotların tasarlanıp üretilmesi konusunda birikim oluşmasını sağlamak da hedeflenmiştir.

Anahtar kelimeler: Robot platformu, hareketli robot, modüler robot yapısı

ACKNOWLEDGMENTS

I am deeply grateful to my thesis Supervisor Asst. Prof. Dr. Buğra Koku and Co-Supervisor Asst. Prof. Dr. İlhan Konukseven for their guidance, advice, criticism, encouragement and insight throughout the research.

I am grateful to Res. Asst. Orhan Ölçücüoğlu for his continuous help, encouragement and his unbelievable effort even in the times when I felt hopeless and weak in solving some problems.

I am grateful to my family for their endless love, support, trust and encouragement.

I would like also to thank my colleagues Özgür Başer, Erdinç İyiyay and Ömer Necati Cora for their support and help.

Finally, I would like to send my special thanks to My Sun.

TABLE OF CONTENTS

PLAGIARISM	iii
ABSTRACT	iv
ÖZ	vi
ACKNOWLEDGMENTS	viii
TABLE OF CONTENTS	ix
LIST OF TABLES	xii
LIST OF FIGURES	xiii
LIST OF SYMBOLS	xviii
CHAPTER	
1. INTRODUCTION.....	1
2. TYPES OF DRIVING SYSTEMS FOR THE MOBILE ROBOTS.....	16
2.1 Important Keys for Locomotion	19
2.2 Legged Mobile Robots	20
2.3 Tracked Mobile Robots	21
2.4 Wheeled Mobile Robots	22
2.4.1 Stability.....	26
2.4.2 Maneuverability.....	26
2.4.3 Controllability.....	27
2.5 Legged - Wheeled Mobile Robots.....	27
3. DESIGN PROCEDURE	29
3.1 Shaft Design.....	29
3.2 Set Screw Selection	36
3.3 Bearing Selection.....	34

3.4 Key Design.....	37
3.5 Palette Selection.....	39
3.6 Frame Design.....	41
3.7 Bearing Hup Design.....	43
3.8 Motor Mounting Design.....	43
3.9 Palette Strecher Design.....	44
3.10 Palette Wheel Design.....	45
3.11 Movable Beam Carrier Design.....	45
3.12 Motor Selection.....	46
3.13 Robot Base Control.....	50
3.14 Batery Evaluation.....	52
4. CONFIGURATIONS OF THE DESIGNED ROBOT BASE.....	54
4.1 Robot Base Driving Up Hill.....	57
4.2 Robot Base Moving Along an Incline Surface.....	63
4.3 Turning Capability of the Robot Base.....	69
4.4Obstacle Handling.....	75
5. RESULTS AND DISSUSSIONS.....	79
6.CONCLUSIONS AND FUTURE WORK.....	87
REFERENCES.....	89
APPENDICES.....	93
Appendix A: Kinetik and Dynamic Analysis of the Robot Base.....	93
Appendix B: Technical Drawings.....	102
Appendix C: PIC 16F877 Pin connections.....	119
Appendix D: LMD 18200 Pin Connections.....	121
Appendix E: Police Department Specifications for the Moile Robots ..	123

LIST OF TABLES

TABLE

1.1 Indoor Mobile Robots	13
1.2 Outdoor Mobile Robots.....	14
2.1 Locomotion Mechanisms Used in Biological Systems.....	17
2.2 Types of Locomotion for the Mobile Robots.....	23
3.1 Load Factors.....	35
3.2 Reliability Factor Table.....	37
3.3 Comparing Features of Mobile Robot Motor Types	47
3.4 Data of the Motors Placed on the Robot Base	50
4.1 Material List.....	56
4.2 User Interface for the Robot Base Climbing Slope.....	68
4.3 Comparison of Robot Base Configurations	68
4.4 Coefficient of Lateral Resistance	71
4.5 Robot Base Turning Capability on Different Soil Characteristics.....	74
4.6 Equations for Driving Step Over for the Robot Base.....	77
5.1 Simulation and Tests Results for the Slope Angle that Robot Base Climb	79
5.2 Test results Related to Crossing Over an Obstacle	80
5.3 Comparison between tests and analytical results	80
5.4 Power Consumption for Indoor Tests	83
5.5 Power Consumption for Outdoor Tests.....	83
5.6 Working Conditions with the configurations	86

LIST OF FIGURES

FIGURE

1.1 Plant-spot welding robot of Kuka	2
1.2 Illustration of the mobile robot base designed	3
1.3 Plustech's walking robot	5
1.4 Underwater Vehicle.....	5
1.5 The mobile robot Sojourner	5
1.6 Pioneer Robot with Different Configurations	6
1.7 Tour-guide robots.....	6
1.8 AGV	7
1.9 Helpmate mobile robot.....	7
1.10 Industrial Cleaning Robot 700	8
1.11 Magellan Mobile Robot of iRobot	8
1.12 Khepera	8
1.13 Alice robot.....	9
1.14 Koala robot.....	9
1.15 ATRV mobile robot	10
1.16 PackBot mobile robot.....	10
1.17 MR-5 remotely operated mobile robot.....	11
1.18 Nomad robot.....	11
1.19 Talon robot	12
1.20 Talon robot in operation.....	12
2.1 Attainable speeds of various locomotion mechanisms	18

2.2 RoboTrack.....	19
2.3 Arrangement of the legs	21
2.4 The Microrover Nanokhod.....	21
2.5 Cye a two wheel differential robot base.....	26
2.6 Uranus robot built by Carnegie Mellon.....	27
2.7 Shrimp having six motorized wheels	28
3.1 Shaft design	29
3.2 CAD drawing of the designed shaft	31
3.3 Assembling two shafts for using wheels and tracks at the same time.....	31
3.4 Screw used for the shafts connection	32
3.5 Loads applied to the bearings.....	34
3.6 Key dimensions	37
3.7 Double-sided timing belt.....	39
3.8 Aluminum profile.....	42
3.9 Frame with movable beams.....	42
3.10 Bearing hups.....	43
3.11 Motor mountings	44
3.12 Palette strecher	45
3.13 Palette pulley	45
3.14 Movable beam carrie.....	45
3.15 Robot base model used in selecting the proper motor	48
3.16 The required data for the motor selection	49
3.17 Main board containing PIC 16F877	51
3.18 Graphical user interface for robot base control.....	51
3.19 Batery duration under load.....	52
4.1 Two different configurations of the robot base with tracks and wheels	55
4.2 Wheeled & Tracked robot base (solid model and manufactured robot)	55
4.3 Robot base driving slope up.....	57
4.4 Normal force caused from ground	59
4.5 Minimum coefficient of friction required for the robot not to slip	60
4.6 Maximum slope angle that robot base can climb.....	63
4.7 Robot base moving along an incline surface.....	64

4.8 Normal forces caused from ground.....	65
4.9 Maximum slope angle that robot base can climb.....	67
4.10 Robot base turning	69
4.11 Robot Base contacts with the obstacle from outside.....	75
4.12 Robot base contacts with the obstacle from inside	76
4.13 Normal forces between the front wheel(s) and the obstacle	78
4.14 Total tractive effort required to cross over the obstacle.....	78
5.1 Robot base that works to cross over an obstacle.....	81
5.2 Robot base goes step down	81
5.3 Wheeled robot base crosses over a step	82
5.4 Tracked robot base crosses over a step	82
5.5 Robot base motion simulator	84
5.6 Simulatation results	85
A.1 Robot base turning a circular path with constat speed	95
A.2 Robot base orientation during turning a circular path.....	98

LIST OF SYMBOLS

D_{rw}	Rear wheel diameter (mm)
D_{fw}	Front wheel diameter (mm)
L_w	Distance center of front wheel to center of gravity (mm)
h	Height of center of mass about plane (mm)
θ	Slope angle (degree)
m	Robot mass (kg)
N	Robot weight (N)
g_{rw}	Maximum drive torque applied to both rear wheels (N-mm)
g_{fw}	Maximum drive torque applied to both front wheels (N-mm)
μ	Coefficient of friction
F_{Nr}	Normal force between both rear wheels and ground (N)
F_{Nf}	Normal force between both front wheels and ground (N)
$F_{rw_{max}}$	Maximum rear wheel tractive force from drive torque (N)
$F_{fw_{max}}$	Maximum front wheel tractive force from drive torque (N)
$F_{rw_{\mu_{max}}}$	Maximum rear wheel tractive force before slip (N)
$F_{fw_{\mu_{max}}}$	Maximum front wheel tractive force before slip (N)
F_{Tr}	Total tractive force generated by both rear wheels (N)
F_{Tf}	Total tractive force generated by both front wheels (N)
F_{Tm}	Total tractive effort of the machine (N)
F_g	Force from gravity acting along the incline (N)

h_{step}	Step height (mm)
θ_{step}	Contact angle (degree)
μ_{rw}	Rear wheel coefficient of friction
μ_{fw}	Front wheel coefficient of friction
F_{Nr}	Normal force between a rear wheel and the ground (N)
F_{Nf}	Normal force between a front wheel and the step (N)
μ_{min}	Minimum required coefficient of friction
g_m	Total motor tractive effort (N)
g_{mu}	Total friction limited tractive effort (N)
g_{min}	Total minimum tractive effort required (N)
V	Ideal forward velocity required to get over the step (mm/s)
Δ	Potential energy on top of step
r_m	Motor shaft radius (mm)
ω_m	Motor angular velocity
τ_m	Motor torque (Nm)
V_{in}	Input voltage (V)
V_m	Motor voltage (V)
I_{in}	Input current (A)
I_m	Motor current (A)
I_0	No-load current (A)
R_m	Motor resistance (ohm)
P	Power (W)
k_v	Linear coefficient between ω_m and V_m
k_τ	Linear coefficient between τ_m and I_m
ω_w	Wheel angular velocity
x, y, θ	Position / orientation of the robot base
v	Robot base velocity (m/s)
ω_l	Angular velocity of the left motor

ω_r	Angular velocity of the right motor
h	key height (mm)
t_1	key way depth (mm)
t_2	key depth (mm)
l	key length (mm)
b	key width (mm)
P	power to be transmitted (kw)
n	rpm
z_1	Number of teeth of pulley1
z_2	Number of teeth of pulley2
t	Pitch (mm)
a	Center distance (mm)
F_i	Spec. peripheral force per engaging tooth and per cm of belt width
M_i	Transferable torque per engaging tooth and per cm of belt width
b	Width of the belt (mm)
D_1	Diameter of Pulley 1 (mm)
D_2	Diameter of Pulley 2 (mm)
P	Required power (kW)
N	Driving speed (rpm)
L_R	Rating life
L	Life expected for radial load, F_r
C	Rated load capacity of bearing
A_p	Placed area
F_{T_f}	Total friction force
M_f	Friction moment
M_t	Moment to be transmitted

CHAPTER I

INTRODUCTION

The word robot has been coined by Karel Capek back in early nineties and the idea of having robots serving human kind has always been attractive for public however, creating these robots has imposed great challenges to scientists. Considering the fact that imagination of man roams freely, but technological achievements goes through a slow and iterative evolution it is not a surprise that the expectations of people from robots are quite different that what technology can feasibly offer to these people. Robotics has achieved its first success to date in the world of industrial manufacturing. Robot arms, or manipulators, comprise a 2 billion dollar industry. Bolted at its shoulder to a specific position in the assembly line, a robot arm can move with great speed and accuracy to perform repetitive tasks such as spot welding (Figure 1.1). For example, in electronics industry, manipulators place surface-mounted components with superhuman precision, making the portable telephone and laptop computer possible [Siegwart, 2004]. Yet, for all of their successes, these commercial robots suffer from a basic disadvantage: *lack of mobility*. A fixed manipulator has a restricted scope of motion that depends on where it is bolted down. In contrast, a mobile robot would be able to travel throughout the manufacturing plant, flexibly applying its abilities wherever it is most effective [Arkin, 1998].

Mobile robot world has several examples of outdoor robots and however they are generally designed for special applications and their prices are quite expensive. For instance a teleoperated robot named Matilda designed for US army and police force is sold for over 4000\$. DARPA is sponsoring the development of a robot dog

project, namely TAKOM for the army for 2250\$. Another example is Pioneer 3AT. The base price for this robot is over 6000\$ and it has very limited capabilities on the rough terrain. With additional hardware, the robot price easily gets above 50000\$. The cost for iRobot Company's mobile robots is ranged from 3500 \$ to 150 000 \$.



Figure 1.1 Plant-spot welding robot of Kuka [Kuka, Siegart 2004]

We do foresee that the use of such robot bases will only increase in time. With this study our purpose is to start building up on the know-how of designing and manufacturing mobile robot platform. Several situations considered, we have decided to start with a small/medium size mobile robot that can be configured to operate on various terrains. This robot base will be able to move on mixed terrain and have at least the average speed of a walking person (or a soldier). Differently from other mobile robot bases, our design will be able to use both tracks (palettes) and wheels either at the same time or individually as illustrated Figure 1.2. The necessity of the use of both tracks and wheels was recognized and Turkish Police Department demanded a mobile robot base which use both track and wheel (Appendix E). This type of a configuration is not common in mobile robots; hence the results of this work will contribute to the field by providing information on the feasibility of this specific configuration and its comparison with tracked and wheeled configurations. Another purpose of this thesis it to facilitate the mobile robotics research in Turkey by providing a design that is suitable for mixed terrain applications that can be manufactured by making use of the domestic resources as much as possible. Also

during the design process, Turkish Police Department's specifications for mobile robots used to destroy bomb have been followed (Appendix D).

The rest of the chapter will provide a brief introduction of many mobile robots that has been built so far followed by the layout of this thesis.

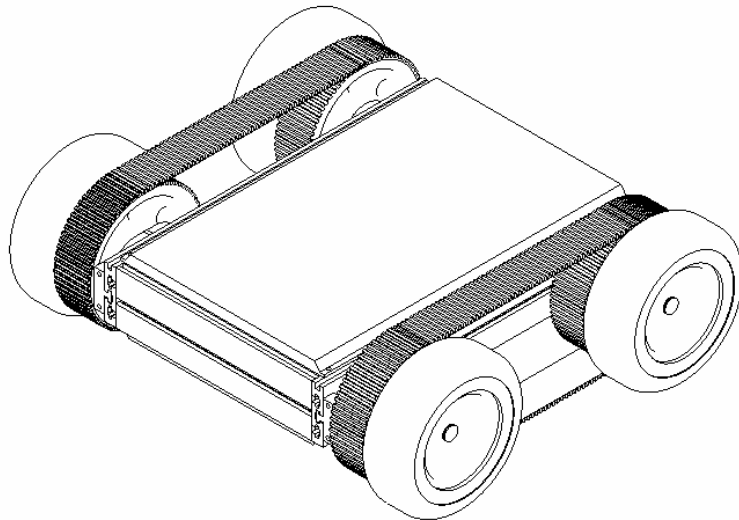


Figure 1.2 Illustration of the mobile robot base designed

Mobile robots are being used in a variety of environments to accomplish different tasks. Most common differentiation between operational environments is based on whether the robot operates indoors or outdoors. Indoors generally provide well structured environments with smooth surfaces to move on. Some common and also potential indoor robotic tasks can be listed as:

Cleaning (floors, windows etc.)

- Patient assistance (distribution of medication)
- Customer assistance (museum tour guide, shopping floor assistance)
- Entertainment
- Surveillance
- Delivery (office boy)

Outdoors have almost no structure at all and impose an uncontrolled environment. From forests to deserts, from earth's atmosphere to outer space, from air to underwater outdoors provide a wide range of environments. Some common and also potential outdoor robotic tasks can be listed as:

- Mining
- Search and rescue
- Cleaning (such as sewage tubes)
- Military applications
- Surveillance
- Fire fighting
- Exploration (such as underwater or space exploration)
- Construction
- Agriculture

Various types of actuation methods are used on mobile robots. For example, Plustech's walking robot provides automatic leg coordination while the human operator chooses an overall direction of travel (Figure 1.3). This robot is the first application driven walking robot. It is designed to move wood out of the forest. The leg coordination is automated, but navigation is still done by the human operator on the robot. Figure 1.4 depicts an underwater vehicle that controls six propellers to autonomously stabilize the robot submarine in spite of underwater turbulence and water currents while the operator chooses position goals for the submarine to achieve.

Hostile environments such as Mars trigger even more unusual locomotion mechanisms. In dangerous and inhospitable environments, even on Earth, such teleoperated systems have gained popularity. In these cases, the low-level complexities of the robot often make it impossible for a human operator to directly control its motion. The human performs localization and cognition activities, but relies on the robot's control scheme to provide motion control [Siegwart, 2004].

Other commercial robots operate on which humans cannot go. These robots do not compel for reasons of mobility but they may compel because of their autonomy, and so their ability to maintain a sense of position and to navigate without human intervention is superior. The mobile robot base Sojourner (Figure 1.5) was used during the Pathfinder mission to explore Mars in summer 1997 [Ranier]. It was almost completely teleoperated from Earth. However, some on board sensors allowed for obstacle detection.



Figure 1.3 Plustech's walking robot [Siegwart, 2004]

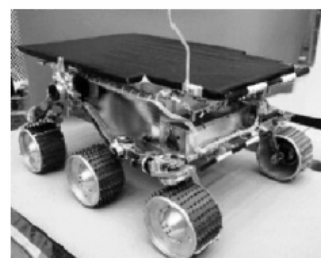


Figure 1.4 Underwater vehicle **Figure 1.5** The mobile robot Sojourner [Ranier]

As seen Figure 1.6, Pioneer is one of the most popular mobile robot bases. It was used in the exploration of Sarcophagus at Chernobyl. And also Pioneer I is a configurable mobile robot platform which gives some opportunities to the robot scientists like having a gripper or a camera. It is attached with a mapping library [Pioneer].

Tour-guide robots (Figure 1.7) can present exhibitions to the guests [Burgard, 2000]. Ten tour-guide robots which have been developed by EPFL have helped people for 5 months at the Swiss exhibition EXPO .02, drawing attention lots of visitors [Siegwart, 2003].

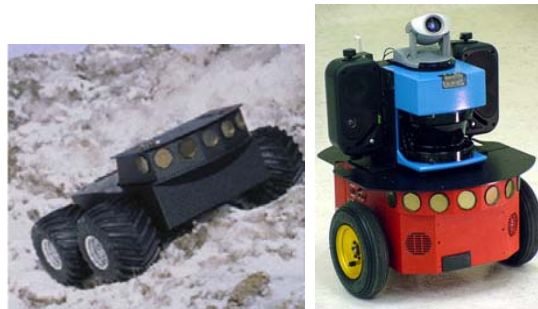


Figure 1.6 Pioneer Robots with different configurations [Pioneer]

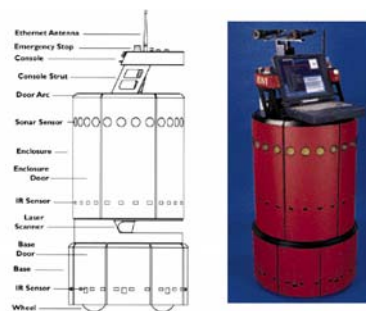


Figure 1.7 Tour-guide robots [Burgard, 2000]

Newest generation of the autonomous guided vehicle (AGV) of SwissLog used to transport motor blocks from one assembly station to another. It is guided by an electrical wire installed in the floor. There are thousands of AGVs transporting products in the industry, warehouses, and even hospitals (Figure 1.8) [Zelinsky, 1992].



Figure 1.8 AGV: Autonomous Guided Vehicle [Zelinsky, 1992]

Helpmate is a mobile robot used in hospitals for transportation tasks [Rosetti, 1998]. It has various on board sensors and cameras for autonomous movement in the corridors. The main sensor for the localization is a camera looking to the ceiling. It can detect the lamps on the ceiling as references, or landmarks (Figure 1.9).



Figure 1.9 Helpmate mobile robot [Rosetti, 1998]

BR 700 industrial cleaning robot designed and manufactured and sold by Alfred Karcher GmbH & Co., Germany. BR 700 has a navigation system having sophisticated sonar system and a gyro [Siegwart, 2004] (Figure 1.10).



Figure 1.10 Industrial cleaning robot 700 [Siegwart, 2004]

Magellan of iRobot (Figure 1.11) is a sophisticated mobile robot with up to three Intel Pentium processors on board. It has a large variety of sensors for high performance navigation tasks [Dis, 2002].



Figure 1.11 Magellan mobile robot of iRobot [Dis, 2002]

Khepera is a small mobile robot for research and education purposes. It is just about 60 mm diameter [Khepera]. Various additional modules such as cameras, sensors and grippers can be equipped (Figure 1.12).

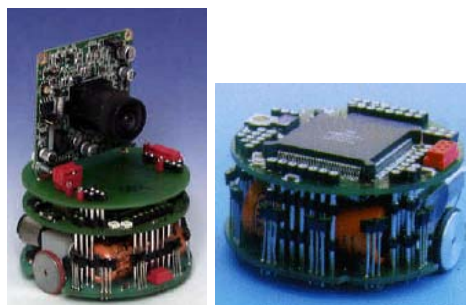


Figure 1.12 Khepera [Khepera]

Alice is one of the smallest fully autonomous robots. It is approximately 2x2x2 cm, it has a battery life of about 8 hours and uses infrared distance sensors, tactile whiskers, and even a small camera for navigation (Figure 1.13) [Kalice].



Figure 1.13 Alice robot [Kalice]

The Koala robot (Figure 1.14) is a mobile robot platform. It was designed for easy use, easy transport and it could work on indoor environment as well as outdoor environment [Koala]. Compact size, modularity, high computational power, easy control and low cost are noticeable be the features of the robot base Koala.



Figure 1.14 Koala robot [Koala]

The ATRV manufactured by iRobot (Figure 1.15) is a mobile robot. It was designed for the projects that require a mobile robot to be all terrain capable [Irobot]. The ATRV Micro is a robotic vehicle, in a family of all terrain robots, with a low center of gravity, a weather-resistant enclosure, and big wheels to traverse uneven terrain. For the military or commercial applications, these all terrain mobile robots are elected [Sadhukhan, 2004].



Figure 1.15 ATRV Micro [Sadhukhan, 2004]

PackBot (Figure 1.16) is a tough, light weight robot designed to conduct explosive ordnance disposal, search-and-surveillance, hostage rescue, and other vital tasks for bomb squads, swat teams, and military purposes [Packbot]. PackBot can be used a full range of improvised explosive device and conventional ordnance disposal tasks. This versatile robot quickly adapts to different configuration, conventional ordnance, and swat missions. With its compact profile and patented mobility platform, PackBot operates with confidence on the rough terrain - from the stairs, curbs, and rubble of urban terrain to the rocks, sand, and mud of battlefield environments.



Figure 1.16 PackBot mobile robot [Packbot]

MR-5 (Figure 1.17) is a remotely controlled mobile robot ideally suited for explosive ordnance disposal, swat, harmful material search, surveillance and other hazardous tasks [MR5]. As a mobile robot rugged and reliable, MR-5 can be used in any weather condition and on any terrain. This highly controllable mobile robot can be

operated on wheels or tracks. The obstacle over and climbing stair capability of this mobile robot are famously known.



Figure 1.17 MR-5 remotely controlled mobile robot [MR5]

Four-wheeled mobile robot, Nomad, (Figure 1.18) was placed in Antarctica by Carnegie Mellon University's Robotics Institute. In Antarctica, it is aimed to search autonomously for the meteorites and classify them [Nomad].



Figure 1.18 Nomad mobile robot [Nomad]

Talon (Figure 1.19 and 1.20) is a powerful, lightweight, versatile robot designed for missions ranging from exploration to weapons delivery [Talon, 2004]. Its large base accommodates sensor and cameras making Talon a one robot solution to a variety of mission requirements.



Figure 1.19 Talon mobile robot [Talon, 2004]

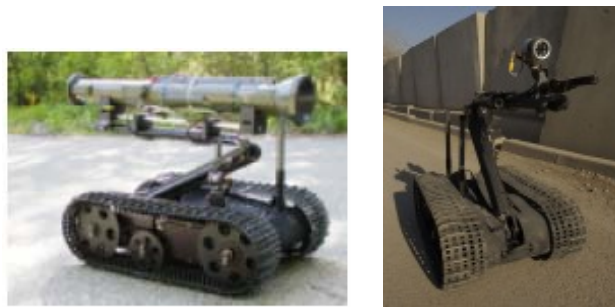


Figure 1.20 Talon robot in operation [Talon, 2004]

Built with all-weather, day/night and amphibious capabilities standard, Talon robot can operate under the most adverse conditions so as to overcome almost any terrain. The Talon began helping with military operations in Bosnia in 2000, deployed to Afghanistan in early 2002 and has been in Iraq since the war started, assisting with improvised explosive device detection and removal. Talon robots had been used in about 20,000 missions in Iraq and Afghanistan by the end of 2004. As of late 2004 there were four Talon robot in existence; 18 were requested for service in Iraq. Each system has cost about \$230,000 to produce. When they go into production, it is estimated the cost per unit will drop to the range of \$150,000 to \$180,000.

After this brief qualitative information about many mobile robots, in order to be able to quantitatively compare these robots, two tables (Table 1.1 and 1.2) are formed. The first table focuses on indoor robots whereas the second table presents

information on outdoor robots and also there is a comparison the outdoor robots with the robot base that we designed and manufactured.

Table 1.1 Indoor mobile robots [adapted from Robosoft]

INDOOR MOBILE ROBOTS							
	Cye	Magellan	Pioneer 2-DXE	B21r	RobuLab 80	RobuLab 150	Pekee
Payload (kg)	4	9,1	22,7	25	80	150	-
Max. Velocity (m/s)	4	2,5	1,6	1	1,5	2	1,11
Dimensions(mm)	225*400*130	Ø 368 h:198	440*380*220	Ø 525 h:1060	600*480*465	1025*680*440	380*250*220
Autonomy (hrs)	2	10	24-30	6	4-5	5-6	1
Wheel / Motors	2*12V DC	2*24V DC	2*12V DC	4*24V DC	2*48V DC	2*48V DC	2*12V DC
Microcontrolller	16Mhz/16 bits	-	Siemens C166	Embedded PC	MPC555	MPC555	16Mhz/16 bits
FirmWare	-	rFlex Cont. Sys	P20S Server	rFlex Cont. Sys	Syndex	Syndex	Instinct Software
Development Tools	(API) for Visual Basic or C++ MatLab	ASCI to speech Interface C++ compilers	ASCI to speech Interface C++ compilers	ASCI to speech Interface C++ compilers	ASCI strings API C for Linux	ASCI strings API C for Linux	(API) for Visual Basic or C++ MatLab
Software	MAP'n ZAP	Mobility robot integration Soft.	Pioneer simulator ACTS	Mobility robot integration Soft.	Libraries of Primitives C Under Linux	Libraries of Primitives C Under Linux	SDK-Pr
Sensors / Detection and other Equipment	Infrared-Ultrasonic Sensor	Odometer -Infrared- Gyro- Light Captor	Ultrasonic sensor- Inf. Sen.- Tactiles sen.-Laser scanner- Navig. compass- Vision sys.- Bumpers- GPS sys. Arms- Grippers- Pan Tilt Camera	Ultrasonic sensor-Inf. Sen.- Tactiles sen.-Laser scanner- Navig compass- Vision sys.- Bumpers- GPS sys. Arms- Grippers- Pan Tilt Camera	Ultrasonic sensor-Inf. Sen.- Tactiles sen.-Laser scanner- Navig compass- Vision sys.- GPS sys. Arms- Grippers- Pan Tilt Camera	Ultrasonic sensor- Laser scanner- Navig compass- Vision sys.- Arms- Grippers- Pan Tilt Camera	Ultrasonic sensor-Inf. Sen.-Laser scanner- Navig compass- Vision sys.- Arms- Grippers- Pan Tilt Camera
Safety	-	Temp. Sensor	Emergen. Stop	Emergen. Stop	Emergen. Stop	Emergen. Stop	Emergen. Stop
Communication	Serials Port Tx, Rx Video Data Trans. Radio Data Trans.	IR Between Robot and RS232, I2C OPP Buses Radio Data Trans.	Radio Data Trans., Wireless RS232 or Ethetnet, Video Data Trans., Joystisk, RS232	Radio Data Trans., Wireless RS232 or Ethetnet, Video Data Trans., RS232	Radio Data Trans., Wireless RS232 or Ethetnet, Video Data Trans., Joystisk, RS232	Radio Data Trans., Wireless RS232 or Ethetnet, Video Data Trans., CAN Bus	Radio Data Trans., Wireless RS232 or Ethetnet, Video Data Trans., CAN Bus

Table 1.1 Continued

Computer Devices	Remote PC or Laptop Win / Linux	Remote PC Win / Linux	Onboard mini PC, Remote PC or Laptop Win / Linux	Onboard or Remote PC or Laptop Win / Linux	Onboard or Remote PC or Laptop Win / Linux	Onboard or Remote PC or Laptop Linux	Onboard or Remote PC or Laptop Linux
Application	Education Beginners	Education Beginners	Appli. Prototy. Educa. Researc	Appli. Prototy. Educa.Re searc	Appli. Prototy. Educa.Re searc	Appli. Prototy. Educa.Re searc	Appli. Prototy. Educa.Re searc
Price Range €	3500-4500 €	11500-16000 €	5000-20000 €	49500-80000 €	20000-40000 €	28000-50000 €	4600-12000 €

Table 1.2 Outdoor mobile robots [adapted from Robosoft]

OUTDOOR MOBILE ROBOTS						
	Pioneer 2-AT	ATRV Mini	ATRV Jr	ATRV-2	RobuCar	Our Robot Base
Payload (kg)	22,7	9,1	25	100	300	10
Max. Velocity (m/s)	0,7	1,5	1	2	1,5	0,9
Dimensions(mm)	500*490*260	605*450	775*550	1050*650Ø	1900*1200*650	300*450*200
Autonomy (hrs)	10	2-4	3-5	4-6	4-6	2-3
Wheel / Motors	2*24V DC	4*24V DC	2*12V DC	4*24V DC	4*24V DC	2*12V DC
Max Slope Capability	40%	45%	45%	45%	10 to 35%	60%
Microcontrolller	Siemens C166	-	-	-	2*MPC555	PIC
Software	Mobility Robot Integration Soft.	Pioneer Simulator ACTS	Mobility Robot Integration Soft.	Mobility robot integration Soft	Libraries of Primitives C Under Linux	Robot Base Simulator
Communication	Radio Data Trans., Wireless RS232 or Ethetnet, Video Data Trans., Joystisk, RS232	Radio Data Trans., Wireless RS232 or Ethetnet, Video Data Trans., Joystisk, RS232	Radio Data Trans., Wireless RS232 or Ethetnet, Video Data Trans., Joystisk, RS232	Radio Data Trans., Wireless RS232 or Ethetnet, Video Data Trans., Joystisk, RS232	Radio Data Trans., Wireless RS232 or Ethetnet, Video Data Trans., Joystisk, RS232	Joystisk, RS232

Computer Devices	Onboard mini PC, Remote PC or Laptop Win / Linux Compatiple	Onboard mini PC, Remote PC or Laptop Win / Linux Compatiple	Onboard mini PC, Remote PC or Laptop Win / Linux Compatiple	Onboard mini PC, Remote PC or Laptop Win / Linux Compatiple	Onboard mini PC, Remote PC or Laptop Win / Linux Compatiple	PC,or Laptop Win Compatiple
Application	Applications Prototyping Education Research	Applications Prototyping Education Research	Applications Prototyping Education Research	Applications Prototyping Education Research	Applications Prototyping Education Research	All Areas
Price Range	9000-25000 €	11500-30000 €	27500-50000 €	43500-70000 €	50000-100000 €	1000-2000 €

Clearly, a useful, mobile robot does more than just move. It polishes the supermarket floor, keeps guard in a factory, mows the golf course, provides tours in a museum, or provide guidance in a museum or it can be a guard like a policeman or a soldier. Therefore, the mobile robots become popular very fastly in the world. Lots of scientists and research companies try to find the right mobile robot configuration which can move on different types of terrain and perform the different tasks that human cannot do. While these developments have been occurring all around the world, we have intended to design our own configurable robot base. At the end, we wish robot base that we have designed will be used by the Turkish Police Department, Military Force and other organizations in Turkey.

The outline of the following chapters of the thesis can be given as follows:

In Chapter II, the driving systems for the mobile robots will be introduced.

In Chapter III, design procedure that we have followed will be presented.

Studies related to the configurations of the robot base will be given in Chapter IV.

Chapter V will be devoted to the results and discussions.

Finally, Chapter VI touches on the conclusions and future work.

CHAPTER II




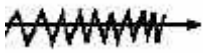








TYPES OF DRIVING SYSTEMS FOR THE MOBILE ROBOTS

In this chapter alternative driving systems that are applicable to mobile robots will be discussed. Appropriate steering type for our design will be sought. Today's wheeled, tracked, and legged mobile robots will be detailed and advantage and disadvantage of them will be discussed.

A mobile robot needs locomotion mechanisms that enable it to move throughout its environment. But there are a large variety of possible ways to move, and so the selection of a robot's approach to locomotion is an important aspect of mobile robot design. In the laboratory, there are research robots that can walk, jump, run, slide, skate, swim, fly, and roll. Most of these locomotion mechanisms have been inspired by their biological counterparts (Table 2.1).

There is, however, one exception: the actively powered wheel is a human invention that achieves extremely high efficiency on the flat ground. This mechanism is not completely foreign to biological systems. Our bipedal walking system can be approximated by a rolling polygon. As the step size decreases, the polygon approaches a circle or wheel. However, nature did not develop a fully rotating, actively powered joint, which is the technology necessary for wheeled locomotion [Todd, 1985]. Mobile robots generally are driven either by using wheeled mechanisms, a well-known human technology for vehicles, or using a small number of articulated legs, the simplest of the biological approaches to locomotion (Table 2.1).

Table 2.1 Locomotion mechanisms used in biological systems [Siegwart, 2004]

Types of motion		Resistance to Motion	Basic Kinematics of Motion	
Flow in a Channel		Hydrodynamic Forces	Eddies	
Crawl		Friction Forces	Longitudinal Vibration	
Sliding		Friction Forces	Transverse Vibration	
Running		Loss of Kinetic Energy	Oscillatory Movement of a Multi-Link Pendulum	
Jumping		Loss of Kinetic Energy	Oscillatory Movement of a Multi-Link Pendulum	
Walking		Gravitational Forces	Rolling of a Polygon	

In general, legged locomotion requires higher degrees of freedom and therefore greater mechanical complexity than wheeled locomotion. Wheels, in addition to being simple, are extremely well suited to flat ground. As Figure 2.1 depicts, on flat surfaces wheeled locomotion is one to two orders of magnitude more efficient than legged locomotion. Railways are ideally engineered for wheeled locomotion because rolling friction is minimized on a hard and flat steel surfaces. But as the surface becomes soft, wheeled locomotion accumulates inefficiencies due to rolling friction whereas legged locomotion suffers much less because it consists only of point contacts with the ground. This is demonstrated in Figure 2.1 by the dramatic loss of efficiency in the case of a tire on soft ground [Todd, 1985].

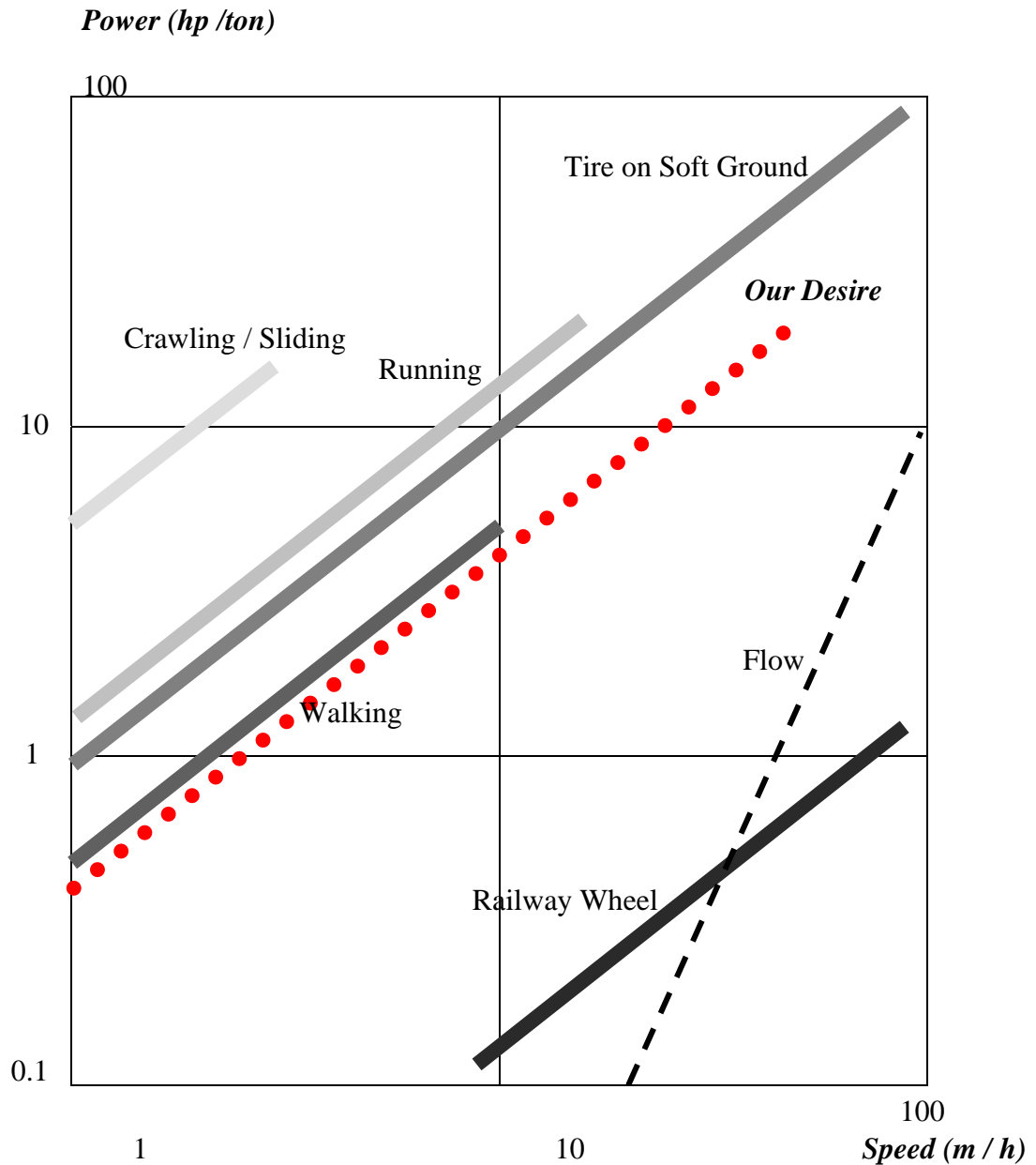


Figure 2.1 Attainable speeds of various locomotion mechanisms [Todd, 1985]

In effect, the efficiency of wheeled locomotion depends greatly on environmental qualities, particularly the flatness and hardness of the ground.

It is understandable therefore that nature favors legged locomotion, since locomotion systems in nature must operate on rough and unstructured terrain. For example, in the case of insects in a forest the vertical variation in ground height is often an order of magnitude greater than the total heights the insect. Whereas, human touched

environments frequently consists of engineered, smooth surfaces, both indoors and outdoors. Therefore, it is also understandable that virtually all industrial applications of mobile robotics utilize some form of wheeled locomotion. Recently, for more natural outdoor environments, there has been some progress toward hybrid and legged industrial robots such as the forestry robot shown in Figure 2.2 [Schweitzer, 2001].

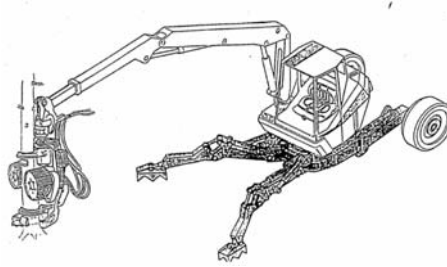


Figure 2.2 RoboTrac, a hybrid wheel-leg robot for rough terrain [Schweitzer, 2001]

2.1 Important Keys for Locomotion

Locomotion is the complement of manipulation. In manipulation, the robot arm is fixed but moves objects in the workspace by imparting force to them. In locomotion, the environment is fixed and the robot moves by imparting force to the environment. In both cases, the scientific basis is the study of actuators that generate interaction forces, and mechanisms that implement desired kinematics and dynamic properties. Locomotion and manipulation thus share similar core issues of stability, contact characteristics and environmental type:

Stability

- Number and geometry of contact points
- Center of gravity
- Static/dynamic stability
- Inclination of terrain
- Characteristics of contact
 - Contact point/path size and shape
 - Angle of contact
 - Friction
- Type of environment
 - Structure
 - Medium (e.g. water, air, soft or hard ground)

2.2 Legged Mobile Robots

Legged locomotion is characterized by a series of point contacts between the robot and the ground. The key advantages include adaptability and maneuverability in terrain. Because only a set of point contacts is required, the quality of the ground between those points does not matter so long as the robot can maintain adequate ground clearance. In addition, a walking robot is capable of crossing a hole or chasm so long as its reach exceeds the width of the hole. A final advantage of legged locomotion is the potential to manipulate objects in the environment with great skill. An excellent insect example (Figure 2.3), the dung beetle, is capable of rolling a ball while locomotion by way of its dexterous front legs.

The main disadvantages of legged locomotion include power and mechanical complexity. The leg, which may include several degrees of freedom, must be capable of sustaining part of the robot's total weight, and in many robots must be capable of lifting and lowering the robot. Additionally, high maneuverability will only be achieved if the legs have a sufficient number of degrees of freedom to impart forces in a number of different directions.

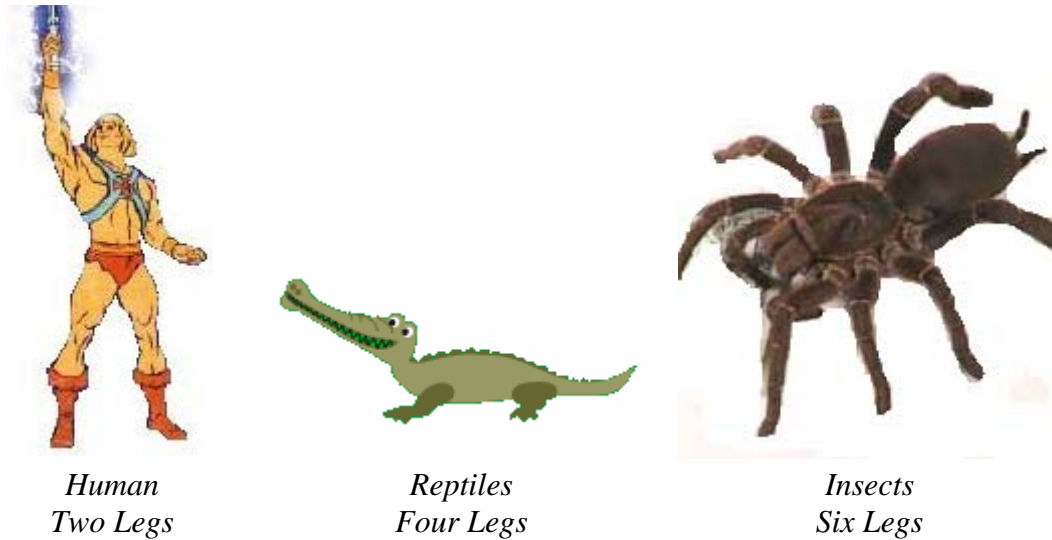


Figure 2.3 Arrangement of the legs

2.3 Tracked Mobile Robots

This type of locomotion can be named as tracked slip/skid locomotion. In the wheel configurations which will be discussed soon, it has been made an assumption that wheels are not allowed to skid against the surface [Steinmetz, 2001]. An alternative form of steering, termed slip/skid, may be used to reorient the robot by spinning wheels that are facing the same direction at different speeds or in opposite directions. An army tank operates this way and the Nanokhod (Figure 2.4) is an example of a such mobile robot based [Winnendael, 1999].

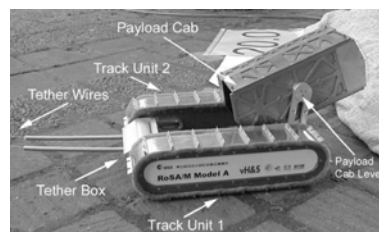


Figure 2.4 The Microrover Nanokhod [Winnendael, 1999]

Robots that make use of tread have much larger ground contact patches and this can significantly improve their maneuverability in loose terrain compared to the conventional wheeled designs. However, due to this large ground contact patch, changing the orientation of the robot usually requires a skidding turn, wherein a large portion of the track must slide against the terrain.

The disadvantage of such configurations is due to the large amount of skidding during a turn, the exact center of rotation of the robot is hard to predict and the exact change in position and orientation is also subject to variations depending on the ground friction. Therefore, dead reckoning on such robots is highly inaccurate. This is the trade-off that is made in return for extremely good maneuverability and traction over rough and loose terrain. Furthermore, a slip/skid approach on a high friction surface can quickly overcome the torque capabilities of the motors being used. In terms of power efficiency, this approach is reasonably efficient on loose terrain but extremely inefficient otherwise [Steinmetz, 2001, Winnendael, 1999]. Detailed analysis of tracked driving systems is presented in Chapter III.

2.4 Wheeled Mobile Robots

The wheel has been by far the most popular locomotion mechanisms in mobile robotics and in man-made vehicles in general. It can achieve very good efficiencies, as demonstrated Figure 2.1, and does so with a relatively simple mechanical implementation.

In addition, balance is not usually a research problem in wheeled robot designs, because most wheeled robots are designed so that all wheels are in ground contact at all times. Thus, three wheels are sufficient to guarantee stable balance although two-wheeled robots can also be stable. When more than three wheels are used, a suspension system is required to allow all wheels to maintain ground contact when the robot encounters uneven terrain.

Table 2.2 Types of wheeled mobile robots (Legend for wheel icons are provided at the end of the table)


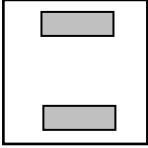
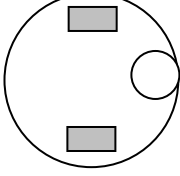
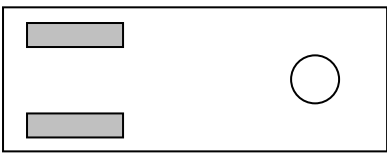
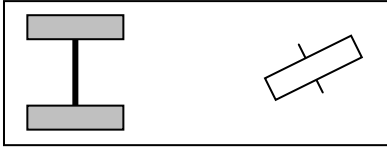

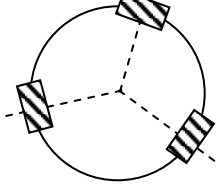
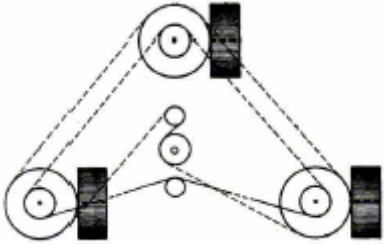
Number of Wheels	Arrangement	Description	Example
2		One steering wheel in the front, one traction wheel in the rear	Bicycle, motorcycle
		Two-wheel differential drive with the center of mass (COM) below the axle	Cye personal robot
		Two-wheel centered differential drive with a third point of contact	Nomad Scout, SmartRob EPFL
		Two independently driven wheels in the rear/front, one unpowered omnidirectional wheel in the front/rear	Many indoor robots, EPFL, Alice, Pygmalion
		Two connected traction wheels(differential) in rear, one steered free wheel in front	Piaggio minitruacts
		Two free wheels in rear, one steered traction wheel in front	Neptune, Hero-1
		Three motorized Swedish or spherical wheels arranged in a triangle; omnidirectional movement is possible	Stanford wheel Tribolo EPFL, PalmRobot
		Three synchronously motorized and steered wheel; the orientation is not controllable	Denning MRV-2, iRobot B24, Nomad 200

Table 2.2 Continued

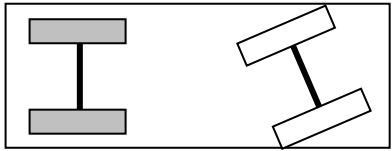
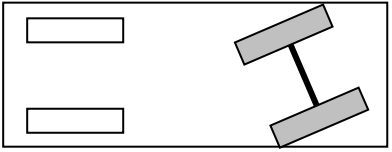
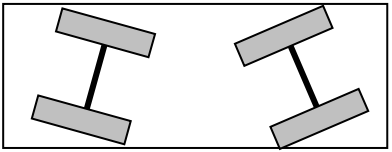
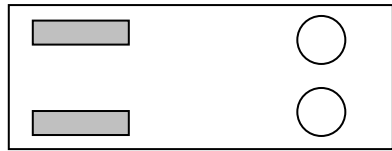
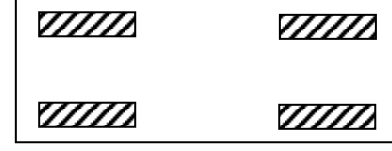
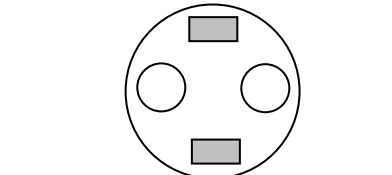
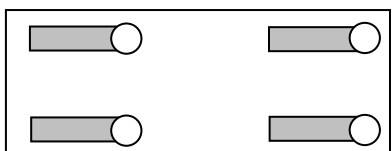
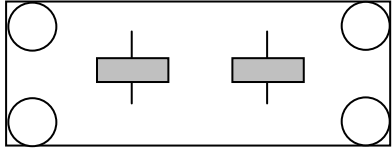
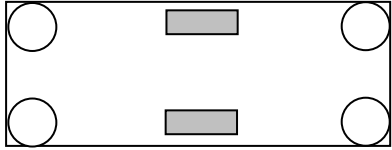
Number of Wheels	Arrangement	Description	Example
4		Two motorized wheels in the rear, two steered wheels in the front; steering has to be different for the two wheels to avoid slipping/skidding	Car with rear-wheel drive
		Two motorized and steered wheels in the front, two free wheels in the rear; steering has to be different for the two wheels to avoid slipping/skidding	Car with rear-wheel drive
		Four steered and motorized wheels	Four wheel drive and steering Hpperion
		Two traction wheels (differential) in rear/front, two omnidirectional wheels in the front/rear	Charlie (DMT-EPFL)
		Four omnidirectional wheels	Carnegie Mellon Uranus
		Two wheel differential drive with two additional points of contact	EPFL Khepera, Hyperbot Chip
		Four motorized and steered castor wheels	Nomad XR4000

Table 2.2 Continued

Number of Wheels	Arrangement	Description	Example
6		Two motorized and steered wheels aligned in center, one omnidirectional wheel at each corner	First
		Two traction wheels (differential) in center, one omnidirectional wheel at each corner	Terragator (Carnegie Mellon University)

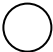

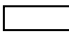



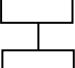
Icons for the each wheel type	
	Unpowered omnidirectional wheel (spherical, castor, Swedish)
	Motorized Swedish wheel (Stanford wheel)
	Unpowered standard wheel
	Motorized standard wheel
	Motorized and steered castor wheel
	Steered standard wheel
	Connected wheels

Table 2.2 (adapted from [Siegwart, 2004]) shows great majority of the mobile robot wheel configurations that were designed and manufactured up to now.

2.4.1 Stability

The minimum number of wheels required for static stability is two. As shown Figure 2.5, a two wheel differential drive robot can achieve static stability if the center of mass is below the wheel axle. Cye is a domestic robot base that uses this wheel configuration.



Figure 2.5 Cye a two wheel differential robot base [Acroname]

However, under ordinary circumstances such a solution requires wheel diameters that are impractically large. Dynamics can also cause a two-wheeled robot to strike the floor with a third point of contact, for instance, with sufficiently high motor torques from standstill. Conventionally, static stability requires a minimum of three wheels with the additional caution that the center of gravity must be contained within the triangle formed by the ground contact points of the wheels.

2.4.2 Maneuverability

Some robots are omnidirectional that they can move at any time in any direction along the ground plane (x, y) regardless of the orientation of the robot around its vertical axis. This level of maneuverability requires wheels that can move in more than just one direction and so omnidirectional robots usually employ Swedish or spherica wheels that are powered. A good example is Uranus, shown in Figure 2.6. This robot uses four Swedish wheels to rotate and translate indepently and without constraints [Uranus].

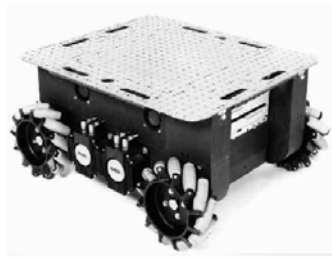


Figure 2.6 Uranus Robot built by Carnegie Mellon University [Uranus]

2.4.3 Controllability

There is generally an inverse correlation between controllability and maneuverability. For instance, the omnidirectional designs such as the four castor wheel configuration require significant processing to convert desired rotational and translational velocities to individual wheel commands. Furthermore, such omnidirectional designs often have greater degrees of freedom at the wheel. For instance, the Swedish wheel has a set of free rollers along the wheel perimeter. These degrees of freedom cause an accumulation of slippage.

Controlling an omnidirectional robot for a specific direction of travel is also more difficult and often less accurate when compared to less maneuverable designs. For example, an acherman steering vehicle can go straight simply by locking the steerable wheels and driving the drive wheels. In a differential drive vehicle, two motors attached to the two wheels must be driven along exactly the same velocity profile. With four wheel omnidrive, such as the Uranus robot, which has four Swedish wheels, the problem is even harder because all four wheels must be driven at exactly the same speed for the robot to travel in a perfectly straight line.

2.5 Legged - Wheeled Mobile Robots

Legged - wheeled mobile robots might offer the best maneuverability in rough terrain. However, they are inefficient on flat ground and need sophisticated control. Hybrid solutions, combining the adaptability of legs with the efficiency of wheels,

offer an interesting compromise. Solutions that passively adapt to the terrain are of particular interest for field and space robotics. The Sojourner robot of Nasa/JPL (Figure 1.5) represents such a hybrid solution, and it is able to overcome objects up to the size of the wheels. A more recent mobile robot design for similar applications has recently been produced called Shrimp (Figure 2.7). It has six motorized wheels and is capable of climbing objects up to two times its wheel diameter [Lauria, 1991]. This enables it to climb regular stairs although the robot is even smaller than the Sojourner.



Figure 2.7 Shrimp having six motorized wheels [Lauria, 1991]

In this chapter alternative driving systems that are applicable to mobile robots are presented. Wheeled, tracked and legged mobile robots are presented in detail, their advantages and disadvantages are discussed. Appropriate steering types for our design are evaluated. As a result of this discussion, it is decided to design a configurable robot base that can be driven by wheels and tracks. Next chapter will explain the design steps and calculations regarding this robot base.

CHAPTER III

DESIGN PROCEDURE

The purpose of this thesis is to design and manufacture a mobile robot that is not only capable of successfully traversing over mixed terrains but also a configurable. The requirement of configurability has certain implications on how the robot body and the parts attached to it are designed. In this chapter, the design procedure carried out to determine the details of these parts are presented.

3.1 Shaft Design

Our robot is intended to be used in three different configurations: with wheels, with tracks and with both wheels and tracks. Therefore, rather than using only one shaft it is considered to use two shafts that can be attached to each other.

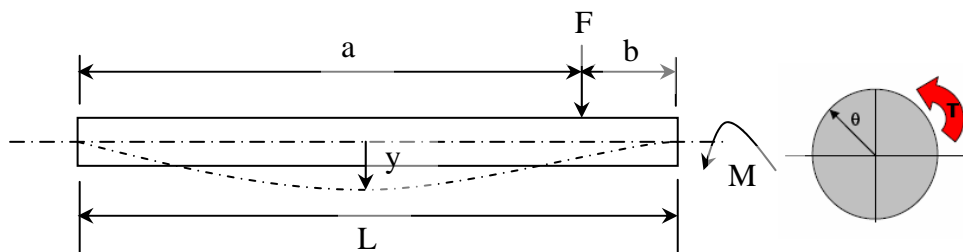


Figure 3.1 Shaft loading

The allowable shaft diameter given in Figure 3.1 can be given as follows:

$$d = \left[\frac{32Fb}{3E\pi L\theta_{allowable}}(b^2 - L^2) + \frac{32M}{3E\pi L\theta_{allowable}}(3a^2 - 6aL + 2L^2) \right]^{\frac{1}{4}} \quad (3.1)$$

where

$$y = \sum \frac{F_i b_i x}{6EIL} (x^2 + b_i^2 - L^2) + \sum \frac{M_i x}{6EIL} (x^2 + 3a_i^2 - 6a_i L + 2L^2) \quad (3.2)$$

$$\theta_{allowable} = \sum \frac{F_i b_i}{6EIL} (b_i^2 - L^2) + \sum \frac{M_i x}{6EIL} (3a_i^2 - 6a_i L + 2L^2) \quad (3.3)$$

The shaft diameter should be checked in terms of torsional deflection and bending stress.

$$\tau \leq \tau_{safety} \quad \text{and} \quad \tau = \frac{T}{W_t} \Rightarrow \tau = \frac{T}{\pi d^3 / 16} \leq \tau_{safety} \quad (3.4)$$

$$\sigma \leq \sigma_{safety} \quad \text{and} \quad \sigma = \frac{M}{W_m} \Rightarrow \sigma = \frac{M}{\pi d^3 / 32} \leq \sigma_{safety} \quad (3.5)$$

Using the allowable shaft diameter equation (Eqn. 3.1), the required shaft radius R and length L are computed to be around 10 mm and 75 mm respectively. Finalized details for all dimensions are available in Appendices B.11, B.12, and B.16. As mentioned above, there are two shafts to be designed and they should be easily connected to one another as in Figure (3.2) and (3.3). Dimensions of the shaft shown in figure 3.2 is calculated as follows:

$$A_p = l(2\pi r + 2d) \quad (3.6)$$

$$F_{T_f} = A_p \mu P \quad (3.7)$$

$$M_f = F_{T_f} \frac{d}{2} \quad (3.8)$$

where A_p is placed area, P is the pressure on placed area, F_{T_f} is total friction force, M_f is friction moment, and M_t is moment to be transmitted. In order to transmit moment safely, M_f should be greater than M_t .

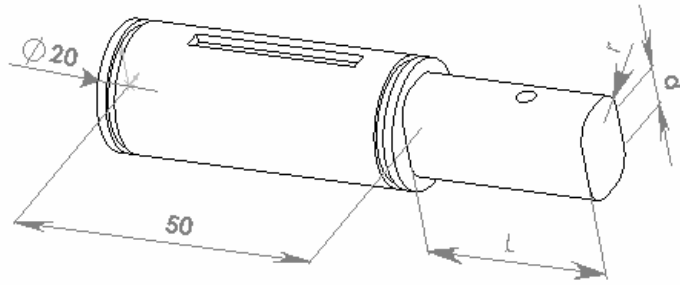


Figure 3.2 CAD drawing of the designed shaft

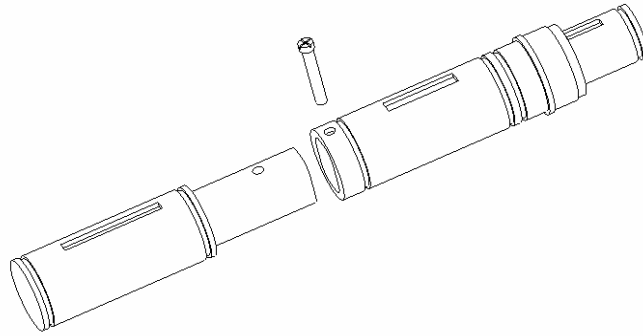


Figure 3.3 Assembling two shafts for using wheels and tracks at the same time

$$\frac{\sigma_{safety}}{2} = \tau_{max} = \frac{P_{max}}{1 - C^2} \leq \tau_{safety} \quad (3.9)$$

$$\tau_{safety} = \frac{\sigma_{ys}}{S} \quad (3.10)$$

$$C = \frac{r}{R} \quad (3.11)$$

Friction moment is expected to be larger than transmitted moments.

$$M_f = SM_t \quad (3.12)$$

$$M_f = \mu l (2\pi + 2d) P \frac{d}{2} \quad (3.13)$$

The pressure generated over the placed area should be less than the critical stress to yield the material.

$$P_{\max} = \frac{\sigma_{\text{safety}}}{2}(1 - C^2) \quad (3.14)$$

$$P_{\min} = \frac{2M_f}{\mu dl(2\pi r + 2b)} \quad (3.15)$$

So P should be in between P_{\min} and P_{\max}

$$P_{\min} < P < P_{\max} \quad (3.16)$$

As a result r , d and l dimensions were found as 4.25, 6.50 and 30 mm respectively. All dimensions are presented in Appendix B.16.

3.2 Set Screw Selection

Two shafts are connected to each other as shown in figure 3.3. To maintain the shafts in place, a screw is used (Figure 3.4). The reliability of this screw is very important for the safe motion. Therefore, the screw selection should be carefully made. Material properties of the selected screw are as follows:

Iron 70, $\sigma_{ys} = 365 \text{ N/mm}^2$ and $\tau_{ys} = 260 \text{ N/mm}^2$

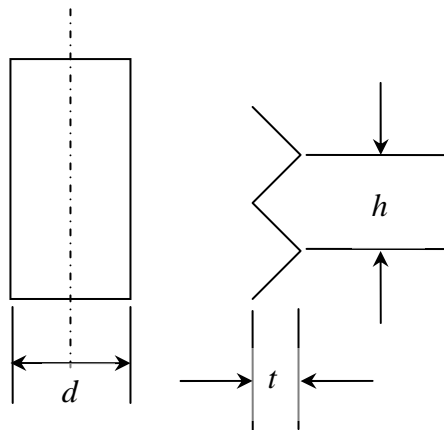


Figure 3.4 Screw used for the shafts connection

Screw used to connect the shafts should resist the maximum shear force that occurs when a 200N loading is assumed for each wheel. Axial loads are assumed to be less than 200N.

$$\tau = \frac{F}{\pi dh} \leq \tau_{safety} \quad (3.17)$$

$$\tau_{safety} = \frac{\tau_{ys}}{S} \quad (3.18)$$

For M3 screw, $h = 0,5$ mm, $t = 0,3$ mm and, safety factor S is taken to be 2.

$$\tau = 21N / mm^2 \quad (3.19)$$

$$\tau_{safety} = 130N / mm^2 \quad (3.20)$$

Since $\tau < \tau_{safety}$, selection of M3 set screw is safe against shear.

Screw used to connect the shafts should also resist the maximum bending stress.

$$\sigma = \frac{3Ft}{\pi dh^2} \leq \sigma_{safety} \quad (3.21)$$

$$\sigma_{safety} = \frac{\sigma_{ys}}{S} \quad (3.22)$$

$$\sigma = 60N / mm^2 \quad (3.23)$$

$$\sigma_{safety} = 183N / mm^2 \quad (3.24)$$

Since $\sigma < \sigma_{safety}$ selection of M3 set screw is sound when bending stresses are considered.

As a result, M3 screw can be safely be used as the set screw in this design.

3.3 Bearing Selection

Bearing selection is done by first identifying the loading conditions, followed by theoretical calculations. These calculations are then adjusted by making use of the guidelines presented in the manufacturer's catalogue to compensate for the actual loading conditions and finally a bearing is selected. The details of this selection is presented in the next section.

The loads applied to the bearings generally include the weight of the shaft and the robot body as illustrated in figure 3.5.

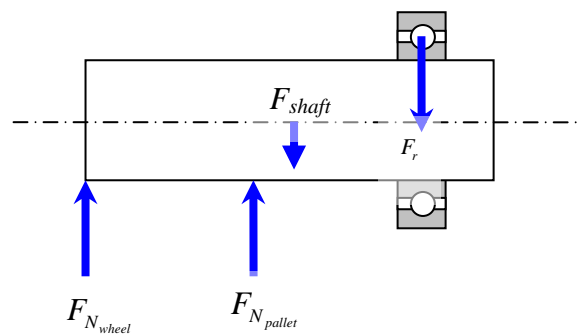


Figure 3.5 Loads applied to a bearing

The following procedure is used in selecting the proper bearing from manufacturer's catalogue.

- Radial and axial loads are to be determined.
- Equivalence load (F) is to be calculated. (manufacturer catalog will be used)
- Appropriate bearing type is to be determined.
- Rough life expectation is to be determined.
- Dynamic load number (C) is to be determined.

When a radial or axial load is mathematically calculated, the actual load on the bearing may be greater than the calculated one because of possible vibration and shocks that the robot will be exposed to during motion.

The actual load may be calculated using the following equations;

$$F_r = f_w F_{r_c} \quad (3.25)$$

$$F_a = f_w F_{a_c} \quad (3.26)$$

where F_r and F_a are loads applied on bearing (N), F_{r_c} and F_{a_c} are theoretically calculated loads (N), and f_w is load factor. Commonly used values for selecting the load factors f_w is given in Table 3.1.

Table 3.1 Load factors

Operating Conditions	Typical Applications	f_w
Smooth operation free from shock	Electric motors, machine tools, air conditioners	1 - 1,2
Normal operation	Air blower, compressors, elevators, cranes	1,2 – 1,5
Operation accompanied any vibration	Construction equipment, crushers, rolling mills	1,5 - 3

The key value that we have used in manufacturer’s catalog data is the bearing rated dynamic load capacity, C.

Life expectancy L can be calculated as follows:

$$L = L_R \left(\frac{C}{F_r} \right)^{3.33} \quad (3.27)$$

where

$L_R = \text{rating life } (1 \times 10^6)$

$L = \text{life expected for radial load, } F_r$

$C = \text{rated load capacity of bearing}$

For design purposes it is more convenient to determine the required rated load C_{req} so that bearing selection can easily be done from the manufacturer's catalogue:

$$C_{req} = F_r \left(\frac{L}{L_R} \right)^{0.3} \quad (3.28)$$

To obtain a reliability value greater than 90%, a reliability factor $K_r = L/L_0$ must be applied to the rated life. Proper K_r values are given in Table 3.2. (e.g. for reliability = 99%, $K_r = 0.21$)

Combining all of the above equations gives the yields equations (3.29) and (3.30).

$$L = K_r L_R \left[\frac{C}{(F_r + F_a) K_a} \right]^{3.33} \quad (3.29)$$

$$C_{req} = (F_r + F_a) \left[\frac{L}{K_r L_R} \right]^{0.3} \quad (3.30)$$

where K_a is the application factor for case in which the load on the bearing has some degree of impact. We have used it as 1.

As a result, SKF deep groove ball bearing with single row has been selected; inner and diameter outer diameter are 20 mm and 32 mm respectively.

Table 3.2 Reliability factor table

Reliability %	Life Rating	Reliability factor $K_r = L/L_0$
90	L ₁₀	1,00
95	L ₀₅	0,62
96	L ₀₄	0,53
97	L ₀₃	0,44
98	L ₀₂	0,33
99	L ₀₁	0,21
99,5	L ₀₀₅	0,15
99,7	L ₀₀₃	0,105
99,9	L ₀₀₁	0,055

3.4 Key Design

In order to secure the rotating parts, keys must be used. First of all, to obtain the required design equations, key dimensions must be specified. A square prism key is selected as illustrated in Figure 3.6.

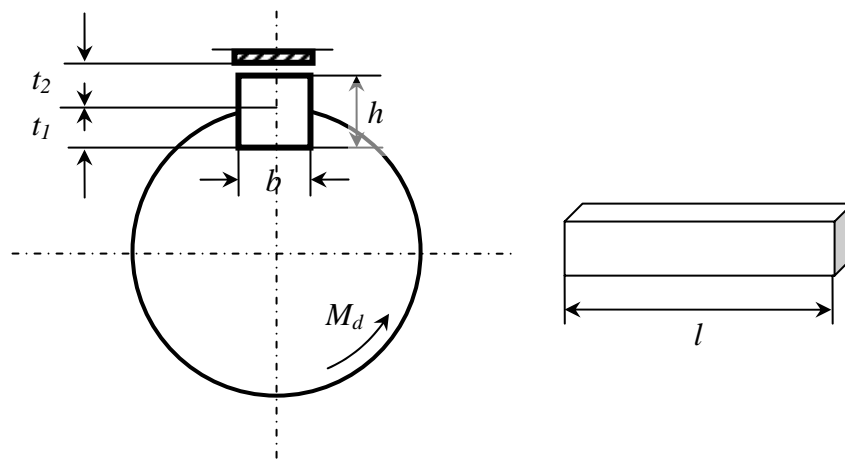


Figure 3.6 Key dimensions

The legend for Figure 3.6 is as follows:

h key height

t_1 key way depth

t_2 key depth

l key length

b key width

P power (kw)

n rpm

For the sake of design calculations, following assumption is made:

$$t_2 \cong h - t_1 \quad (3.31)$$

We have selected alloy steel as key material and Al 6061 as shaft material. Shaft housing material is polyamide or Al 6061 for tracks and wheels respectively.

Equations (3.32) and (3.33) can be used for key, shaft, and shaft housing materials.

$$P_{safety} = \frac{\sigma_{ys}}{S} \quad (3.32)$$

$$\tau_{safety} = \frac{\tau_{ys}}{S} \quad (3.33)$$

where S is the safety factor.

Moment to be transmitted that indicated by M_t (N-m).

$$M_t = 9550 \frac{P}{n} \Rightarrow d = M_t \sqrt[3]{\frac{P}{n}} \text{ (mm)} \quad (3.34)$$

Length of key is to be determined after strength calculations.

$$F_t = \frac{M_t}{d/2} \text{ (N)} \quad (3.35)$$

where F_t is the tangential force.

$$P = \frac{F_t}{l.t_2} < P_{safety} \quad (3.36)$$

P can be equal to P_{safety} . In this case

$$l = \frac{F_t}{t_2 P_{safety}} \text{ (mm)} \quad (3.37)$$

Control of key for cutting $\tau = \frac{F_t}{b.l} \leq \tau_{safety} \quad (3.38)$

Control of shaft $P = \frac{F_t}{l.t_1} \leq (P_{safety})_{shaft} \quad (3.39)$

As a result the keys dimensions are selected as 30 x 3 x 4 (l x h x b).

3.5 Palette (Track) Selection

Double-Sided Timing Belt as shown in Figure 3.7 is chosen to be used as a palette.



Figure 3.7 Double-Sided Timing Belt

The details of the double sided timing belt selection can be given as the follows.

Transferable torque of the timing belt is:

$$M = \frac{z_e M_i d \pi b}{t} \quad (3.40)$$

Maximum number of engaging teeth that can be used for selection of the timing belt is:

$$z_e = z_1 \left[0,5 - \frac{t(z_2 - z_1)}{19,74a} \right] \quad (3.41)$$

Peripheral force of the two sided timing belt is:

$$F_u = F_i z_e b \quad (3.42)$$

Required torque (N-m) and torque listed for belt are:

$$T = \frac{P * 9549}{n} \text{ and } T_b = \frac{T}{b} \quad (3.43)$$

Reference circle diameter (mm) is:

$$d = \frac{z t}{\pi} \quad (3.44)$$

Length of the belt (mm) is:

$$L = 2a + 1,57(D_1 + D_2) + \frac{(D_1 - D_2)^2}{4a} \quad (3.45)$$

Also notations used above can be listed in order to easy realization as follows:

z_1	<i>Number of teeth of pulley1</i>
z_2	<i>Number of teeth of pulley2</i>
t	<i>Pitch (mm)</i>
a	<i>Center distance (mm)</i>
F_i	<i>Spec. peripheral force per engaging tooth and per cm of belt width</i>
M_i	<i>Transferable torque per engaging tooth and per cm of belt width</i>
b	<i>Width of the belt (cm)</i>
D_1	<i>Diameter of Pulley 1</i>
D_2	<i>Diameter of Pulley 2</i>
P	<i>Required power (kW)</i>
N	<i>Driving speed (rpm)</i>

After required calculations are carried out, M_i turns out to be 0,195Nm/cm = 19,5Nmm/mm. To meet this need, T10 with steel cord is selected (NSW Company SECA Timing Belts [Track]). The pulleys to be used with the selected belt are designed and manufactured by us.

3.6 Frame Design

To construct the frame of the robot base aluminum profiles are designed and manufactured. Figure 3.8 shows the aluminum profile used in building the frame of the robot body. The robot body is illustrated in figure 3.9. Aluminum profiles are the building blocks of the robot body. The slots are intended to facilitate the configurability of the robot base. A total of 4 slots are used, two on one face, one on the other, and one slot along the top edge of the aluminum profile as illustrated in figure 3.8.

Two slotted side faces the inner side of the robot body. Movable bars are inserted into these slots. By using these beams, internal elements of the robot can easily be managed within the robot body. For example, the batteries, computer mainboard and other accessories within robots body can easily be moved around. Additional elements can also easily be added to this robot structure in the future. These slots are

also used for carrying the motor mountings, and connecting the profiles. The slot placed outside is used for mounting the bearing hubs. Top groove is reserved for future use.

Detailed drawing of the aluminum profile is given in Appendix B.5.

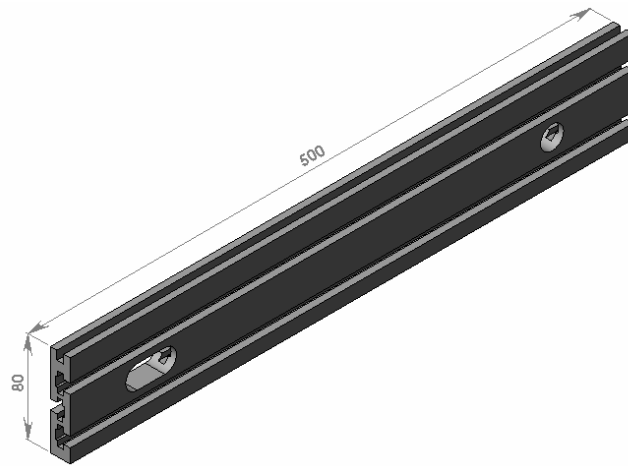


Figure 3.8 Aluminum profile

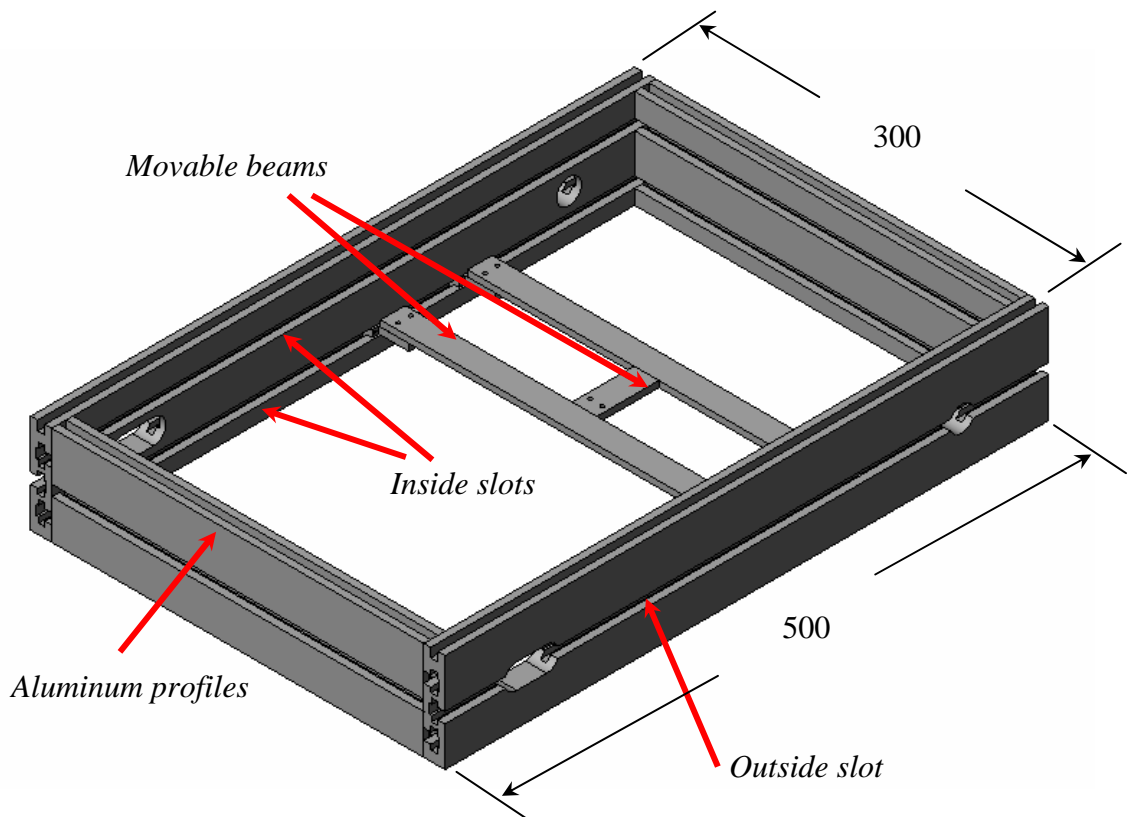


Figure 3.9 Frame with movable beams

3.7 Bearing Hub Design

Our robot design requires that the robot can be used with and without tracks. When tracks are used, their tension has to be arranged by using some mechanism. The proposed solution in this design is to shift bearing hubs in the aluminum profile slots and fix them at desired locations. Since only one of the two shafts on one side of the robot is to be sliding, the other can be fixed. This implies that two different hubs are to be designed. The first hub (Figure 3.10a) is for the fixed shafts which are connected to the motor, the second one (Figure 3.10b) is for the movable shafts which are used for stretching the palettes. Dimensions of the bearing hubs are available in Appendix B.3 and B.4.

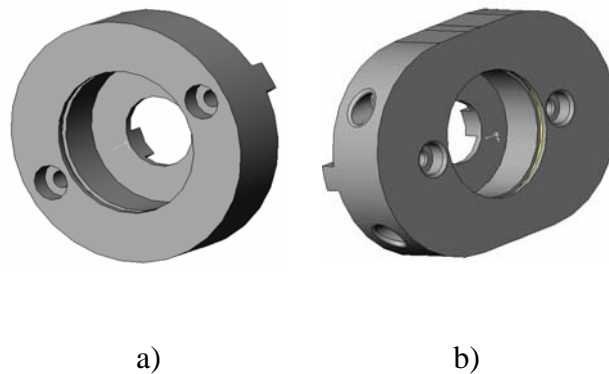


Figure 3.10 Bearing Hubs

a) Hub for fixed shafts, b) Hub for stretching the palettes

3.8 Motor Mounting Design

Almost all motors can be mounted given a little ingenuity and elbow grease. Nevertheless, the material of the motor mounting should be selected very carefully. Considering the required shape of the motor mounting (illustrated in figure 3.11), without further analysis, we preferred steel to aluminum as the mounting material.

The mountings are designed to be able to move inside the slot of the aluminum profiles so that motor positions can easily be adjusted within the robots body. This

feature is also important from the configurability point of view of this design. For example, if the reduction ratio between the motor output and robot wheel shaft is to be changed, this adjustment will not have any implications on neither on the mounting nor on the robot body frame. All dimensions of the motor mounting can be seen in Appendix B.6.

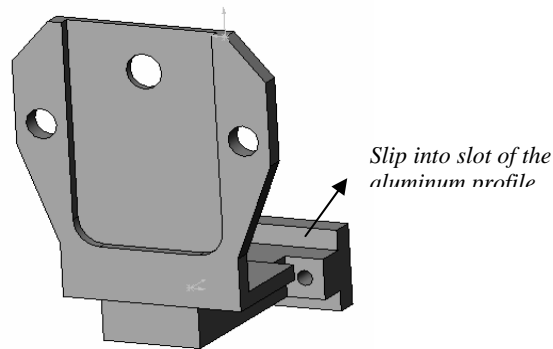


Figure 3.11 Motor Mounting

3.9 Palette Stretcher Design

To stretch the palettes, a stretcher is designed as illustrated in figure 3.12. This part is fixed to the frame then bearing hub is stretched by using two screws. Dimensions of the palette stretcher can be seen in Appendix B.15.

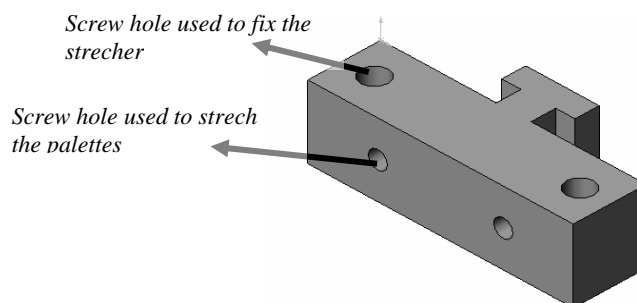


Figure 3.12 Palette Stretcher

3.10 Track Pulley (*Wheel*) Design

Appropriate pulley for the selected belt is designed. It is manufactured from polyamide to decrease the weight. The track wheel is shown in figure 3.13.

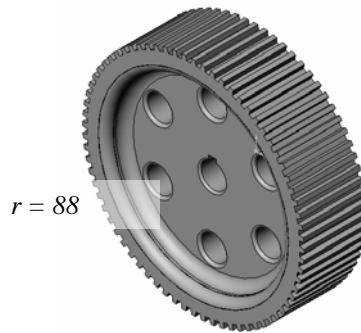


Figure 3.13 Palette pulley

3.11 Movable Beam Carrier Design

To carry the movable beams as well as the motor mountings, a carrier is designed and manufactured. This beam carrier is shown in Figure 3.14. Dimensions of the movable beam carrier can be seen in Appendix B.1.

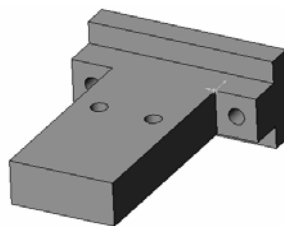


Figure 3.14 Movable beam carrier

3.12 Motor Selection

Motors are the most important part of the robot base since they do provide the motion of it. Various types of motors are available for the mobile robots. In order to have a successful robot, the motors should be selected very carefully. Alternative motors are DC, RC servo and stepper motors and a comparison of these are given in Table 3.3. RC servos are commonly used for hobby purposes, their use is very easy. With slight manipulation continuous rotation can be obtained from these motors, however, they are neither efficient, nor strong enough for our applications, therefore, they are opted out. Stepper motors also provide ease of use and easy open loop position control. However, their power vs. size performance is definitely not appropriate for our applications. As a result, permanent magnet brushed DC motors are chosen as the actuators of our robots. Permanent magnet brushed motor is selected due to its availability, simplicity of the control circuitry and low cost. However, the configurable nature of this robot base allows the users to switch to any kind of motor as long as it is physically possible to fit it into the robot base. In terms of manufacturing, the only overhead of switching motors will be the design and manufacturing of motor mountings.

To figure out what we need to look for in a motor, it is needed to define how we want our robot base to perform. The procedure used in selecting an appropriate motor is given as follows.

1. Deciding on the environment in which the robot base will be driven and also possible external forces.
2. Deciding on the maximum speed of the robot base that we want it to reach.
3. Deciding on the maximum acceleration of the robot base that we want it to achieve.
4. Estimating all the parameters of the robot base.
5. Constructing a dynamic equation for the robot base. (A control procedure is also presented for this model in Appendix A.)
6. Checking whether robot base can achieve the desired maximum speed and acceleration or not.

This procedure is iteratively used in selecting a proper motor from manufacturer's catalogue. Maxon manufactures high quality motors, and they are preferred not only in many other mobile robots, but also in several different industrial applications. Therefore, at the end of this analysis, a Maxon motor will be selected.

Table 3.3 Comparing features of mobile robot motor types

Motor Type	Benefits	Detractors	Best For
DC Motor	<ul style="list-style-type: none"> • Commonly available • Great variety • Most powerful • Easy to interface • A must for large robots 	<ul style="list-style-type: none"> • Too fast, needs gearbox • High current usually • Harder to mount wheels • More expensive • Complex control(PWM) 	✓ Large robots
Hobby Servo Motor	<ul style="list-style-type: none"> • Gearbox included • Great variety • Good indoor robot speed • Inexpensive • Good small robot power • Easy to mount • Easy to mount wheels • Easy to interface • Medium power required 	<ul style="list-style-type: none"> • Low weight capability • Little speed control 	*Small robots *Legged robots
Stepper Motor	<ul style="list-style-type: none"> • Precise speed control • Great variety • Good indoor robot speed • Easy to interface • Inexpensive 	<ul style="list-style-type: none"> • Heavy for their power • High current usually • Bulky size • Harder to mount wheels • Not very powerful • Complex controls needed 	*Line follower *Maze solver

As mentioned within the given procedure above, a model for the robot base is necessary in order to select a proper motor. The Figure 3.15 illustrates a basic way to model the moving robot base.

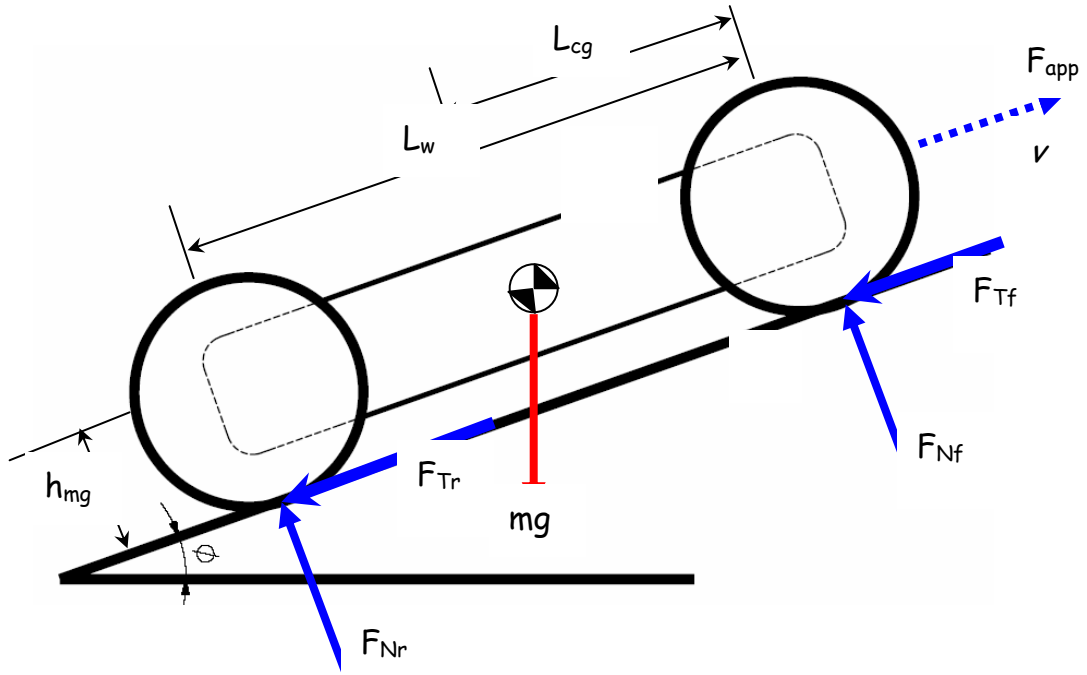


Figure 3.15 Robot base model used in selecting the proper motor

For choosing the motors for the robot base, we need to know how the performance criteria of the robot along with the forces that the base will be in interaction with. After some manipulations, the required forces to move the robot base can be given as:

$$F_{app} = F_{Nf} \mu + F_{Nr} \mu + mg \sin \theta \quad (3.46)$$

where θ is the slope angle, m is the total mass of the robot base (+wheel + track), and μ is the coefficient of friction.

Note that robot base's velocity is desired between 0,6-1 m/s that is the speed of a walking soldier / person. Motor velocities based on robot's translational velocity can be computed as:

$$V_{robot} = V_{motor} D_w \frac{\pi}{60} \quad (3.47)$$

Figure 3.16 illustrates how force, torque and power requirements of the robot base change with the change in slope of the surface that the robot moves on. Police and military specs suggest that such robots should be able to climb slopes of 30°.

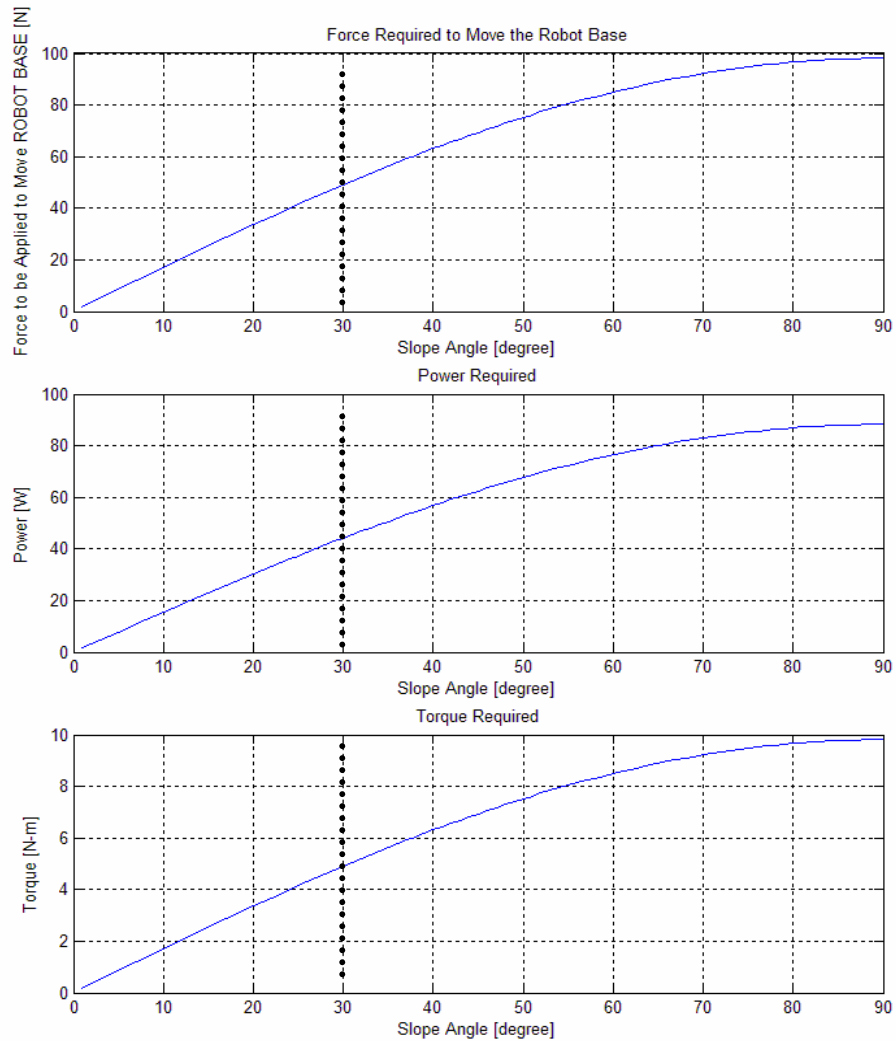


Figure 3.16 The required data for the motor selection

As a result, RE-Max series 40 Watt DC motor is selected from Maxon's catalogue. All the data about this motor is given in the Table 3.5.

Table 3.4 Data of the Motors Placed on the Robot Base

Voltage		No Load		At Maximum Efficiency				Stall	
Operating Range	Nominal (V)	Speed (rpm)	Current (A)	Speed	Current	Torque (g-cm)	Output (W)	Torque (g-cm)	Current
12-24	12	72	0,35	36	3,5	54600	40	240000	6
12-24	24	36	0,5	18	1,75	54600	20	120000	3

3.13 Robot Base Control

Within the scope of this thesis, only the design and manufacturing of a mixed terrain robot base is planned. Application of advanced control techniques is left for future studies. However, in order to carry out the experiments on mixed terrain, it is still necessary to easily move this robot around. It is also important to demonstrate for future users that this robot can easily be controlled via a PC. Hence, basic drivers on the PC side should be written. This involves development of a microcontroller based system on the robot side, and a sample software package on the PC side.

On the robot side, a small microcontroller board with PIC 16F877 is designed and manufactured (Figure 3.17). A small motor driver board with LMD 18200 H-bridges are also manufactured and connected to the microcontroller board. PIC 16F877 is chosen not only because it is commonly available on the market. 16F877 has many pins that can be reserved for future use, and also available bootloaders for this microcontroller provides a simple development environment with minimal hardware installed on the robot. LMD 18200 is also selected for its simplicity in use. With this IC a simple motor driver that will survive long enough to carry out the basic driving test can be constructed quickly.

On the PC side, a small program is written. A snapshot of this program is illustrated in figure 3.18. This program opens a serial connection to the robot via RS232 and

talks to the robot. With this program, the microcontroller algorithms can be debugged, individual motors can be controlled for test purposes, and by using the virtual joystick, the robot base can easily be driven around. In the future, this wired RS232 connection to the robot will be replaced with wireless links. Currently, an RF and WI-FI connection is planned.



Figure 3.17 Main Board containing PIC 16F877

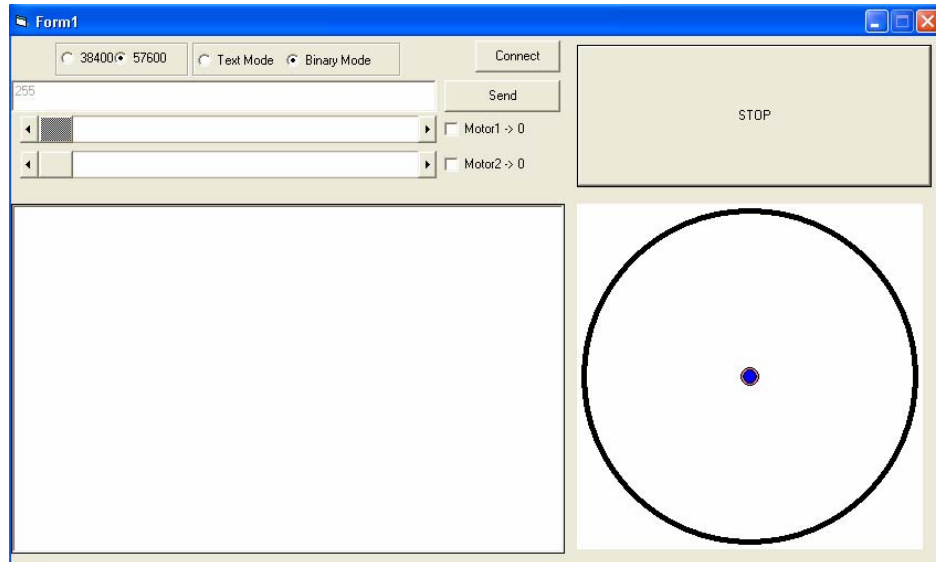


Figure 3.18 Graphical user interface for robot base control

3.14 Battery Evaluation

Robot base carries two 12 V – 7 A batteries. When robot base is taken out for mission, it is important to be able to estimate how long these batteries will last at an approximate rate of discharge. Therefore, battery capacity must be taken into account during the design procedure. To calculate how long the battery will really last, “Peukert’s Formula” can be used.

$$T = C / I^n \quad (3.48)$$

C is theoretical capacity (in amp-hours, equal to actual capacity at one amp), I is current drawn from the battery during operation (in amp), T is the time the battery will last (in hours), and n is the Peukert Number for the battery. The Peukert Number shows how well the battery holds up under right rates of discharge. This number n most ranges from 1.1 to 1.3. The closer n gets to 1, the better the performance. This number is determined empirically, by testing the battery at different rates. For the batteries that we used, the Peukert Number is taken as 1.3 (according to our experiences). Figure 3.19 illustrates the performance curve of the battery plotted for n = 1.3.

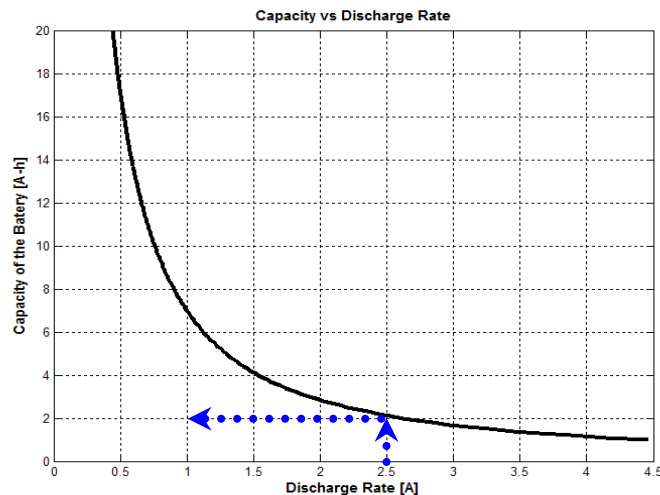


Figure 3.19 Battery duration under load

It is seen from the graph that discharge rate of 2.5 A the batteries can hold up to 2 hours. This prediction is consistent with our tests results. The battery is chosen based on availability and price. It is needless to say that better (more expensive) batteries will perform better, yet, even these batteries provided enough energy to carry out several experiments with a single charge.

This chapter presented the details of the design procedure that was carried out prior to the manufacturing of the robot base. All of the essential parts of the robot base are introduced, and critical calculations used in determining the dimensions of these parts are presented. As a result, this chapter provides the design steps towards manufacturing a configurable robot base that can be driven both by wheels and tracks. Next chapter will present detailed analysis on the configurable structure of the robot.

CHAPTER IV

CONFIGURATIONS OF THE DESIGNED ROBOT BASE

Generally, robots designed for rough terrain are not very successful on smooth surfaces, and it is also true that robots designed for indoors are doomed to fail outdoors. This thesis attempts to design and manufacture a configurable robot base that is capable of handling mixed terrains. This is done by combining wheels and tracks on a single robot through which, smooth surfaces are traversed mainly on wheels, whereas tracks provide the extra support necessary when the surface becomes uneven. The configurable nature of this design also allows the user to choose either the wheels or the tracks, and only keep it on the robot by uninstalling the other. Especially, if the robot will be used in an environment in which the surface conditions are not going to change, this will improve the usability of the proposed robot design.

In this chapter, alternative robot base configurations will be discussed. As mentioned in the previous chapters, robot base is designed to be used in three different configurations: with track, wheel (Figure 4.1) and track + wheel (Figure 4.2). In the design stage, the related parts are designed in order to realize these configurations. If both tracks and wheels will be used, tracks are connected to the robot body first, then the wheels are connected to the tracks. Two shafts that easily interlock with each other are used for this purpose. The time to convert the robot base from the wheeled + tracked to the tracked and from tracked to wheeled takes a short time (a few minutes). The system is specifically designed to fulfill this since switching between configurations might be necessary in the field, and proposed design is ready to

handle it. Note that all the materials used can be seen from the Table 4.1. Kinematic and dynamic analysis of the robot base can also be seen in Appendix A.

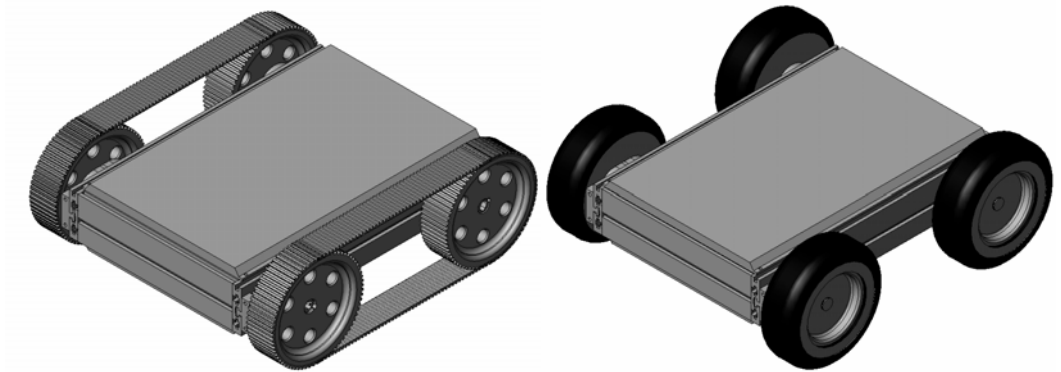


Figure 4.1 Two different configurations of the robot base with tracks and wheels

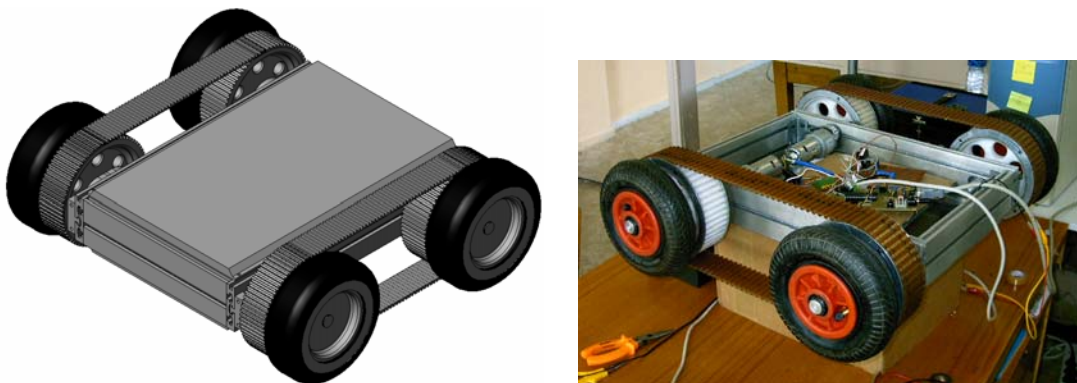


Figure 4.2 Wheeled & Tracked robot base (solid model and manufactured robot)

Throughout this chapter, performance of different robot configurations while moving up hill and moving along an inclined surface will be discussed. The required models for these configurations are given in detail and their performance with increasing slope angles is evaluated, results are presented in terms of plots. Secondly, tracked robot base configuration will be modeled and it will be detailed. For all the configurations, different conditions will be tested such as turning and climbing capabilities, tip over angle, etc.

Table 4.1 Material List

Part Name	Material	Weight (gr)	Tracked & Wheeled	Wheeled	Tracked
Profile Right	Aluminum	1080	1080	1080	1080
Profile Left	Aluminum	1080	1080	1080	1080
Profile Front	Aluminum	660	660	660	660
Profile Back	Aluminum	660	660	660	660
Top Shield	Aluminum	250	250	250	250
Bottom Shield	Aluminum	250	250	250	250
Pallet Shaft	Aluminum	60	240	0	240
Wheel Shaft	Aluminum	120	480	480	0
Bearing	Steel	100	400	400	400
Bearing Hub	Aluminum	100	400	100	400
Bolts	Steel	100	100	100	100
Movable Beam	Aluminum	300	900	900	900
Profile Holder	Steel	50	200	200	200
Movable Beam Holder	Steel	30	180	180	180
Track Stretcher	Aluminum	40	80	0	80
Palette	Rubber	320	640	0	640
Wheel	Rubber	600	2400	2400	0
Key for Wheel	Aluminum	10	40	40	0
Key for Palette	Aluminum	13	52	0	52
Pulley for Palette	Polyamide	900	3600	0	3600
Pulley M. Belt	Aluminum	40	80	80	80
Pulley Motor	Aluminum	40	80	80	80
Motor	Aluminum	510	1020	1020	1020
Motor Housing	Aluminum	80	160	80	80
Battery		1000	1000	1000	1000
Cables	Plastic	50	50	50	50
		Total (gr)	16082	11090	13082

The last topic investigated in this chapter is on the robot's obstacle handling capability. The required speed for the robot to go over obstacles of different heights is investigated. This is modeled for two cases. In the first case the obstacle only contacts with one side of the robot, or in other terms, only wheels on one side of the robot touch the obstacle. In the second case, the whole robot is expected to go over the obstacle.

4.1 Robot Base Driving Up Hill

Robot base is designed so that it can move on mixed terrain and on mixed terrain driving up hill is unavoidable. To investigate the climbing performance of this robot a robot model is formed as shown in figure 4.3. In this set it is assumed that, palletes and wheels always contact with the ground. Equations required are as follows.

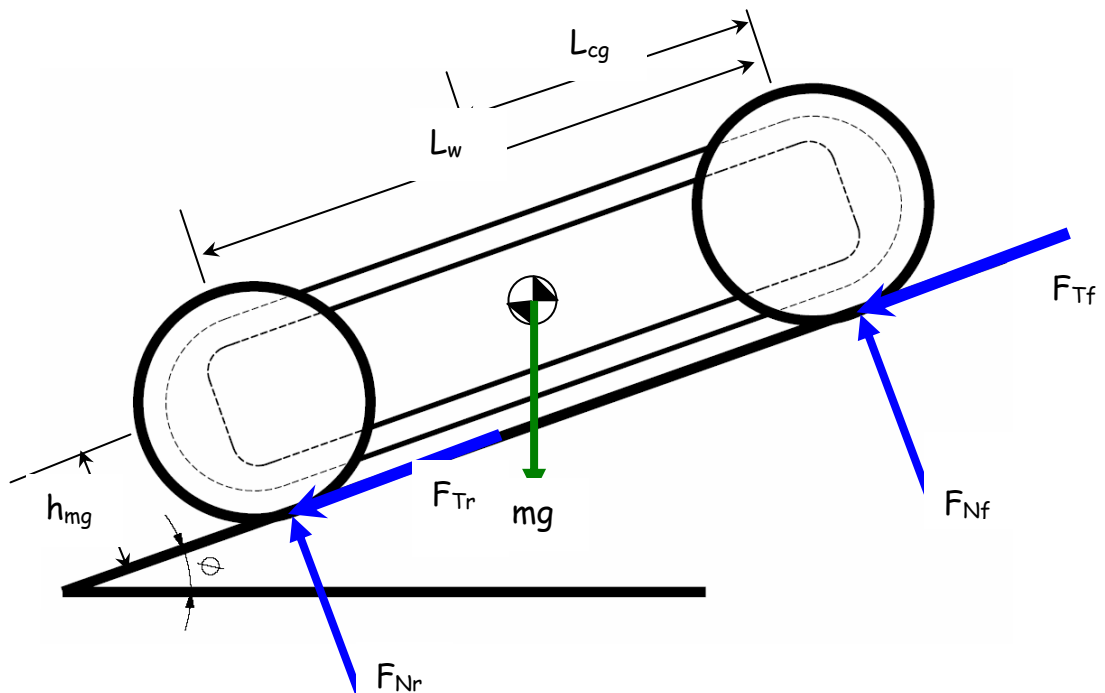


Figure 4.3 Robot base driving slope up

The design equations are:

$$\sum F_x = \mu_w \gamma_r F_{Nr} + \mu_w \gamma_f F_{Nf} - mg \sin \theta \quad (4.1)$$

$$\sum F_y = F_{Nr} + F_{Nf} - mg \cos \theta \quad (4.2)$$

$$\sum M = F_{Nr} L_w - mg(L_{cg} \cos \theta + h \sin \theta) \quad (4.3)$$

Normal forces (Figure 4.3) between ground and the contact points can be obtained as follows:

$$F_{Nr} = \frac{mg(L_{cg} \cos \theta + h \sin \theta)}{L_w} \quad (4.4)$$

$$F_{Nf} = \frac{mg((L_w - L_{cg}) \cos \theta - h \sin \theta)}{L_w} \quad (4.5)$$

where

D_{rw} Rear wheel diameter (mm)

D_{fw} Front wheel diameter (mm)

L_w Distance center of front wheel to center of gravity (mm)

h Height of center of mass about plane (mm)

θ Slope angle (degree)

m Robot mass (kg)

N Robot weight (N)

g_{rw} Maximum drive torque applied to both rear wheels (N-mm)

g_{fw} Maximum drive torque applied to both front wheels (N-mm)

μ Coefficient of friction

F_{Nr} Normal force between both rear wheels and ground (N)

F_{Nf} Normal force between both front wheels and ground (N)

F_{Tr} Total tractive force generated by both rear wheels (N)

F_{Tf} Total tractive force generated by both front wheels (N)

F_{Tm} Total tractive effort of the robot (N)

F_g Force from gravity acting along the slope(N)

$$\left. \begin{array}{l} \gamma_f = 1 \\ \gamma_r = 0 \end{array} \right\} \text{For FWD (Front Wheel Drive)}$$

$$\left. \begin{array}{l} \gamma_f = 0 \\ \gamma_r = 1 \end{array} \right\} \text{For RWD (Rear Wheel Drive)}$$

$$\left. \begin{array}{l} \gamma_f = 1 \\ \gamma_r = 1 \end{array} \right\} \text{For AWD (All Wheel Drive)}$$

While robot base is simulated using the equations given above, tracked and tracked & wheeled robot bases provide an AWD robot whereas wheeled robot base can be considered as FWD or RWD depending on the way it is driven. Normal forces between ground and the contact points for these configurations are illustrated in Figure 4.4. These plots tell us that while slope angle is continuously changed, normal forces at the front decrease and tip over case occurs when the normal force becomes zero. That means contact between wheel and ground disappears, however, this is more of a theoretical observation than a practical one, since before tipping over, the robot will slide on this surface.

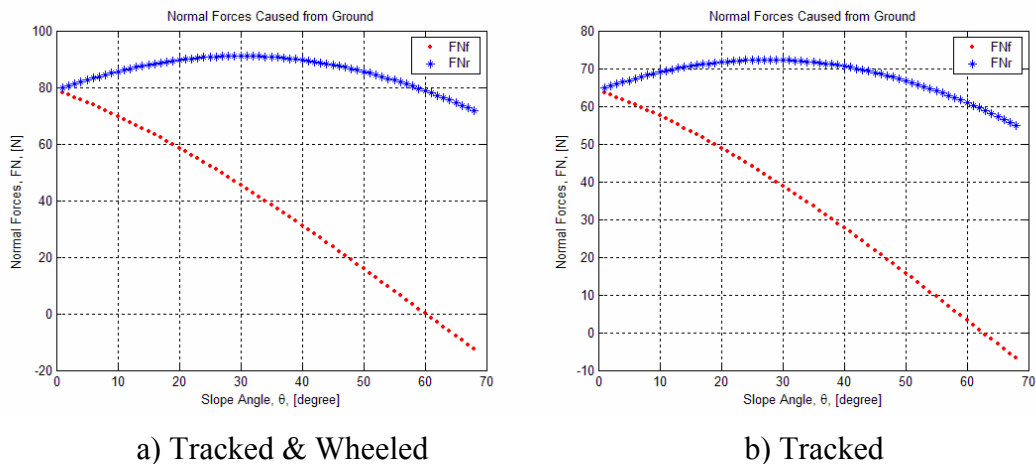
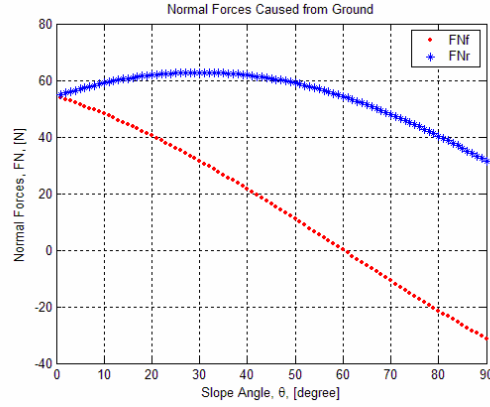


Figure 4.4 Normal force caused from ground



c) Wheeled

Figure 4.4 (continued) Normal force caused from ground

A range of coefficient of friction for robot base configurations can be obtained from:

$$\mu \geq \frac{L_w \sin \theta}{(\gamma_r - \gamma_f)(h \sin \theta + L_{cg} \cos \theta) + \gamma_f L_w \cos \theta} \quad (4.6)$$

Wheeled & tracked robot base that we designed is assumed as all wheel drive. The advantage of all wheel drive can also be seen by comparing the coefficient of friction values for front, rear and all wheel drive types as seen in Figure 4.5. The plot shows that the required minimum coefficient of friction for the robot to remain on an inclined surface without slippage.

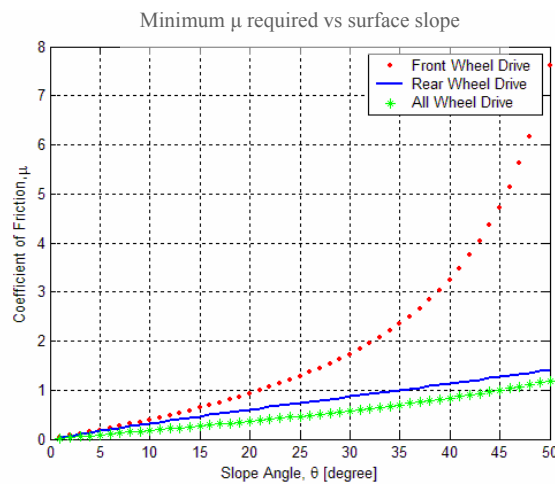


Figure 4.5 Minimum coefficient of friction required for the robot not to slip on inclined surfaces

The critical slope angle that causes tipping over condition for the robot base is:

$$\theta = \tan^{-1}\left(\frac{L_w - L_{cg}}{h}\right) \quad (4.7)$$

Plot of normal force between ground and the contact points is seen in Figure 4.6. When slope angle is nearly 60 degrees, normal force between rear and ground becomes zero. That means contact between wheel and ground disappears. After this point, robot base tips over.

Maximum front and rear wheel tractive forces from drive torque are:

$$F_{r_{w_{\max}}} = \frac{2\gamma_r g_{rw}}{D_{rw}} \quad (4.8)$$

$$F_{f_{w_{\max}}} = \frac{2\gamma_f g_{fw}}{D_{fw}} \quad (4.9)$$

where

$F_{r_{w_{\max}}}$ Maximum rear wheel tractive force from drive torque (N)

$F_{f_{w_{\max}}}$ Maximum front wheel tractive force from drive torque (N)

Maximum front and rear wheel tractive forces before slip are:

$$F_{r_{w_{\mu_{\max}}}} = \gamma_r \mu F_{Nr} \quad (4.10)$$

$$F_{f_{w_{\mu_{\max}}}} = \gamma_f \mu F_{Nf} \quad (4.11)$$

where

$F_{r_{w_{\mu_{\max}}}}$ Maximum rear wheel tractive force before slip (N)

$F_{f_{w_{\mu_{\max}}}}$ Maximum front wheel tractive force before slip (N)

Total tractive force generated by both rear wheels is in a range and this range is expressed in Equations 4.12 and 4.13.

$$F_{Tr} = F_{rW_{\mu \max}} \quad \mathbf{if} \quad F_{rW_{\mu \max}} < F_{rW_{\max}} \quad (4.12)$$

$$F_{Tr} = F_{rW_{\max}} \quad \mathbf{if} \quad F_{rW_{\mu \max}} > F_{rW_{\max}} \quad (4.13)$$

And also total tractive force generated by both front wheels is:

$$F_{Tf} = F_{fW_{\mu \max}} \quad \mathbf{if} \quad F_{fW_{\mu \max}} < F_{fW_{\max}} \quad (4.14)$$

$$F_{Tf} = F_{fW_{\max}} \quad \mathbf{if} \quad F_{fW_{\mu \max}} > F_{fW_{\max}} \quad (4.15)$$

Total tractive effort of the robot is:

$$F_{Tm} = F_{Tr} + F_{Tf} \quad (4.16)$$

And force from gravity acting along the incline is:

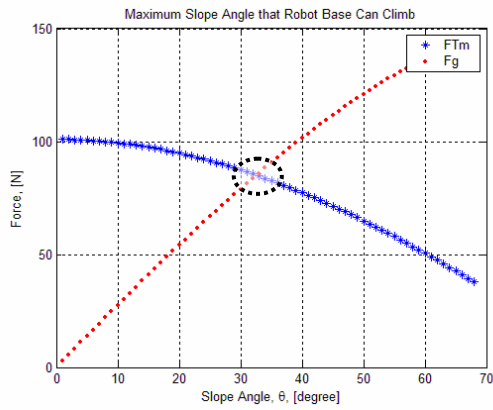
$$F_g = mg \sin \theta \quad (4.17)$$

After these calculations, the case of whether the robot base can climb up a slope or not can be determined as:

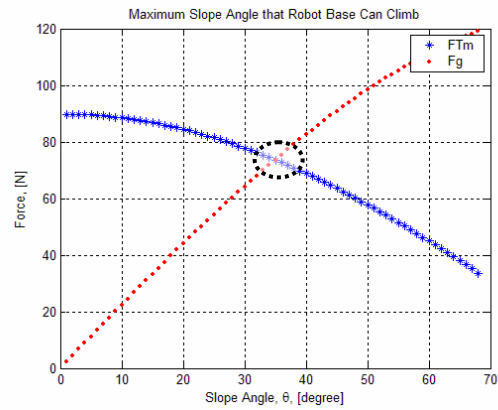
$$\text{Robot can climb up the slope if } F_{Tm} > F_g \quad (4.18)$$

$$\text{Robot cannot climb up the slope if } F_{Tm} < F_g \quad (4.19)$$

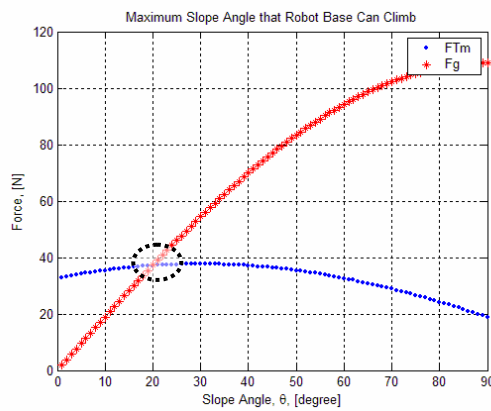
The condition whether the robot base can climb a slope up or not can also be determined from the Figure 4.6. The dashed circle indicates the intersection point of two curves which represent total tractive effort and force from gravity along the slope. This intersection point gives the maximum slope angle that the robot base can climb.



a) Tracked & Wheeled



b) Tracked



c) Wheeled

Figure 4.6 Maximum slope angle that robot base can climb

4.2 Robot Base Moving Along an Incline Surface

Another condition for robot base is the motion along an inclined surface (Figure 4.7). For such a configuration, a basic model is derived as follows. Note that superscript “s” denotes the incline surface and distinguish these equations from the one for hill climbing.

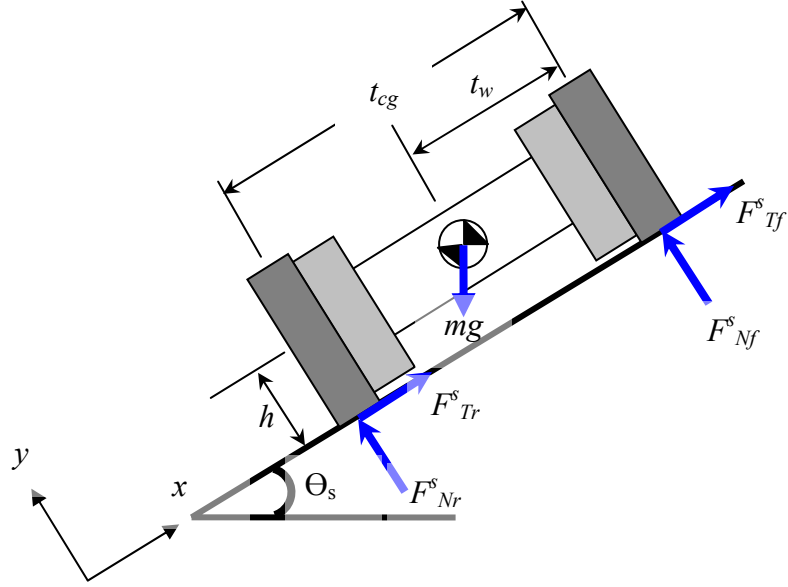


Figure 4.7 Robot base moving along an incline surface

The equations for the modeling are:

$$\sum F_x^s = \mu\gamma_r F^s_{Nr} + \mu\gamma_f F^s_{Nf} - mg \sin \theta_s \quad (4.20)$$

$$\sum F_y^s = F^s_{Nr} + F^s_{Nf} - mg \cos \theta_s \quad (4.21)$$

$$\sum M^s = F^s_{Nr} t_w - mg(t_{cg} \cos \theta_s + h \sin \theta_s) \quad (4.22)$$

Normal force between ground and the contact points can be obtained as follows:

$$F^s_{Nr} = \frac{mg(t_{cg} \cos \theta_s + h \sin \theta_s)}{t_w} \quad (4.23)$$

$$F^s_{Nf} = \frac{mg((t_w - t_{cg}) \cos \theta_s - h \sin \theta_s)}{t_w} \quad (4.24)$$

Plot of the normal forces is given in Figure 4.8.

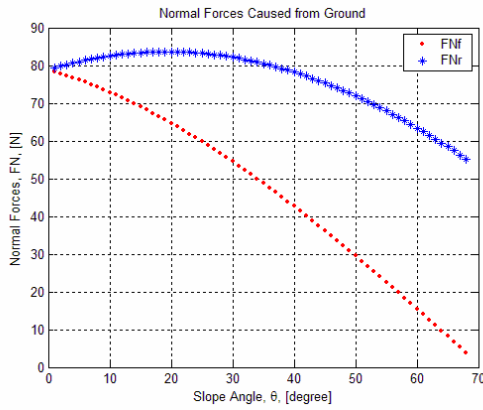
The critical slope angle when the robot base moves along an incline surface is:

$$\theta_s = \tan^{-1} \left(\frac{t_w - t_{cg}}{h} \right) \quad (4.25)$$

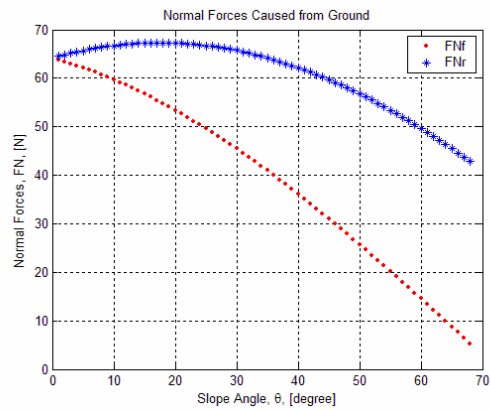
Maximum front and rear wheel tractive forces from drive torque are:

$$F^s_{rw_{\max}} = \frac{2\gamma_r g_{rw}}{D_{rw}} \quad (4.26)$$

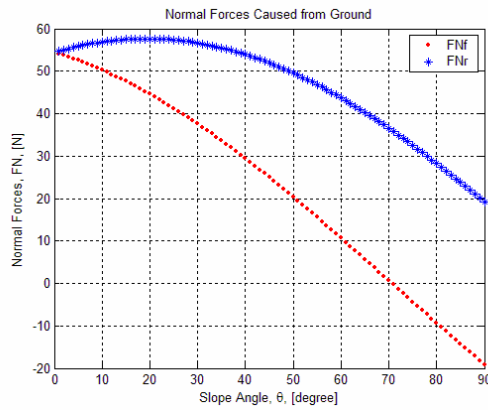
$$F^s_{fw_{\max}} = \frac{2\gamma_f g_{fw}}{D_{fw}} \quad (4.27)$$



a) Tracked & Wheeled



b) Tracked



c) Wheeled

Figure 4.8 Normal Forces caused from ground

Maximum front and rear wheel tractive forces before slip are:

$$F^s_{rw_{\mu_{\max}}} = \gamma_r \mu F^s_{Nr} \quad (4.28)$$

$$F^s_{fw_{\mu_{\max}}} = \gamma_f \mu F^s_{Nf} \quad (4.29)$$

The range of total tractive force generated by both rear is:

$$F^s_{Tr} = F^s_{rW_{\mu \max}} \quad \mathbf{if} \quad F^s_{rW_{\mu \max}} < F^s_{rW_{\max}} \quad (4.30)$$

$$F^s_{Tr} = F^s_{rW_{\max}} \quad \mathbf{if} \quad F^s_{rW_{\mu \max}} > F^s_{rW_{\max}} \quad (4.31)$$

Total tractive force generated by both front wheels are:

$$F^s_{Tf} = F^s_{fW_{\mu \max}} \quad \mathbf{if} \quad F^s_{fW_{\mu \max}} < F^s_{fW_{\max}} \quad (4.32)$$

$$F^s_{Tf} = F^s_{fW_{\max}} \quad \mathbf{if} \quad F^s_{fW_{\mu \max}} > F^s_{fW_{\max}} \quad (4.33)$$

Total tractive effort of the robot is:

$$F^s_{Tm} = F^s_{Tr} + F^s_{Tf} \quad (4.34)$$

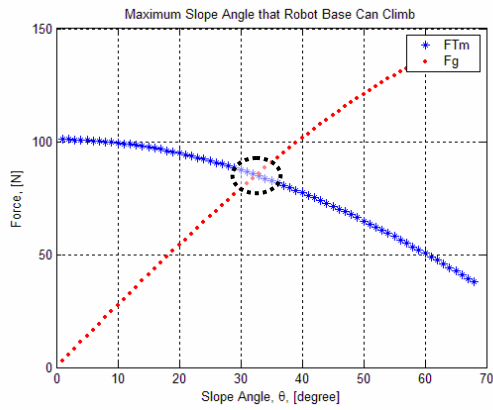
And force from gravity acting along the incline is:

$$F^s_g = mg \sin \theta_s \quad (4.35)$$

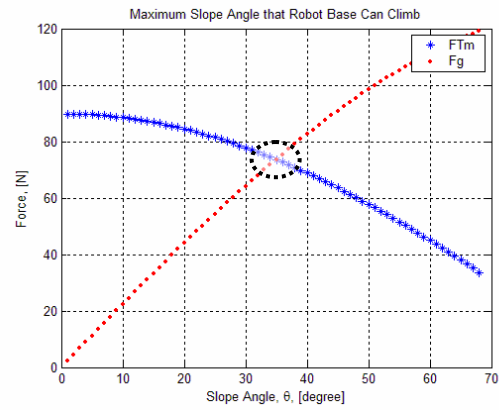
Whether robot base can climb up a slope or not can be determined as:

$$\text{Robot can climb the slope if } F^s_{Tm} > F^s_g \text{ as seen in Figure 4.9.} \quad (4.36)$$

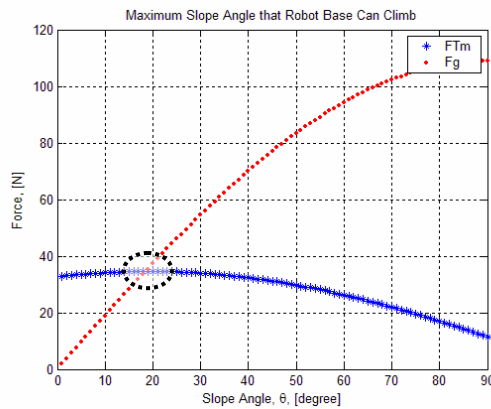
$$\text{Robot cannot climb the slope if } F^s_{Tm} < F^s_g \quad (4.37)$$



a) Tracked & Wheeled



b) Tracked



c) Wheeled

Figure 4.9 Maximum Slope Angle that robot base can climb

All these equations and their implications cannot be visualized very easily. In order to see the results more effectively, an active MS Excel worksheet is constructed. The values in this table can be set as desired and the results are displayed at the output part of this worksheet.

After completing the modeling and simulation of three robot base configurations, a comparison can be made between these three types. It is actually expected that the best slope climber should be tracked robot base; the worst should be wheeled robot. Table 4.3 shows that these expectations are not invalid.

Table 4.2 User Interface for the robot base climbing slope

INPUTS	
Rear wheel diameter (mm)	200
Front wheel diameter (mm)	200
Distance between wheels (mm)	347
Distance center of front wheel to center of gravity (mm)	173,5
Height of center of mass about plane (mm)	100
Slope angle (deg)	34,00
Robot base mass (kg)	16,08
Maximum drive torque applied to both rear wheels (N-mm)	10000
Maximum drive torque applied to both front wheels (N-mm)	10000
Coefficient of friction, mu	0,5
γ_r	1
γ_f	1
OUTPUTS	
Can the robot base climb up the slope?	YES
Tip-over angle (deg, rad)	60,0
Required minimum friction coefficients:	
Front wheel drive only required coefficient of friction	1,28
Rear wheel drive only required coefficient of friction	0,74
All wheel drive required coefficient of friction	0,47

Table 4.3 Comparison of three robot base configurations

	Tip Over Angle	
	Slope Up	Slope Side
Wheeled	60,0422°	70,6652°
Tracked	60,0422°	70,6652°
Wheeled & Tracked	62,5828°	72,4744°

	Slope Angle that Robot can Climb	
	Slope Up	Slope Side
Wheeled	20°	20°
Tracked	35°	35°
Wheeled & Tracked	31°	31°

4.7 Turning Capability of the Robot Base

The handling characteristics of the wheeled & tracked robot base have certain unique features and are quite different from those of wheeled one. In differential steering, the thrust of one pallet is increased and that of the other is reduced so as to create a turning moment to overcome the moment of turning resistance due to the skidding of the pallets on the ground, as shown in Fig. 4.10. Since the moment of turning resistance is usually considerable, significantly more power may be required during a turn than in a straight line motion. Furthermore, braking of the inside pallet is often required in making a turn. [Wong, 1993]

The turning behavior of the robot base depends on the thrusts of the outside and inside tracks F_o and F_i , the resultant resistant force R_{tot} , the moment turning resistance M_r exerted on the track by the ground. Our robot base works at low speed so the centrifugal force may be neglected, and the behavior of the base can be described by the following two equations of motion:

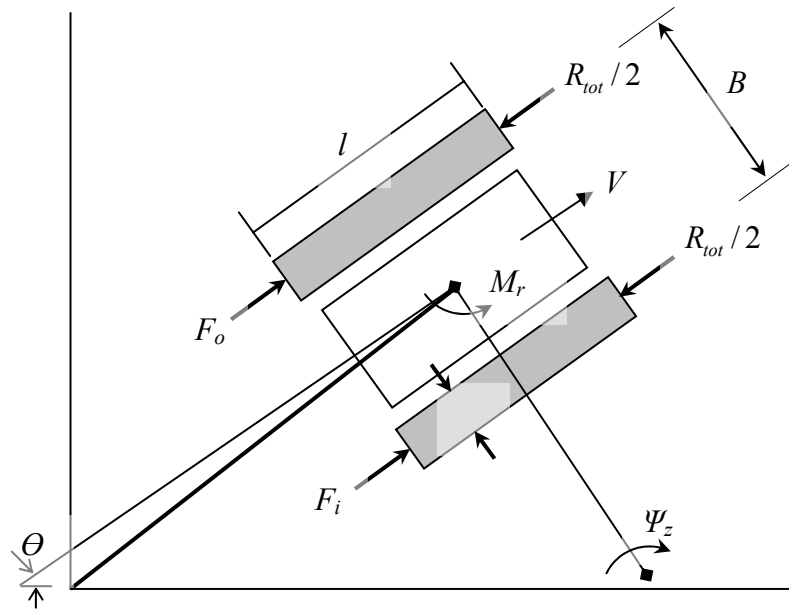


Figure 4.10 Robot base turning [Bekker, 1956 and Nuttall, 1964]

$$m \frac{d^2 s}{dt^2} = F_o + F_i - R_{tot} \quad (4.38)$$

$$I_z \frac{d^2\theta}{dt^2} = \frac{B}{2}(F_o - F_i) - M_r \quad (4.39)$$

where s is the displacement of the center of gravity of the robot base, θ is the angular displacement of the robot base, B is the tread of the robot (the spacing between the centerlines of the two tracks, note that it can be assumed that the wheel and the palette act as one body), and I_z and m are the mass moment of inertia of the robot base about the vertical axis passing through its center of gravity and the mass of the robot base, respectively. The above two differential equations can be integrated and the trajectory of the center of gravity and the orientation of the robot base can be determined as discussed by Bekker [Bekker, 1956].

Under steady state conditions, there are no linear and angular accelerations as mentioned below:

$$F_o + F_i - R_{tot} = 0 \quad (4.40)$$

$$\frac{B}{2}(F_o - F_i) - M_r = 0 \quad (4.41)$$

The thrusts of the outside and inside tracks required to achieve a steady-state turn are therefore expressed by:

$$F_o = \frac{R_{tot}}{2} + \frac{M_r}{B} = \frac{f_r W}{2} + \frac{M_r}{B} \quad (4.42)$$

$$F_i = \frac{R_{tot}}{2} - \frac{M_r}{B} = \frac{f_r W}{2} - \frac{M_r}{B} \quad (4.43)$$

where f_r is the coefficient of motion resistance of the robot base in the longitudinal direction which will be mentioned soon and W is the robot base weight.

To determine the values of the thrusts, F_o and F_i , the moment of turning resistance M_r must be known. This can be determined experimentally or analytically.

If the normal pressure is uniformly distributed along the track, the lateral resistance per unit length of the track, R_l , can be expressed by:

$$R_l = \frac{\mu_l W}{2l} \quad (4.44)$$

where μ_l is the coefficient of lateral resistance and l is the contact length of the track. The value of μ_l depends not only on the terrain, but also on the design of the track. Table 4.4 provides guidelines for properly selecting μ_l .

Table 4.4. Coefficient of Lateral Resistance, μ_l [Hayashi, 1975 and Wong, 1993]

Track Material	Concrete	Hard Ground	Grass
Steel	0,5-0,51	0,55-0,58	0,87-1,11
Rubber	0,9-0,91	0,65-0,66	0,67-1,14

Accordingly, Equations 4.42 and 4.43 can be rewritten in the following forms:

$$F_o = \frac{f_r W}{2} + \frac{\mu_l W l}{4B} \quad (4.45)$$

$$F_i = \frac{f_r W}{2} - \frac{\mu_l W l}{4B} \quad (4.46)$$

The motion resistance of a track is developed by Bekker [Bekker, 1969]. This is based on Bekker's pressure-sinkage relationship and can be given with the following equation:

$$R_{tot} = Wf_r = \left[\frac{1}{(n+1)b^{1/n} \left(\frac{k_c}{b} + k_\phi\right)^{1/n}} \right] \left[\frac{W}{l} \right]^{\frac{n+1}{n}} \quad (4.47)$$

where b and l are width and length of the track, respectively and n , k_c , k_ϕ are pressure-sinkage parameters [Wong, 1993, pp. 118]

The sinkage of a track can be obtained as well as the motion resistance of a track. This has also been developed by Bekker [Bekker, 1969]. By using the pressure-sinkage equation proposed by Bekker, the sinkage for a track with uniform contact pressure can be given by:

$$z_o = \left[\frac{p}{k_c/b + k_\phi} \right]^{\frac{1}{n}} = \left[\frac{\frac{W}{bl}}{k_c/b + k_\phi} \right]^{\frac{1}{n}} \quad (4.48)$$

where p is the average normal pressure on the track and it is equal to $\frac{W}{2A}$. A is the contact area of the track [Wong, 1993 and 1998].

Equations 4.42 and 4.43 are of fundamental importance, and they lead to conclusions of practical significance regarding the steerability of the robot base. For the outside track:

$$F_o \leq cbl + \frac{W \tan \phi}{2} \quad (4.49)$$

where b is the track width and c and ϕ are the cohesion and angle of internal shearing resistance of the terrain, respectively. By rearranging the equations, we obtain the equation below:

$$\frac{l}{B} \leq \frac{1}{\mu_t} \left[\frac{4cA}{W} + 2 \tan \phi - 2f_r \right], \quad (4.50)$$

where A is the contact area of one track. This indicates that, to enable robot base to steer without spinning the outside track, the ratio of the track length to tread of the robot base, l/B , must satisfy the following condition.

$$\frac{l}{B} \leq \frac{2}{\mu_t} \left[\frac{c}{p} + 2 \tan \phi - f_r \right] \quad (4.51)$$

In the Table 4.5, different terrain values and in terms of these values some calculations are given. Z_0 sinkage values, f_r motion resistance, $F_o - F_i$, required inside and outside forces during the turn (in kN) and lastly l/b values are calculated and these results are compared with the real ones.

Note that real l/b value is $\frac{l}{b} = \frac{347}{570} = 0,60877$. This value should be lower than the l/b values which are calculated from the different terrain parameters.

After observing Table 4.5, it can be said that, all the l/b values which are calculated by different terrain parameters are bigger than the real values, so our designed robot base will be able to turn around itself on all kinds of terrain that are specified.

Table 4.5 Robot base turning capability on different soil characteristics.

	Dry Sand	Sandy Loam	Clayey Soil	Heavy Clay	Lean Clay	Clayey Loam	Snow
Moisture (%)	0	15	38	25	22	46	0
n	1,1	0,7	0,5	0,13	0,2	0,73	1,44
k_c (kN/mⁿ⁺¹)	0,95	5,27	13,19	12,7	16,43	41,6	10,55
k_{fi} (kN/mⁿ⁺²)	1528,43	1515,04	692,15	1555,95	1724,69	2471	66,08
c (kPa)	1,04	1,72	4,14	68,95	68,95	6,1	6
fi (deg)	28	29	13	34	20	26,6	20,7
B (m)	0,57	0,57	0,57	0,57	0,57	0,57	0,57
L (m)	0,347	0,347	0,347	0,347	0,347	0,347	0,347
g (m/s²)	9,81	9,81	9,81	9,81	9,81	9,81	9,81
m (kg)	16	16	16	16	16	16	16
W(kN)	0,1569	0,156	0,156	0,156	0,156	0,156	0,156
Z₀ (m)	0,001	2,03E-05	1,23E-06	4,64E-26	1,89E-17	1,57E-05	0,039
f_r	0,001	0,001	0,001	0,001	0,001	0,001	0,001
F_o (kN)	0,015	0,039	0,063	0,087	0,111	0,135	0,158
Fi (kN)	-0,015	-0,039	-0,063	-0,087	-0,110	-0,134	-0,158
P (kPa)	1,361	1,361	1,361	1,361	1,361	1,361	1,361
$\frac{L}{B}$	5,617	2,873	2,642	28,485	22,092	1,939	1,552

4.4 Obstacle Handling

Robot base is designed to be able to move on uneven terrain which means that it will have to move around obstacles. It should easily go over the obstacles, steps etc. This necessitates the use of strong motors at the first place. To analyze obstacle handling capabilities of this robot base two cases are considered. First case is when robot base tries to go over the obstacle and the obstacle is under one side of the robot (marked as one side contact). In the second case, the whole robot is driven towards the obstacle (marked as two side contact).

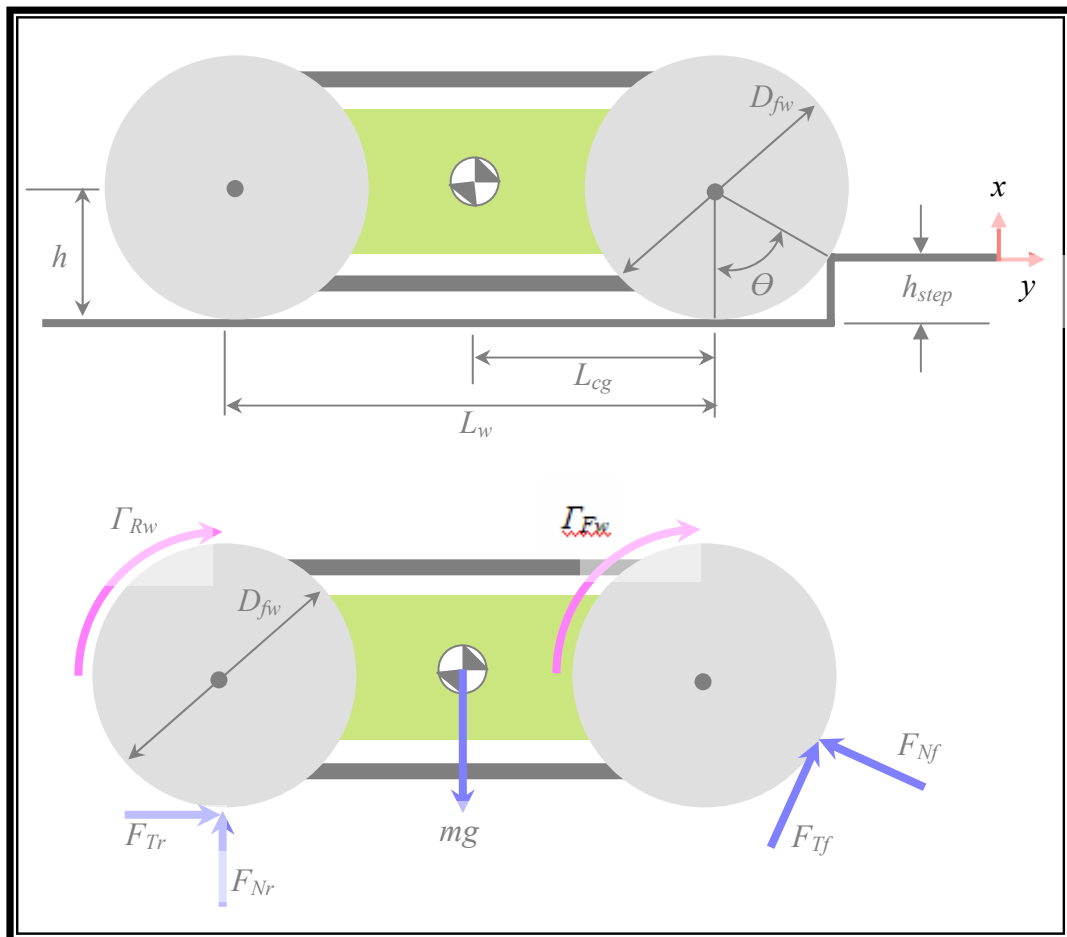


Figure 4.11 Robot Base contacts with the obstacle from outside

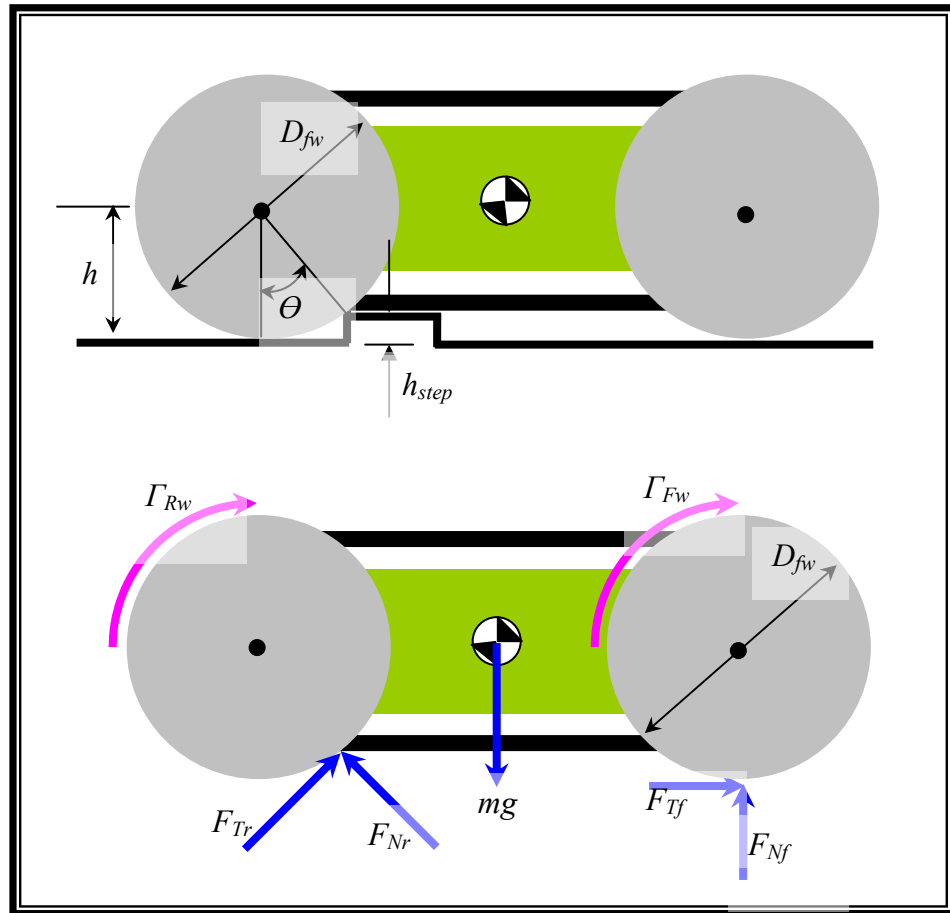


Figure 4.12 Robot Base contacts with the obstacle from inside

Robot base may contact with the obstacle from outside (Figure 4.11) or inside (Figure 4.12).

Table 4.6 shows the required equations which are needed for analyzing the driving over a step condition. Here the details about the equations are not given

Table 4.6 Equations for driving step over for the robot base

	Two Side Contact	One Side Contacts
F_{Nr}	$\frac{2mgA}{L_w + (D_{fw}/2)S}$	$\frac{2mgA}{L_w + (D_{fw}/2)S}$
F_{Nf}	$\frac{2mgB}{(L_w + (D_{fw}/2)S)(C + \mu_{\min_2}\gamma_f S)}$	$\frac{2mgB}{(L_w + (D_{fw}/2)S)(C + \mu_{\min_1}\gamma_f S)}$
μ_{\min}	μ_{2w}	μ_{1w}
$F_{rw_{\max}}$	$\frac{g_{rw}}{\gamma_r D_{rw}/2}$	$\frac{g_{rw}}{\gamma_r D_{rw}/2}$
$F_{fw_{\max}}$	$\frac{g_{fw}}{\gamma_f D_{fw}/2}$	$\frac{g_{fw}}{\gamma_f D_{fw}/2}$
g_m	$F_{rw_{\max}} + F_{fw_{\max}}$	$F_{rw_{\max}} + F_{fw_{\max}}$
$F_{rw_{\mu_{\max}}}$	$2\gamma_r \mu_{rw} F_{Nr}$	$2\gamma_r \mu_{rw} F_{Nr}$
$F_{fw_{\mu_{\max}}}$	$2\gamma_f \mu_{fw} F_{Nf}$	$2\gamma_f \mu_{fw} F_{Nf}$
g_{mu}	$F_{rw_{\mu_{\max}}} + F_{fw_{\mu_{\max}}}$	$F_{rw_{\mu_{\max}}} + F_{fw_{\mu_{\max}}}$
F_{Tr}	$2\mu_{\min_2} F_{Nr}$	$2\mu_{\min_1} F_{Nr}$
F_{Tf}	$2\mu_{\min_2} F_{Nf}$	$2\mu_{\min_1} F_{Nf}$
g_{\min}	$F_{Tr} + F_{Tf}$	$F_{Tr} + F_{Tf}$

After modeling the stepping over a step condition for the robot base, it can be determined whether the robot base can go over the obstacle (step) or not. If the following condition is satisfied, the robot can climb over the specified obstacle, else it cannot.

$$(F_{Tr} \leq F_{rw_{\max}}) * AND (F_{Tr} \leq F_{rw_{\mu_{\max}}}) * AND (F_{Tf} \leq F_{fw_{\max}}) * AND (F_{Tf} \leq F_{fw_{\mu_{\max}}}) \dots (4.52)$$

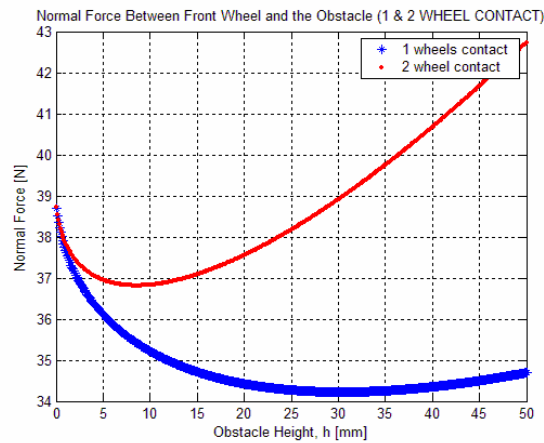


Figure 4.13 Normal Forces Between the front wheel(s) and the obstacle

In Figure 4.13, the normal forces are seen when the robot base contacts with an obstacle. In this figure, forces are given for one side and two side contact, separately.

Figure 4.14 depicts the total tractive effort that is required when robot base crosses over an obstacle. It is understood that robot base can cross over the obstacle with one side contact more easily since it requires less power in this case.

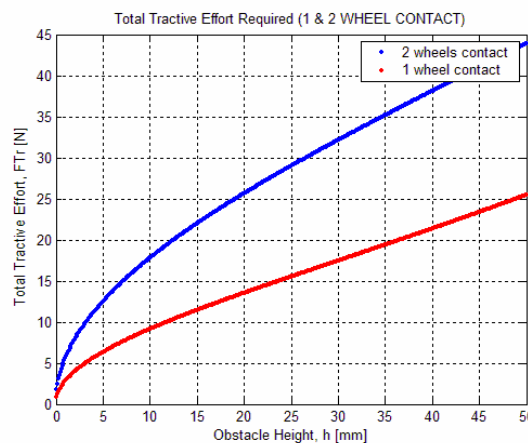


Figure 4.14 Total tractive effort required to cross over the obstacle

In this chapter, designed robot base configurations are discussed. For wheeled, tracked and wheeled + tracked robot base configurations required models are constructed. Simulations are carried out based on these models for all three of the configurations to test the obstacle handling and turning capabilities of the robot.

CHAPTER V

RESULTS AND DISCUSSIONS

These tests aims to observe the performance of the robot while climbing up and moving along an inclined surface, to determine tipping over conditions, capabilities of crossing over an obstacle and power consumption. Also the results are going to be compared with the military specifications given in Appendix E.

The first results were related to the slope performance. Robot base was tested on terrain between A, B and C Buildings of the ME Department. The slope of the inclined surface has been continuously changed to find the critical angle. Simulations are also carried out for these cases on a similar surface. Test results are given as seen Table 5.1.

Table 5.1 Simulation and test results for the slope angle that robot base can climb

	Experimental	Simulation
Tracked	31⁰	34⁰
Wheeled	19⁰	20⁰
Tracked + Wheeled	28⁰	31⁰

Another test was related to the tipping over case. The results were very close to the analytical results. Table 5.2 shows the test and analitical results, respectively. Test

were performed on a terrain which is between the A, B and C Buildings of the Mechanical Engineering Department.

Another test is related to crossing obstacle over. These tests were performed both indoor and outdoor. Robot is driven towards obstacles of various heights and results are recorded and these results are as given in Table 5.2. And a comparison between tests and analytical results is given in Table 5.3.

Table 5.2 Test results related to crossing over an obstacle

Obstacle Height	6,4 cm	8 cm	9 cm	11 cm	13 cm
Tracked	√	√	√	√	√
Wheeled	√	√			
Tracked + Wheeled	√	√	√	√	

Table 5.3 Comparison between tests and analytical results

	Crossing Obstacle Over			
	One Wheel Contact		Two Wheel Contact	
	Analytical Results	Test Results	Analytical Results	Test Results
Wheeled	9 cm	8 cm	7 cm	6,4 cm
Tracked	18 cm	13 cm	11 cm	9 cm
Wheeled & Tracked	14 cm	11 cm	9,5 cm	7 cm

It was observed during the tests if the operation area has lots of steps and obstacles, it is not a good idea to use wheeled robot. Instead of wheeled one, tracked or tracked + wheeled one should be used in such a case. As seen in Figure 5.1, if the robot base meets such a case (obstacle is just stay between two wheels), it may not cross over

the obstacle and it gets stuck. However if the tracked or tracked + wheeled one meet such a case, it can cross over the obstacle that we have observed.

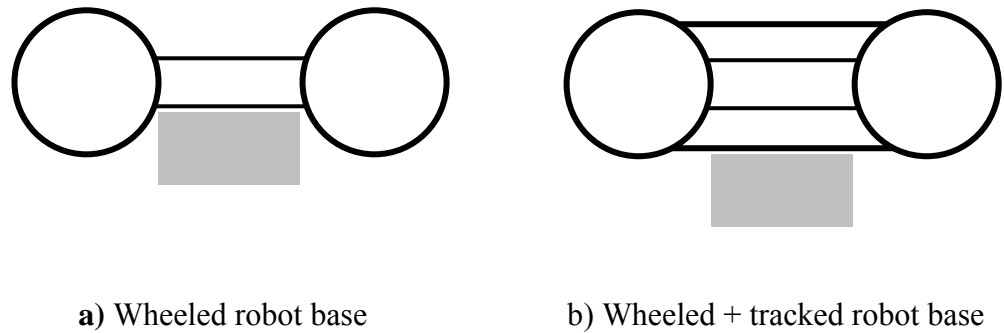


Figure 5.1 Robot base that works to cross over an obstacle

Another observation from the tests, the wheeled robot base may not achieve going step down. However tracked or tracked + wheeled robot base could achieve this task very easily (Figure 5.2).

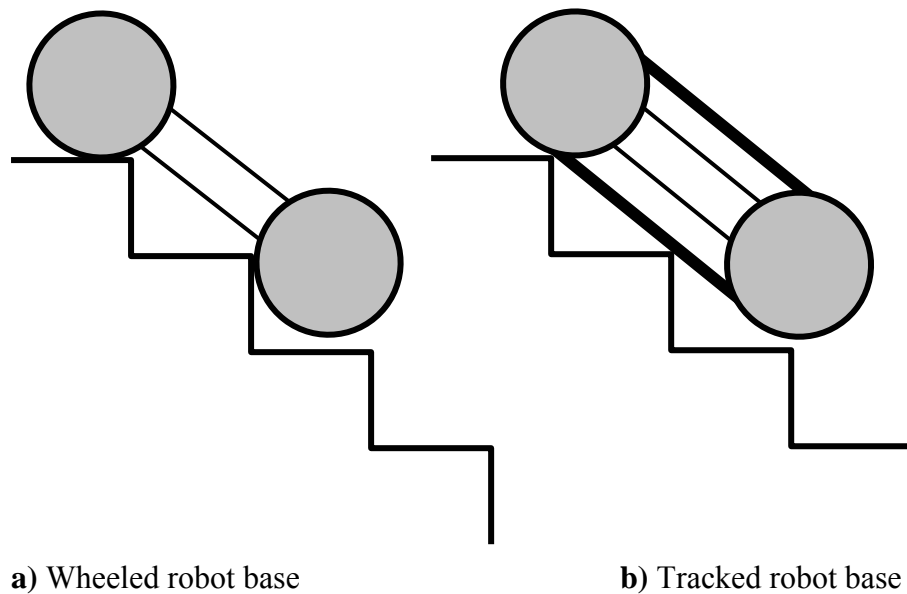


Figure 5.2 Robot base goes step down

During the test, we were aware of the condition given in Figure 5.3. As seen from the picture, wheeled robot base can not cross over the step very easily. Some times it may get stuck in such a condition. On the other hand, tracked and tracked + wheeled robot base can cross over the step very easily (Figure 5.3 and 5.4). This showed us the superiority of the tracks to the wheels.



Figure 5.3 Wheeled robot base crosses over a step



Figure 5.4 Tracked robot base crosses over a step

When robot base works on different types of terrain, power consumption is an important subject. A simulation has been constructed and the simulation results have been compared with the test results since improvement of the robot base in future will be required some predesign tools.

Power consumption data was get from indoor and outdoor environment. Table 5.4 shows the data get from indoor environment. Table 5.5 indicates the results from the

outside working environment. Indoor environment denotes the corridor of the C Block of the ME Department. Outside environment denotes the rough and smooth area between A, B and C Buildings of the ME Department.

Table 5.4 Power consumption for indoor tests

	Current At the Start (A)	Current During Motion (A)	Distance Traveled (m)	Time Traveled (s)	Power Consumption (W)
Tracked	1,65	1,1-1,3	10	16,6	26,4
Wheeled	1,15	0,9-1,1	10	12,5	21,6
Tracked + Wheeled	1,85-1,9	1,3-1,4	10	14,7	27,12

Table 5.5 Power consumption for outdoor tests

	Current At the Start (A)	Current During Motion (A)	Distance Traveled (m)	Time Traveled (s)	Power Consumption (W)
Tracked	1,8-2	1,4-2,2	10	20	33,6
Wheeled	1,3-1,4	1,1-1,5	10	14,5	26
Tracked + Wheeled	2-2,2	1,5-2,5	10	17	36

Table 5.5 and 5.6 show the power consumption obtained from the test results. These results can be compared with the simulation results. Figure 5.5 shows a simulator prepared to obtain the power consumption during travel. In this simulator, after inputs are entered, power consumption, acceleration time, total travel time and peak power can be obtained according to the distance traveled. Also while robot base

travels, a group of plots is obtained. These plots are speed, distance, torque and power versus time.

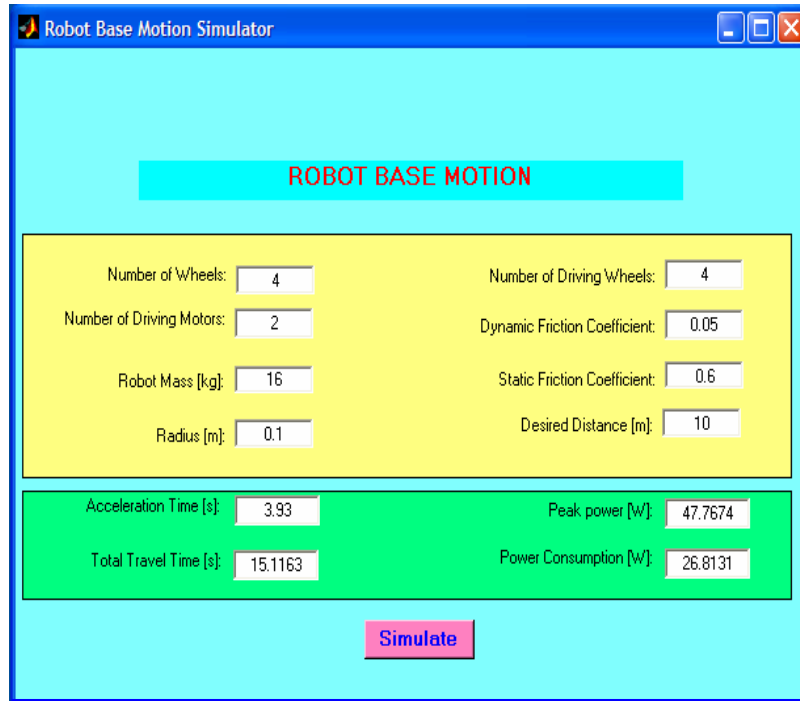


Figure 5.5 Robot Base Motion Simulator

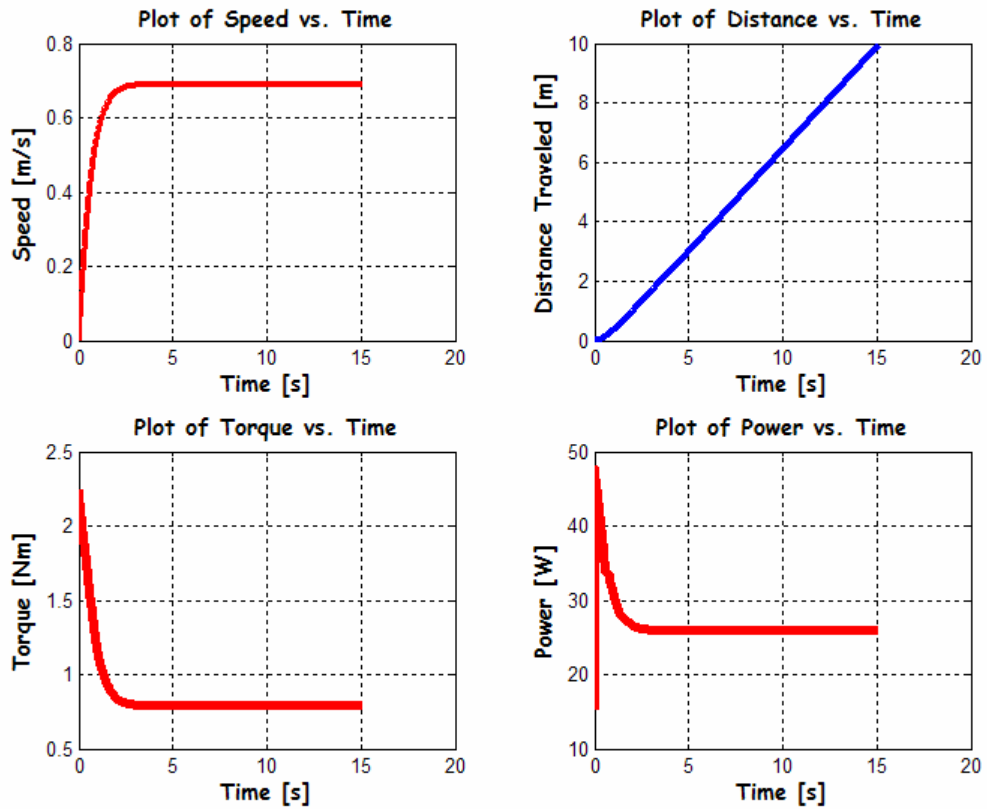


Figure 5.6 Simulation Results

The results obtained in Figure 5.6 are very close to the test results obtained in Table 5.5. Therefore we will have a chance for our future design of the robot base that we can see the results of the robot base motion just before manufacturing.

As mentioned in Chapter IV, robot base can turn a radius of curvature as well as turning around itself. This task is difficult for the wheeled one. Our observation from the test results showed that wheeled robot base was inefficient during turning. Therefore the motors draw high current from the batteries. On the other hand this task was not difficult for the tracked one. It can achieve turning around itself or a curvaure very easily. It was observed in the tests, the motors draw maximum 3,2 A current from the batteries. This current value does not damage the motors, motor controllers and the mainboard.

After completing all the tests, we were able to decide the right configuration with the right working condition. Actually, at the beginning of the design process our aim was to catch these results at the end. Table 5.6 shows the comparison between configurations and the working conditions. In this table, *3 indicates the best* and *1 indicates the worst*. It is clearly said that robot base can work on any types of terrain with its three configurations. According to the desired conditions, it can be reconfigured and used successfully. With such a configurable robot base which has not been designed and constructed yet, lots of tasks can be accomplished.

Table 5.6 Working conditions with the configurations

Working Condition	Wheeled Robot Base	Tracked Robot Base	Wheeled & Tracked Robot Base
<i>Rough Terrain (Low Speed)</i>	3	1	1
<i>Rough Terrain (High Speed)</i>	3	1	1
<i>Smooth Terrain (Low Speed)</i>	3	3	3
<i>Smooth Terrain (High Speed)</i>	3	2	2
<i>Terrain with Obstacles (Low Speed)</i>	1	3	2
<i>Terrain with Obstacles (High Speed)</i>	1	2	3
<i>Step Up</i>	1	3	2
<i>Step Down</i>	1	3	2
<i>Slope Up</i>	1	3	2
<i>Slope Down</i>	1	3	2
<i>Turning Around Itself (Low Speed)</i>	1	3	2
<i>Turning Around Itself (High Speed)</i>	1	3	2

CHAPTER VI

CONCLUSION AND FUTURE WORK

In this thesis, a modular robot base for mixed terrain applications is designed and manufactured. The robot base can be configured to be in three different configurations: wheeled, tracked and both tracked and wheeled at the same time. The modular structure of the design allows the users to switch between configurations in short time by putting on and off the proper modules. Due to this modularity at the actuation level, the robot can work on mixed terrain, in other words it can move on all types of terrain. This robot base can be used for different applications ranging from military applications to agricultural applications. At the design stage, the expected performance of the robot is validated via simulations and these simulation results are then compared to actual data collected from the manufactured robot. Simulations are run under Matlab. Tests tasks are carried out outside of the ME-C building. In these tests data on climbing up and moving along inclined surfaces, tip over, slippage and crossing over obstacles, stepping down between two surfaces are collected. Power consumption is also tested. All the test results are compared with the simulation results. At the end, it was observed that simulation results were very close to the test results. This is very promising in the sense that computed improvements on the base will be expected to yield predicted results. All the tests have been performed for each configuration separately and it can be said that the robot base that uses tracks has an advantage when moving on the terrain having obstacles and stairs. Hence, the superiority of the track to the wheel is justified.

The robot is actuated by two motors housed within the robot body. The control of these motors is done via an LMD 18200 ID that can drive 6 Amps of current at 56 Volts. A microcontroller board is designed and manufactured. This communicates with a PC and handles the actuation of motors based on the commands that are being sent by the PC. A PIC 16F877 microcontroller running at 20 MHz is used on this board. A COM object is created on the PC side. This software module handles the communication with the PIC microcontroller over RS232 and allows the user to drive the robot via a virtual joystick.

In the near future, the cabled connection between this robot and a host PC will be established via wireless communication, cameras and various sensors will be installed and interfaced with the on-board PC. A robot arm is also planned to be designed and mounted on this base. Such modification will especially be useful for police forces and Türkiye Atom Enerjisi Kurumu (TAEK). It is also intended that several of these robots can be connected with each other for specific tasks. Design of a flipper is also considered.

REFERENCES

[Arkin] Arkin, R.C., *Behavior-Based Robotics*. Cambridge MIT Press, MA, 1998.

[Beer] Beer, F.P. and Russell Johnston, E., *Mechanics of materials*, McGraw-Hill, 1981.

[Bekker] Bekker, M.G., *Theory of Land Locomotion*, Ann. Arbor, MI: University of Michigan Pres, 1956.

[Bekker] Bekker, M.G., *Introduction to Terrain-Vehicle Systems*, Ann Arbor, MI: University of Michigan Pres, 1969.

[Burgard] Burgard W., Cremers A., Fox D., Hahnel D., Lakemeyer G., Schulz D., Steiner W., Thrun S., *Experiences with an Interactive Museum Tour-Guide Robot*, *Artificial Intelligence*, 114, 1-53, 2000.

[Dis] <http://www.dis.uniroma1.it/~labrob/people/freda>, last date accessed: July 15, 2005.

[Design] Robot Desing Lecture Notes, School of Mechanical and Manufacturing Engineering, University of New South Wales, <http://www.mech.unsw.edu.au>, last date accessed: June 10, 2005.

[Falcone] Falcone E., Gockley R., Porter E., Nourbakhsh I., *The Personal Rover Project: The Comprehensive Design of a Domestic Personal Robot*, *Robotics and Autonomous Systems*, Special Issue on Socially Interactive Robots, 42, 245-258, 2003.

[Hayashi] Hayashi, I., *Practical Analysis of Tracked Vehicle Steering Depending on Longitudinal Track Slippage*, in Proc. 5th Int. Conf. of the Int. Society for Terrain-Vehicle Systems, Vol.II, Detroit-Houghton, MI, 1975.

[Hibbeler] Hibbeler, R.C., *Mechanics of Materials*, Second edition, Prentice Hall, 1994.

[Irobot] <http://www.irobot.com/atrv>, last date accessed: July 20, 2005.

[Khepera] <http://www.k-team.com/robots/khepera>, last date accessed: June 15, 2005.

[Kalice] <http://www.k-team.com/robots/kalice>, last date accessed: August 10, 2005.

[Koala] <http://www.k-team.com/robots/koala>, last date accessed: August 10, 2005.

[Kuka] <http://www.kuka.com/en>, last date accessed: July 25, 2005.

[Lauria] Lauria J., Barraquand J. *Robot Motion Planning: A Distributed Presentation Approach*, International Journal of Robotics Research, 10: 628-649, 1991.

[Manufacturing] Desing and Manufacturing Lecture Notes, MIT, <http://www.me.mit.edu>, last date accessed: April 20, 2005.

[MR5] <http://www.esit.com/mobile-robots/mr5.html>, last date accessed: March 5, 2005.

[Nomad] D. Wettergreen, M. Bualat, D. Christian, K. Schwehr, H. Thomas, D. Tucker, E. Zbinden, *Operating Nomad during the Atamaca Desert Trek*, Proceedings of Int. Conference on Field and Service Robotics, 1997.

[Nuttall] Nuttall, C. J., *Some Notes on the Steering of Tracked Vehicles*, Journal of Terramechanics, Vol.1, No.1, 1964.

[Packbot] <http://www.packbot.com>, last date accessed: July 15, 2005.

[Pioneer] <http://www.pioneer.com>, last date accessed: July 15, 2005.

[Ranier] <http://ranier.oact.hq.nasa.gov/telerobotics.html>, last date accessed: August 20, 2005.

[Rosetti] Rosetti M.D., Kumar A., Felder R.A., *Mobile Robot Simulation of Clinical Laboratory Deliveries*, Proceedings of Simulation Conference, 1998.

[Roymech] <http://roymech.co.uk>, last date accessed: August 25, 2005.

[Robosoft] <http://www.robosoft.fr>, last date accessed: August 10, 2005.

[Sadhukhan] Sadhukhan D., *AGV Terrain Classification Using Internal Sensors*, MSc Thesis, The Florida State University, College of Eng., 2004.

[Schweitzer] Schweitzer, G., Werder M., *Robotrac – a Mobile Manipulator Platform for Rough Terrain*, in Proceedings of the International Symposium on Advanced Robot Technology, Tokyo, Japan, March, 1991.

[Shigley] Shigley, J.E. and Mischke, C.R., *Mechanical Engineering Design*, Fifth edition, McGraw-Hill, 1989.

[Siegwart] Siegwart R., *Robox at Expo.02: A large Scale Installation of Personal Robots*, Journal of Robotics and Autonomous Systems, 42:203-222, 2003.

[Siegwart] Siegwart R., Lamon P., Estier T., Lauria M., Piguet R., *Innovative Design for Wheeled Locomotion in Rough Terrain*, Journal of Robotics and Autonomous Systems, 40:151-162, 2002.

[Siegwart] Siegwart R., Nourbakhsh, I.R., *Autonomous Mobile Robots*. Cambridge MIT Press, London, 2004.

[Steinmetz, 2001] Steinmetz B.M., Arbter K., Brunner B., Landzettel K., *Autonomous VisionBased Navigation of the Nanokhod Rover*, in Proceedings of i-SAIRAS 6th International Symposium on Artificial Intelligence, Robotics and Automation in Space, Montreal, June 18-22, 2001.

[Stevens] Stevens, B.S., Clavel, R., Rey, L., "The Delta Parallel Structured Robot, Yet More Performant through Direct Drive," in *Proceedings of 23rd International Symposium on Industrial Robots*, Barcelona, pp. 485-493, October 1992.

[Talon] <http://www.foster-miller.com/literature/documents/talon>, last date accessed: June 20, 2005.

[Todd] Todd, D.J., *Walking Machines, an Introduction to Legged Robots*, Kogan Page Ltd., 1985.

[Track] <http://www.nswplastics.com/pdfs/timing>, last date accessed: August 10, 2005.

[Uranus] <http://www.ri.cmu.edu>, last date accessed: July 20, 2005.

[Winnendael] Winnendael V.M., Visenti G., Bertrand R., Rieder R., *Nanokhod Microrover Heading Towards Mars*, in Proceedings of the 5th International Symposium on Artificial Intelligence, Robotics and Automation in Space, Noordwijk, Netherlands, pp. 69-76, 1999.

[Wong] Wong, J.Y., *Theory of Ground Vehicles*, John Wiley Inc., Second Edition, 1993.

[Wong] Wong, J.Y., *Terramechaics and Off-Road Vehicles*, Elsevier, Amsterdam, 1998.

[Zelinsky] Zelinsky A., Dowson I., *Continuous Smooth Path Execution for an AGV*, IEEE Region 10 Conference, Melbourne, Australia, 1992.

APPENDIX A

KINEMATIC AND DYNAMIC ANALYSIS OF THE ROBOT BASE

A.1. Differential Steering

Differential steering system is a reliable method that is commonly used especially in small mobile robots. Differential steering system is also not uncommon to our daily lives. For example it is the drive system of almost all wheelchairs. Two wheels mounted on a single axis are independently powered and controlled, thus providing both drive and steering at the same time. If both drive wheels turn in tandem, the robot moves in a straight line. If one wheel faster than the other, the robot follows a curved path. If the wheels turn at equal speed, but in opposite directions, the robot pivots. Therefore differential steering is just a matter of varying the speeds of the drive wheels to control a mobile platform.

In modeling our differentially driven robot base two modeling methods can be used. First one is an elementary model which does not treat physical issues such as friction, inertia, many mechanical details of motors, gearing, and wheel & palette-based actuators. This method presents a way of computing the trajectory of the robot base that is based on certain simplified assumptions. This method also presents equations for dead reckoning and using odometry for robot base localization so it provides a starting point for the development of algorithms for the future applications of the robot base which are navigation, path planning, and other more challenging problems. The second method provides a more detailed model. It includes friction, gearing, motor details and wheel & palette specifications to the model. The details of both methods are given below.

A.1.1 Simplified Robot Model

Before tackling the differential steering model, let's consider the problem of getting our robot base designed to make a 90-degree turn around a corner in a hallway or a road. An approach would be for the robot base to round the corner, following a gradual circular arc through the intersection while maintaining a steady speed. To accomplish this, the speed of the outer wheel should be higher than the inner one. To start with it is assumed that a circular path is followed by the robot as shown in Figure A.1.

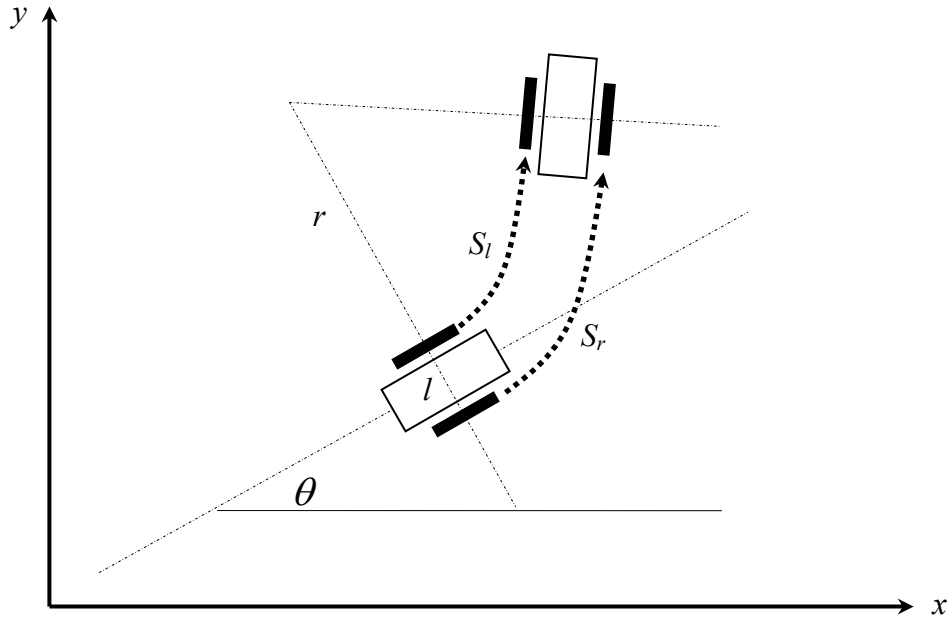


Figure A.1 Robot base turning a circular path with constant speed.

$$S_l = r\theta \quad (\text{A.1})$$

$$S_r = (r + l)\theta \quad (\text{A.2})$$

$$S_M = (r + l/2)\theta \quad (\text{A.3})$$

where S_l , S_r give the displacement (distance traveled) for the left and right wheels respectively, r is the turning radius for the inner wheel, l is the distance between wheels (from center-to-center along the length of the axle), and θ is the angle of the turn in radians ($\theta_{\text{radians}} = \theta_{\text{degrees}} (\pi/180)$). S_M is the displacement of the center point on the main body. Equations (A.1), (A.2), (A.3) confirm that when the wheels turn at fixed velocities, robot base follows a circular path.

Note that there is an important simplifying assumption that the wheels and pallets maintain a steady velocity, and also in this part only, the effects of the acceleration

are neglected. But soon they will also be substituted into the equations. Robot base is considered as a rigid body.

$$d\theta / dt = (v_r - v_l) / l \quad (\text{A.4})$$

Integration of Eqn. A.4 and taking the initial orientation of the base as $\theta(0) = \theta_0$, robot base's orientation can be written as a function of wheel velocity and time.

$$\theta(t) = (v_r - v_l)t / l + \theta_0 \quad (\text{A.5})$$

This change in orientation also applies to the absolute frame of reference. Position as a function of time can be obtained as follows:

$$dx / dt = [(v_r + v_l) / 2] \cos(\theta(t)) \quad (\text{A.6})$$

$$dy / dt = [(v_r + v_l) / 2] \sin(\theta(t)) \quad (\text{A.7})$$

Integration and applying the initial position of the robot base $x(0) = x_0$, $y(0) = y_0$.

$$x(t) = x_0 + \frac{l(v_r + v_l)}{2(v_r - v_l)} [\sin((v_r - v_l)t / l + \theta_0) - \sin(\theta_0)] \quad (\text{A.8})$$

$$y(t) = y_0 + \frac{l(v_r + v_l)}{2(v_r - v_l)} [\cos((v_r - v_l)t / l + \theta_0) - \cos(\theta_0)] \quad (\text{A.9})$$

Finally, when constant accelerations are also considered, equations can be ordered as follows:

$$\theta(t) = Ct^2 + Dt + \theta_0 \quad (\text{A.10})$$

$$\mathbf{x} = (At + B) \cos(Ct^2 + Dt + \theta_0) \quad (\text{A.11})$$

$$\theta = (At + B) \sin(Ct^2 + Dt + \theta_0) \quad (\text{A.12})$$

where

$$A = (a_r + a_l) / 2 \quad (\text{A.13})$$

$$B = (w_r + w_l) / 2 \quad (\text{A.14})$$

$$C = (a_r - a_l) / 2l \quad (\text{A.15})$$

$$D = (w_r - w_l) / l \quad (\text{A.16})$$

where, w_r and w_l are initial velocities, a_r and a_l are constant acceleration.

A.1.2 Detailed Robot Model

The second method is a bit more detailed. It contains friction, gearing, motor detail and wheel specifications. DC motors are expected to have reduction before getting connected to the wheels and pallets.

Robot base shown in Figure A.2 has wheels and pallets that are same radius of r_w and distance of l (Actually the radius of them is very close to each other. They may be considered they are same since it is assumed that wheels and pallets always contact with the ground). Inputs can be specified as follows:

ω_l is the angular velocity of the motor on left [rad/s]

ω_r is the angular velocity of the motor on right [rad/s]

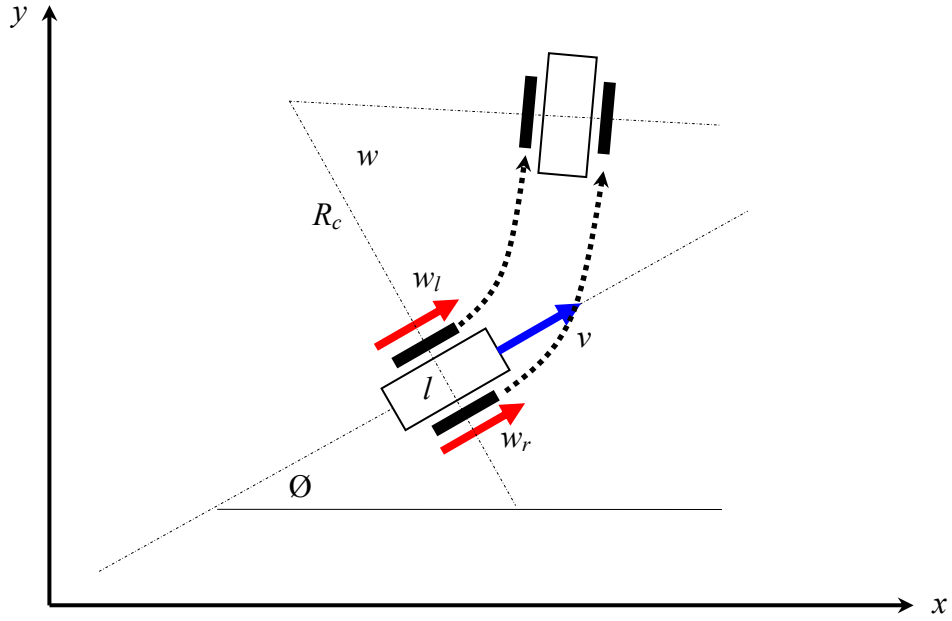


Figure A.2 Robot base turning a circular path.

Instantaneous curvature can be obtained when ω_l is not equal ω_r , shown Figure A.2.

The linear and angular velocities of the center of the robot base are:

$$v = \frac{r_w}{2\Omega}(\omega_l + \omega_r) \quad (\text{A.17})$$

$$\omega = \frac{r_w}{l\Omega}(\omega_l - \omega_r) \quad (\text{A.18})$$

where Ω is gear ratio.

The radius of the instantaneous curvature is then given by

$$R_c = \frac{v}{\omega} \quad (\text{A.19})$$

If v and ω are inserted the above equation, Equation (A.20) is going to be obtained.

$$R_c = \frac{l}{2} \left(\frac{w_l + w_r}{w_l - w_r} \right) \quad (\text{A.20})$$

and the Eqn. (A.21) shows the relationship between the angular velocity of the left side and that of the right.

$$\frac{w_l}{w_w} = \frac{l + 2R_c}{2R_c - l} \quad (\text{A.21})$$

State space equation describing the orientation of the robot can be given from Eqn. (A.18) by

$$\dot{\phi} = \frac{r_w}{l\Omega} (\omega_l - \omega_r) \quad (\text{A.22})$$

From Eqn. (A.17) state space equations describing the position of the robot can be given by

$$\dot{x} = \frac{r_w}{2\Omega} (\omega_l + \omega_r) \cos \phi \quad (\text{A.23})$$

$$\dot{y} = \frac{r_w}{2\Omega} (\omega_l + \omega_r) \sin \phi \quad (\text{A.24})$$

The equation of motion for differential drive robot base can be given by

$$M\ddot{x} = \frac{2\Omega\tau_m}{r_w} - F_{friction} \quad (\text{A.25})$$

where \ddot{x} is acceleration of robot base. Now, it is required that we should mention about friction forces. Typical friction forces include;

- Friction with the ground
- Friction with the rotor shaft
- Friction within the gearhead
- Air friction (neglected in our case due to low speed)

The largest friction value is the ground friction. The friction force can be static (F_s) or dynamic friction (F_d). F_s depends on the mass of the robot base and takes a maximum value just before the base starts moving. This force is called maximum static friction force. If the robot base is located on the horizontal surface parallel to the ground, the maximum static friction is given by

$$(F_s)_{\max} = \mu_s Mg \quad (\text{A.26})$$

where μ_s is friction coefficient. In classical physics, the friction coefficient has a value that is never greater than one and is not a function of the contact surface area. This is generally true when considering rigid materials sliding on rigid surfaces, such as steel on steel. But when it comes to elastic materials such as rubber, the coefficient can vary greatly (0.5-3.0). For practical purposes, this value can be safely taken between 0.3- 1 [Design]. The dynamic friction force is normally proportional to the velocity of the robot base. Such that

$$F_d = \mu_d \dot{x} \quad (\text{A.27})$$

F_s is often much larger than F_d . However, both forces must be considered in the design process as follows:

- The driving torque is large enough to make the robot start moving.

$$M\ddot{x} = \frac{2\Omega\tau_m}{r_w} - F_{friction} > 0 \quad (\text{A.28})$$

Robot base can reach desired maximum speed \dot{x}_{\max} and acceleration \ddot{x}_{\max} by solving the following equation.

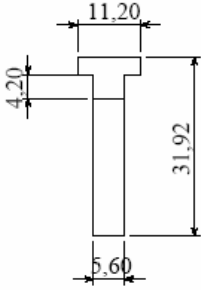
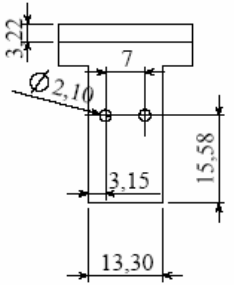
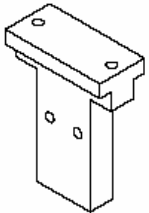
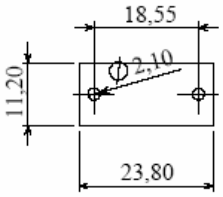
$$M\ddot{x} = \frac{2\Omega\tau_m}{r_w} - \mu_d \dot{x} \quad (\text{A.29})$$

- When robot base is on a slope of angle θ :

$$M\ddot{x} = \frac{2\Omega\tau_m}{r_w} - F_{friction} - mg \sin \theta \quad (\text{A.30})$$

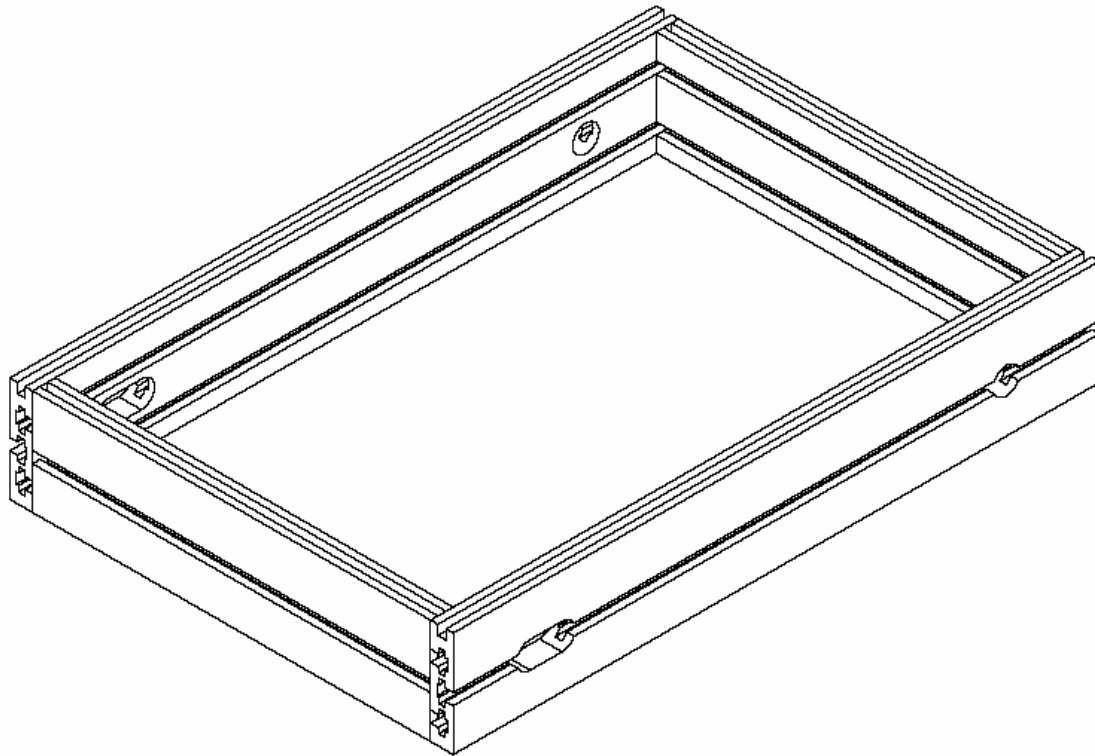
APPENDIX B

TECHANICAL DRAWINGS

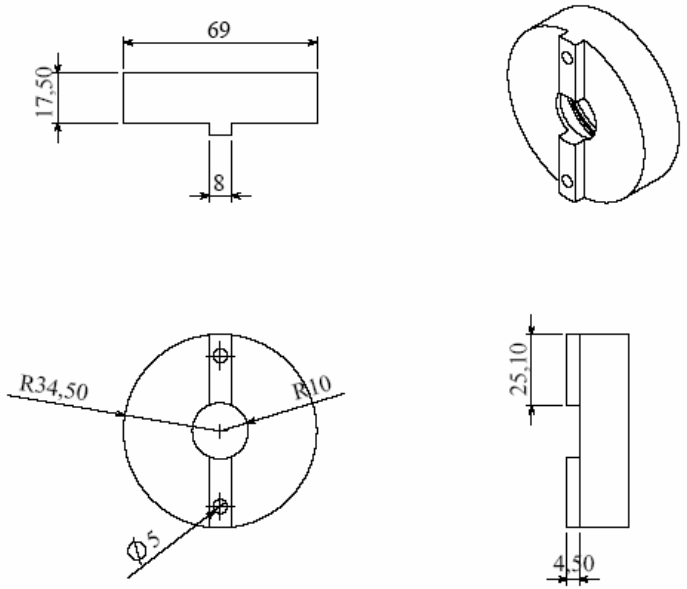


DIMENSIONS ARE IN MM	NAME		Middle East Technical University Mechanical Engineering Department
	DRAWN	Gökhan BAYAR	
	CHECKED	Dr. Bağcı KOKU	
	ENG APPR.		
	MFG APPR.		
MATERIAL	Aluminum	Q.A.	
FINISH	May 15, 2005	COMMENTS:	
SCALE	1/1		
SIZE		PART NAME	
A		SUPPORTER FOR MOVABLE BEAM	
WEIGHT:		PART NO:	

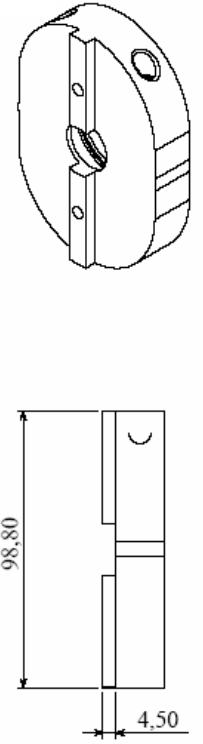
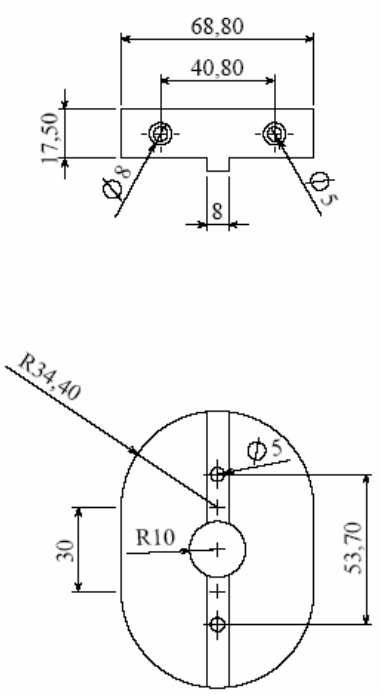
B.1



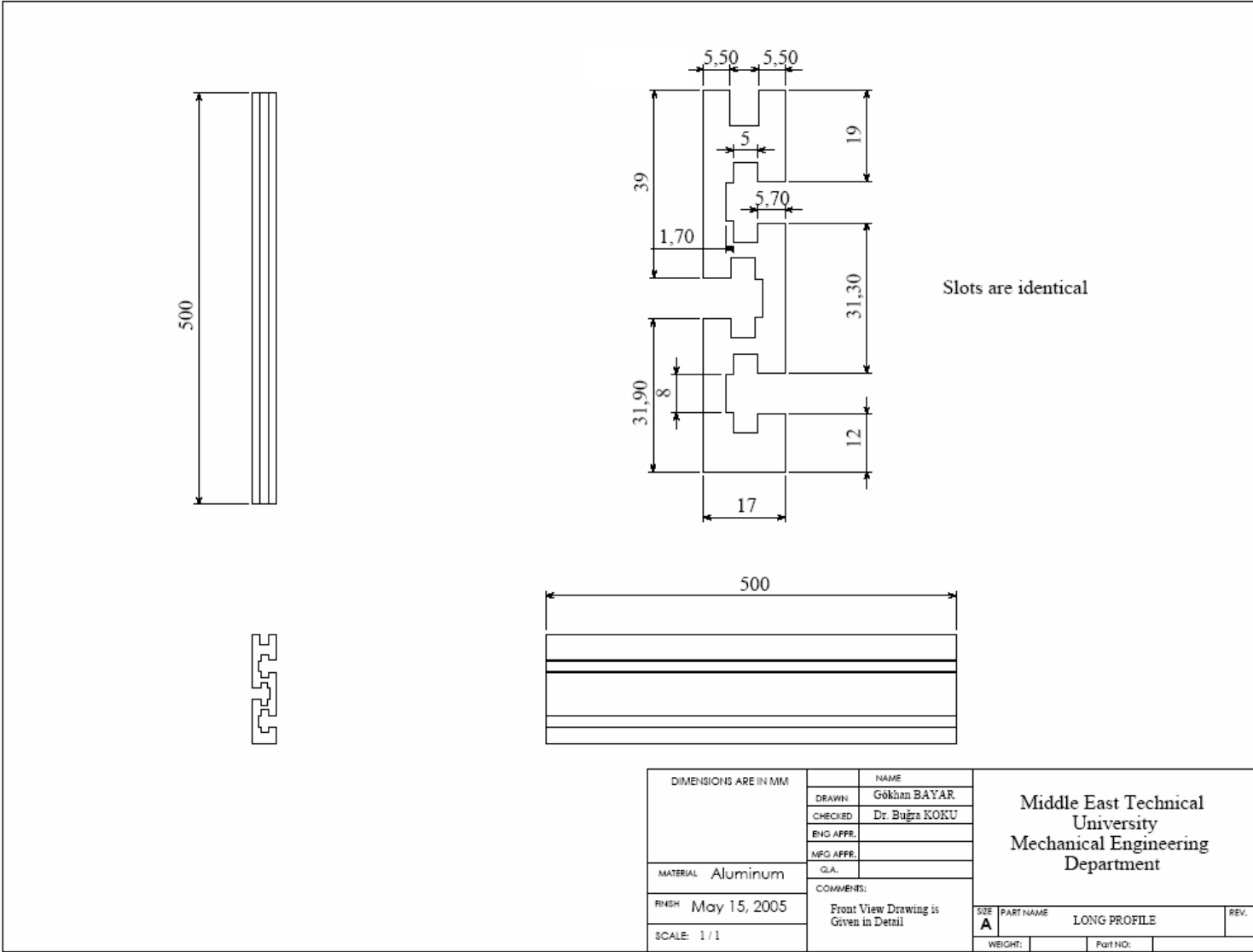
DIMENSIONS ARE IN MM		NAME		Middle East Technical University Mechanical Engineering Department			
		DRAWN:	Gökhan BAYAR			SIZE	PART NAME
		CHECKED:	Dr. Buğra KOKU			A	BASE
		ENG APPR.				WEIGHT:	Part NO.
		MFG APPR.					10
MATERIAL Aluminum		Q.A.		REV.			
FINISH May 15, 2005		COMMENTS:					
SCALE: 1/1							

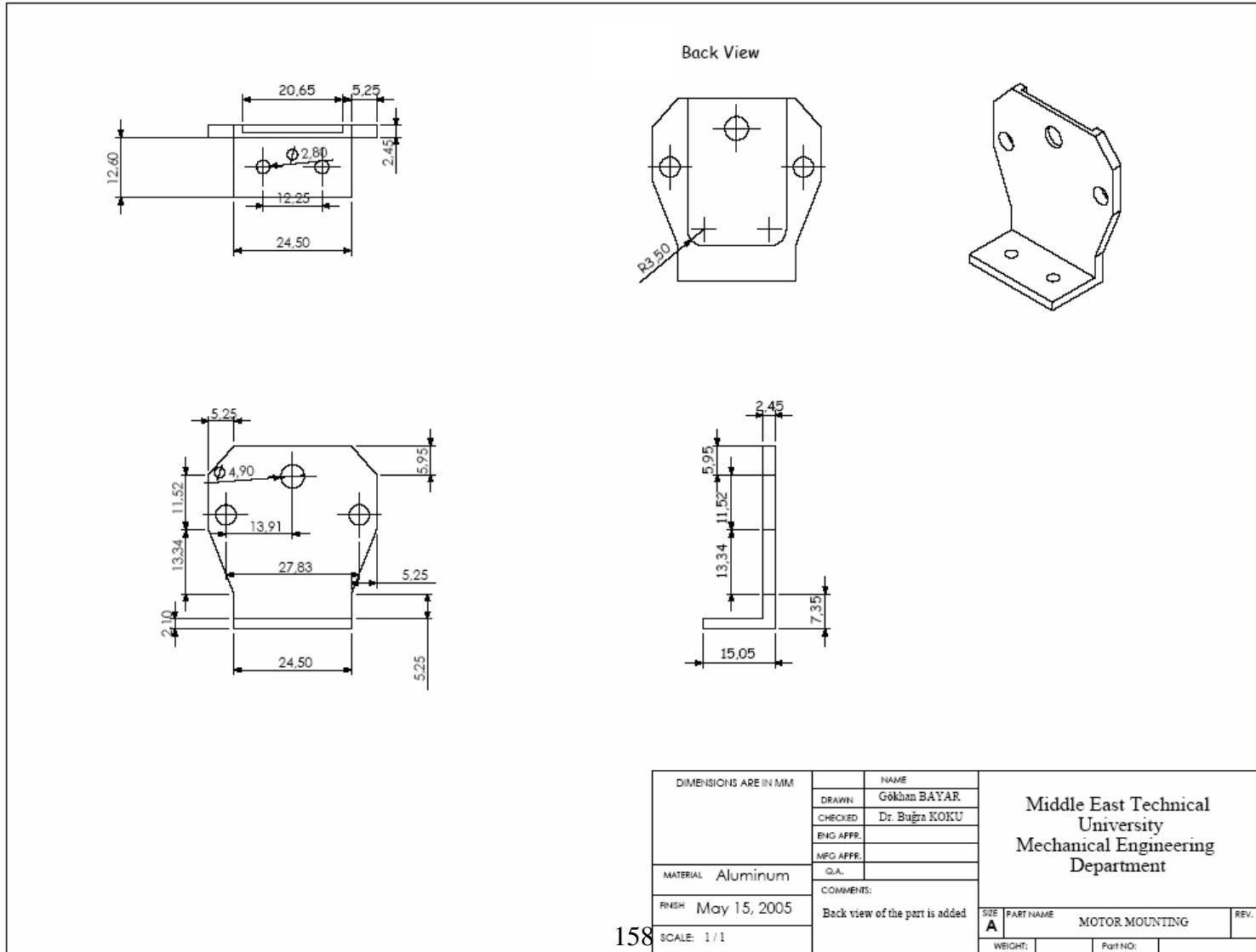


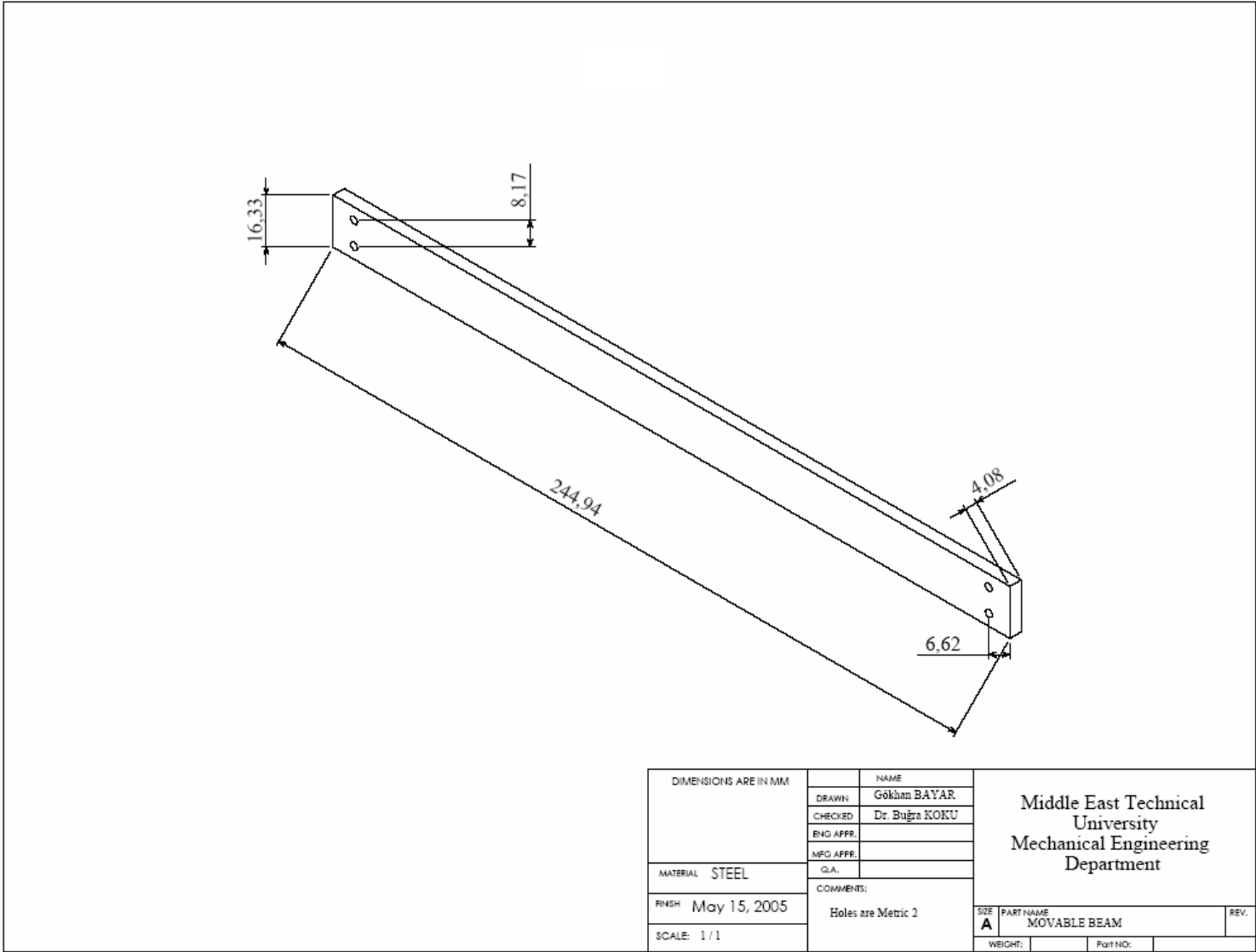
DIMENSIONS ARE IN MM		NAME	Middle East Technical University Mechanical Engineering Department		
DRAWN		Gökhan BAYAR			
CHECKED		Dr. Biğra KOKU			
ENG APPR.					
MFG APPR.					
Q.A.					
MATERIAL	Aluminum	COMMENTS:	SIZE	PART NAME	REV.
FINISH	May 15, 2005		A	BEARING HUP-CIRCLE	
SCALE	1 / 1		WEIGHT:	PART NO.:	

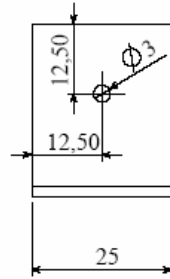
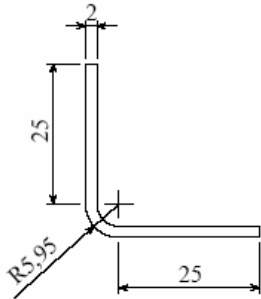
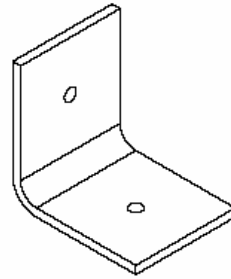
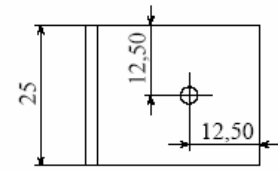


DIMENSIONS ARE IN MM		NAME	Middle East Technical University Mechanical Engineering Department		
		DRAWN: Gökhan BAYAR			
		CHECKED: Dr. Biğra KOKU			
		ENG APPR.			
		MFG APPR.			
		Q.A.			
MATERIAL	Aluminum	COMMENTS:	SIZE	PART NAME	REV.
FINISH	May 15, 2005		A	BEARING HUP-SQUARE	
SCALE	1/1		WEIGHT:	PART NO.	

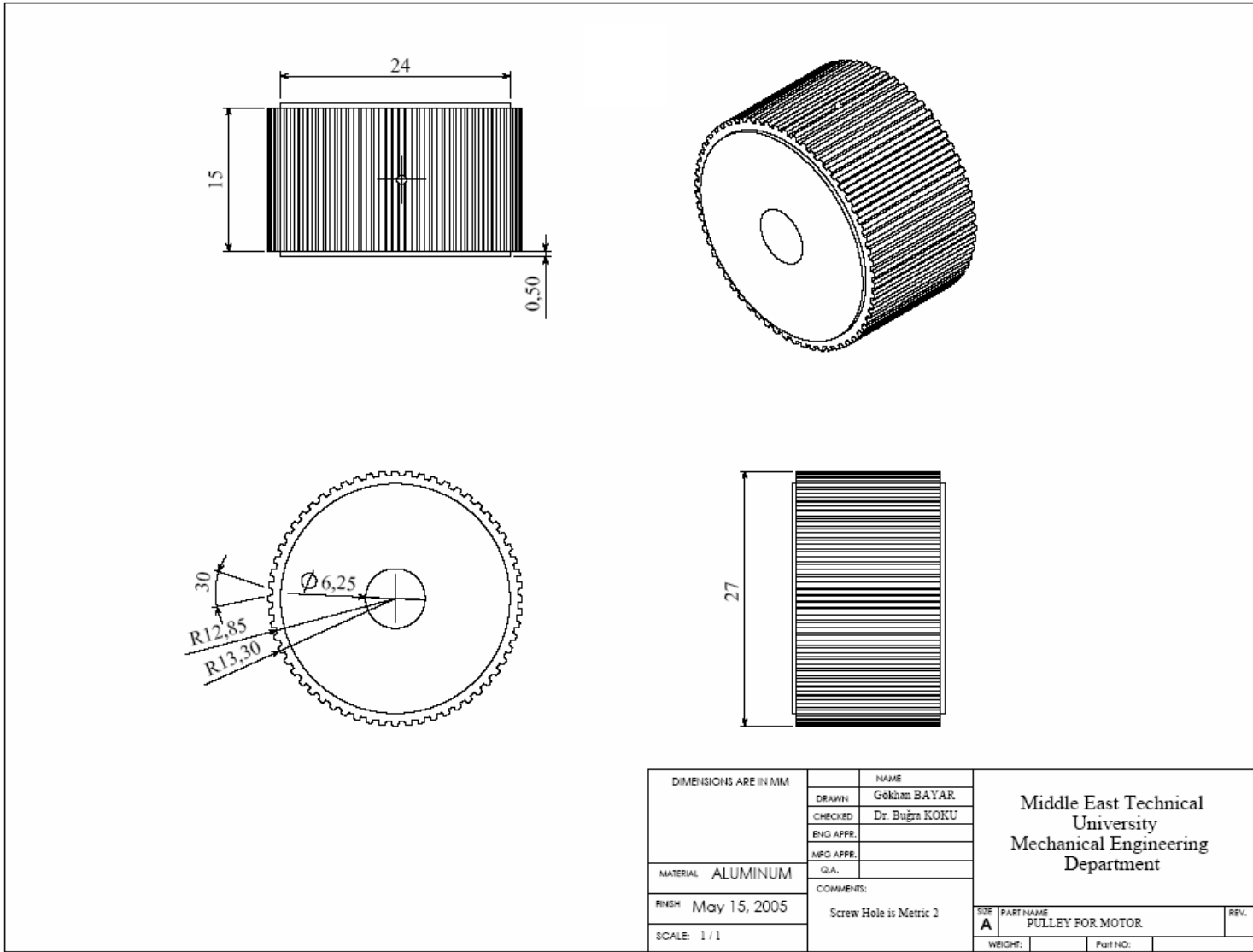


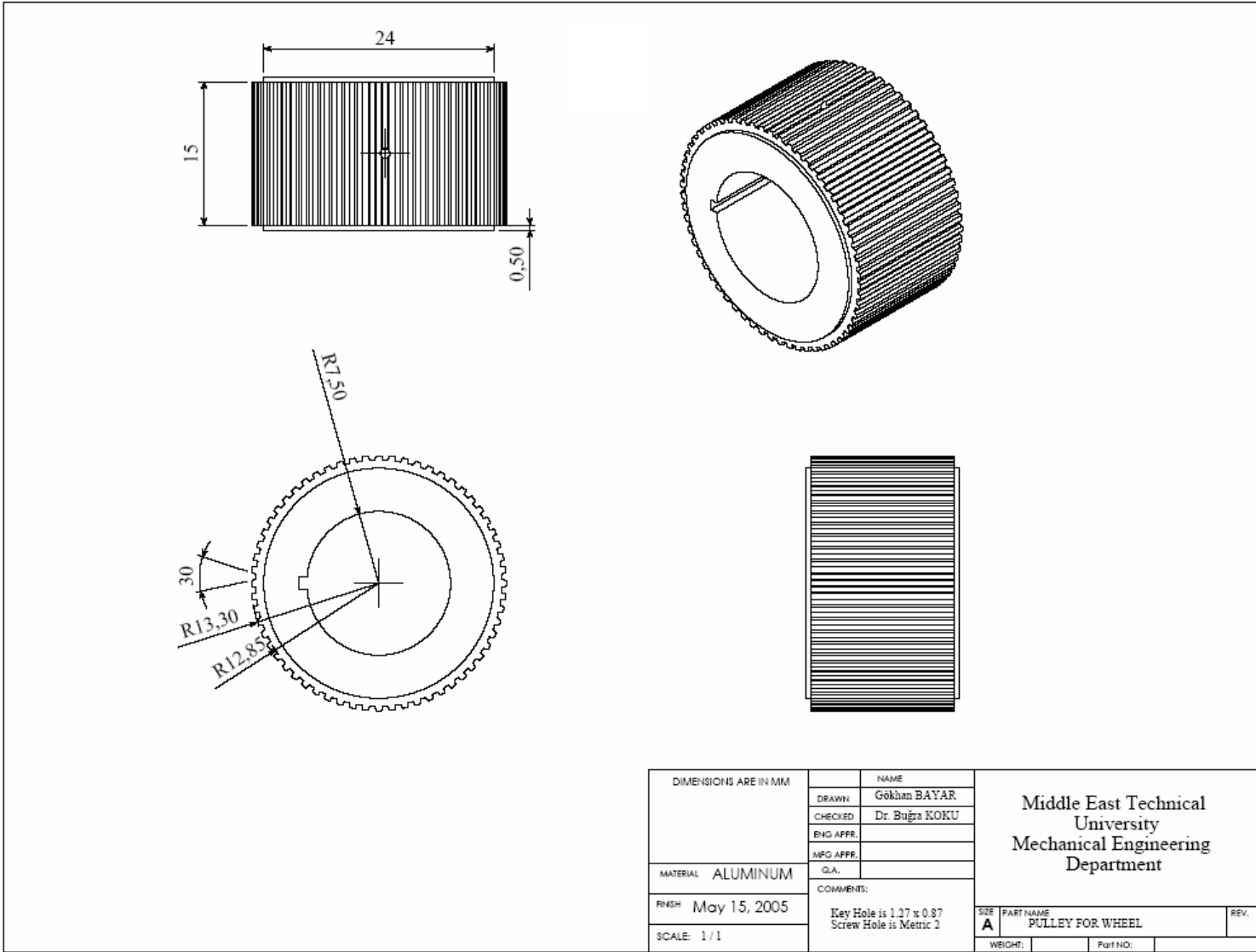


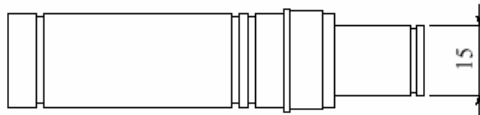
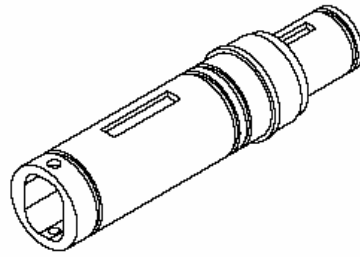
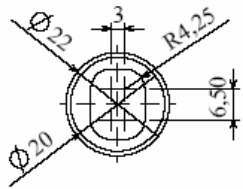
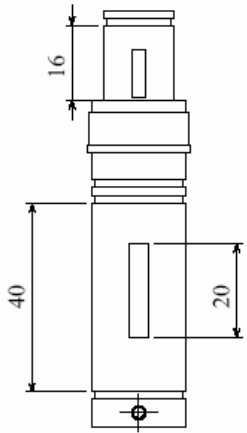




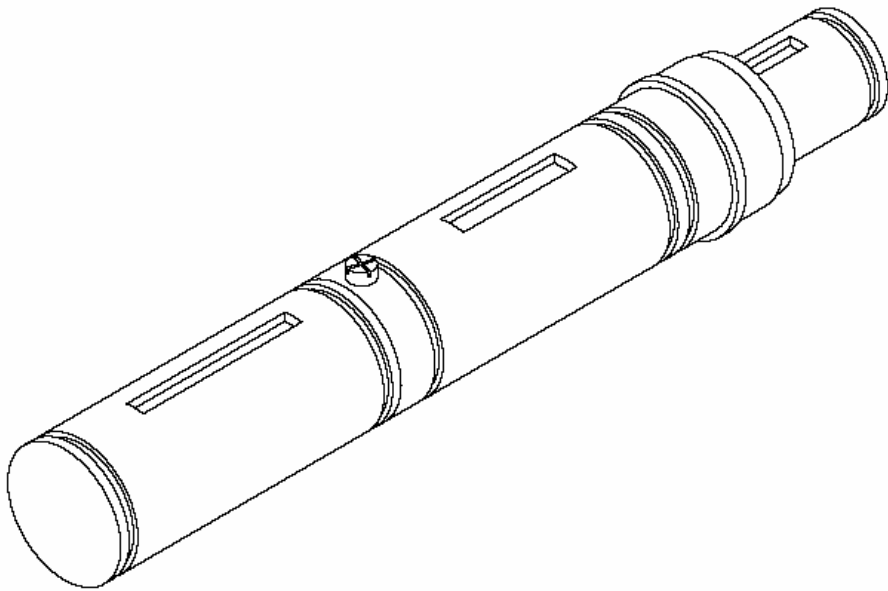
DIMENSIONS ARE IN MM		NAME		Middle East Technical University Mechanical Engineering Department	
		DRAWN	Gökhan BAYAR		
		CHECKED	Dr. Buğra KOKU		
		ENG. APPR.			
		MFG APPR.			
MATERIAL Aluminum		Q.A.			
FINISH May 15, 2005		COMMENTS:		SIZE PART NAME PROFILE HOLDER REV.	
SCALE: 1 / 1				A	
				WEIGHT: Part NO:	





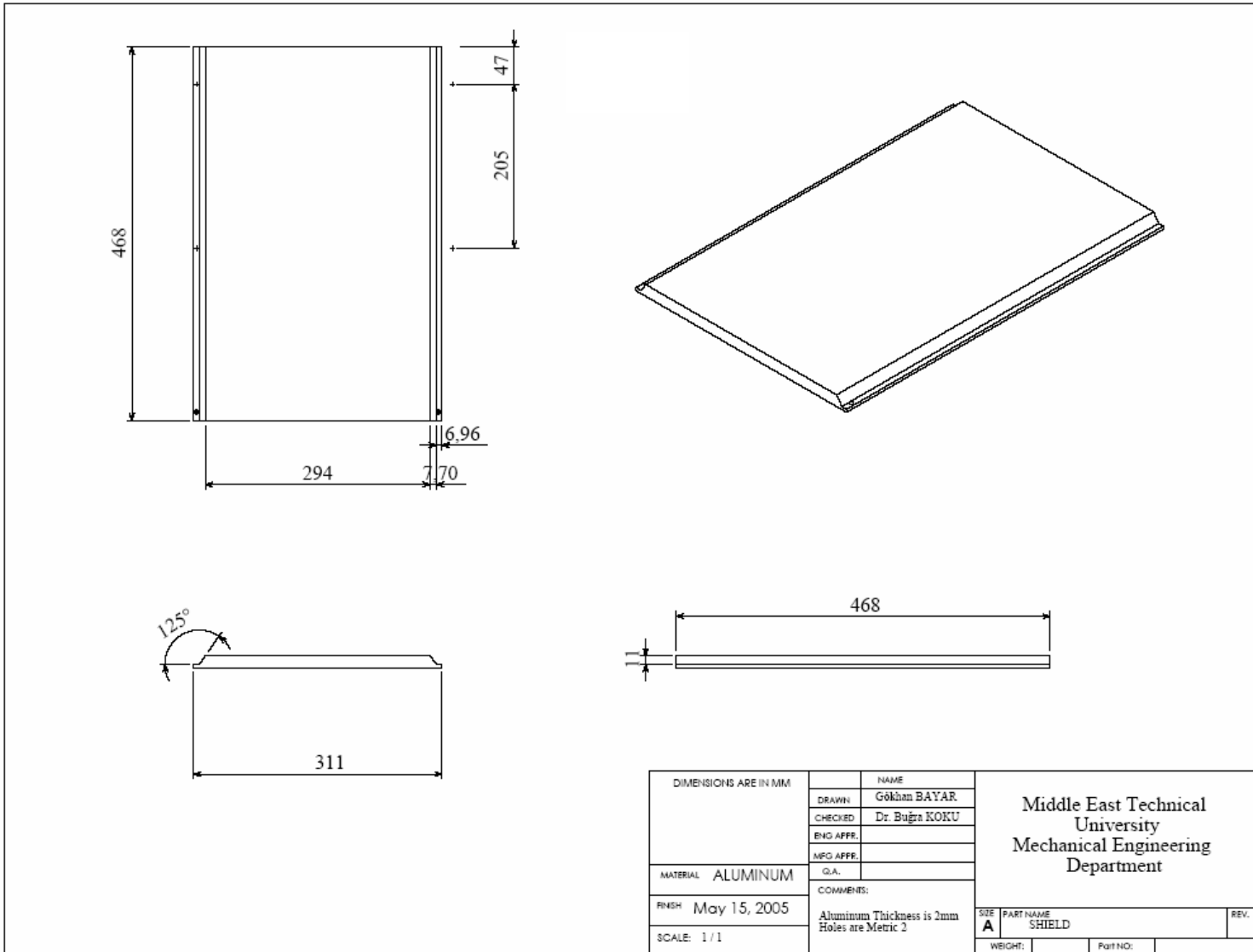


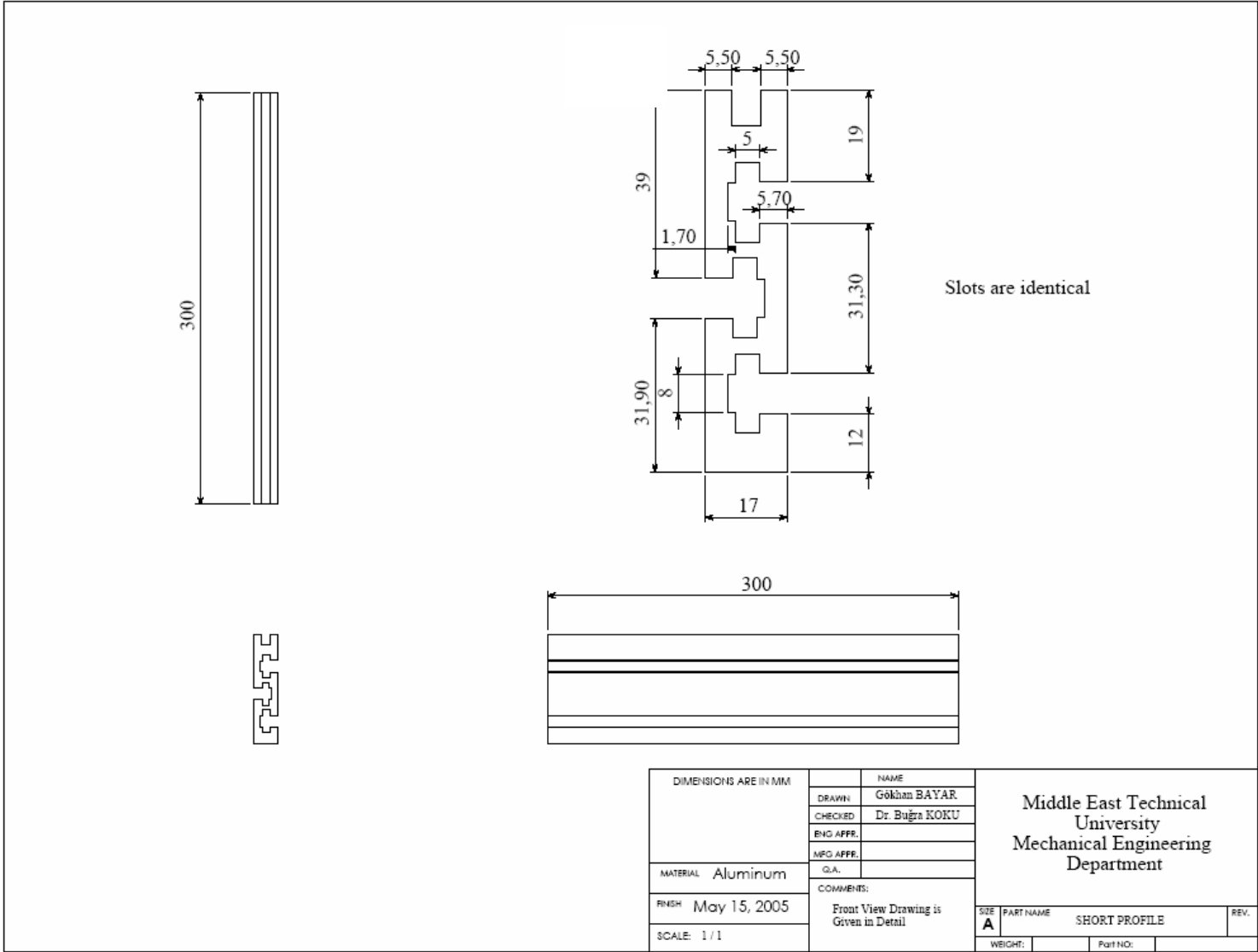
DIMENSIONS ARE IN MM		NAME		Middle East Technical University Mechanical Engineering Department	
DRAWN		Gökhan BAYAR			
CHECKED		Dr. Buğra KOKU			
ENG. APPR.					
MFG. APPR.					
MATERIAL Aluminum		Q.A.		SIZE PART NAME REV. A PALETTE SHAFT	
FINISH May 15, 2005		COMMENTS:		WEIGHT: Part NO: 10	
SCALE: 1/1					

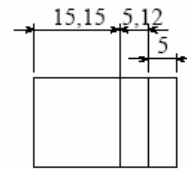
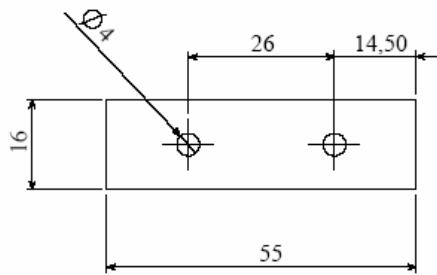
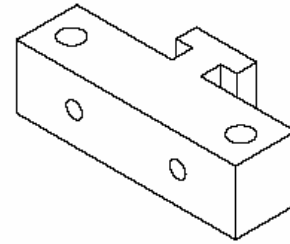
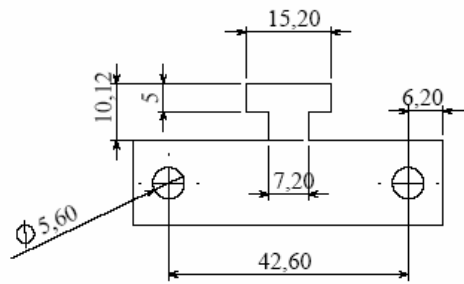


DIMENSIONS ARE IN MM		NAME	Middle East Technical University Mechanical Engineering Department			
		DRAWN			Gökhan BAYAR	
		CHECKED			Dr. Buğra KOKU	
		ENG APPR.				
		MFG APPR.				
		Q.A.				
MATERIAL	Aluminum	COMMENTS:		SIZE	PART NAME	REV.
FINISH	May 15, 2005			A	CONNECTED SHAFTS	
SCALE	1/1			WEIGHT:	PART NO.	10

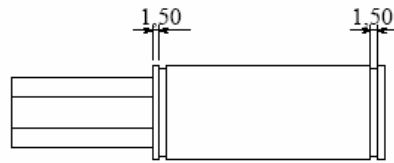
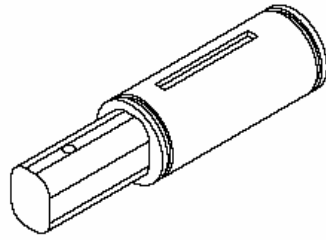
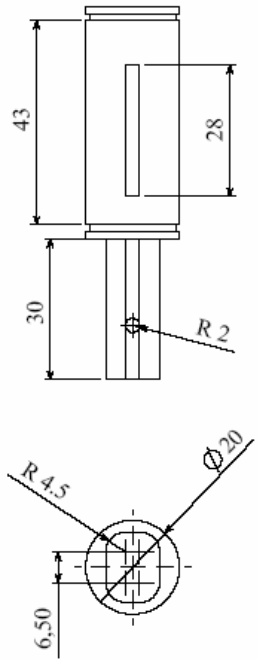
B.12







DIMENSIONS ARE IN MM	NAME	Middle East Technical University Mechanical Engineering Department		
	DRAWN			Gökhan BAYAR
	CHECKED			Dr. Buğra KOKU
	ENG APPR.			
	MFG APPR.			
MATERIAL	Aluminum	Q.A.		
FINISH	May 15, 2005	COMMENTS:		
SCALE	1/1	SIZE	A	
		PART NAME	PALETTE STRETCHER	
		WEIGHT:	PART NO.:	
			REV.	



DIMENSIONS ARE IN MM		NAME	Middle East Technical University Mechanical Engineering Department	
DRAWN		Gökhan BAYAR		
CHECKED		Dr. Buğra KOKU		
ENG. APPR.				
MFG APPR.				
MATERIAL Aluminum		Q.A.		
FINISH May 15, 2005		COMMENTS:		
SCALE: 1/1		SIZE	PART NAME	REV.
		A	WHEEL SHAFT	
		WEIGHT:	PART NO:	10

APPENDIX C

PIC 16 F877 PIN CONNECTIONS

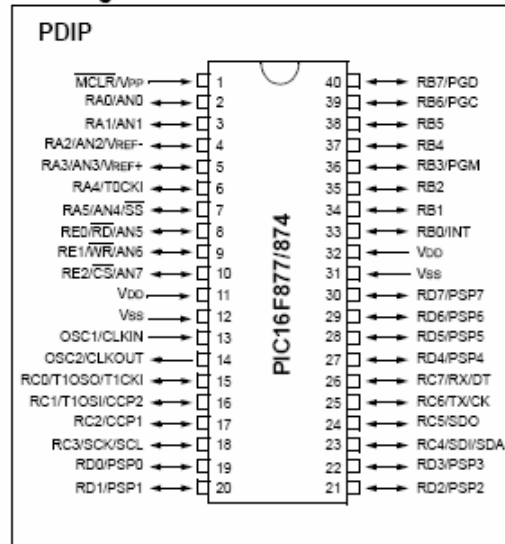
Devices Included in this Data Sheet:

- PIC16F873
- PIC16F876
- PIC16F874
- PIC16F877

Microcontroller Core Features:

- High performance RISC CPU
- Only 35 single word instructions to learn
- All single cycle instructions except for program branches which are two cycle
- Operating speed: DC - 20 MHz clock input
DC - 200 ns instruction cycle
- Up to 8K x 14 words of FLASH Program Memory,
Up to 368 x 8 bytes of Data Memory (RAM)
Up to 256 x 8 bytes of EEPROM Data Memory
- Pinout compatible to the PIC16C73B/74B/76/77
- Interrupt capability (up to 14 sources)
- Eight level deep hardware stack
- Direct, indirect and relative addressing modes
- Power-on Reset (POR)
- Power-up Timer (PWRT) and
Oscillator Start-up Timer (OST)
- Watchdog Timer (WDT) with its own on-chip RC
oscillator for reliable operation
- Programmable code protection
- Power saving SLEEP mode
- Selectable oscillator options
- Low power, high speed CMOS FLASH/EEPROM
technology
- Fully static design
- In-Circuit Serial Programming™ (ICSP) via two
pins
- Single 5V In-Circuit Serial Programming capability
- In-Circuit Debugging via two pins
- Processor read/write access to program memory
- Wide operating voltage range: 2.0V to 5.5V
- High Sink/Source Current: 25 mA
- Commercial, Industrial and Extended temperature
ranges
- Low-power consumption:
 - < 0.6 mA typical @ 3V, 4 MHz
 - 20 µA typical @ 3V, 32 kHz
 - < 1 µA typical standby current

Pin Diagram



Peripheral Features:

- Timer0: 8-bit timer/counter with 8-bit prescaler
- Timer1: 16-bit timer/counter with prescaler,
can be incremented during SLEEP via external
crystal/clock
- Timer2: 8-bit timer/counter with 8-bit period
register, prescaler and postscaler
- Two Capture, Compare, PWM modules
 - Capture is 16-bit, max. resolution is 12.5 ns
 - Compare is 16-bit, max. resolution is 200 ns
 - PWM max. resolution is 10-bit
- 10-bit multi-channel Analog-to-Digital converter
- Synchronous Serial Port (SSP) with SPI™ (Master
mode) and I²C™ (Master/Slave)
- Universal Synchronous Asynchronous Receiver
Transmitter (USART/SCI) with 9-bit address
detection
- Parallel Slave Port (PSP) 8-bits wide, with
external RD, WR and CS controls (40/44-pin only)
- Brown-out detection circuitry for
Brown-out Reset (BOR)

APPENDIX D

LMD 18200 PIN CONNECTIONS

LMD18200 3A, 55V H-Bridge

General Description

The LMD18200 is a 3A H-Bridge designed for motion control applications. The device is built using a multi-technology process which combines bipolar and CMOS control circuitry with DMOS power devices on the same monolithic structure. Ideal for driving DC and stepper motors; the LMD18200 accommodates peak output currents up to 6A. An innovative circuit which facilitates low-loss sensing of the output current has been implemented.

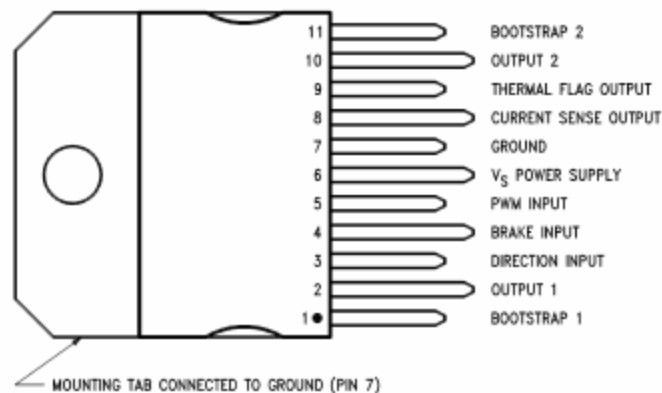
Features

- Delivers up to 3A continuous output
- Operates at supply voltages up to 55V
- Low $R_{DS(ON)}$ typically 0.3 Ω per switch
- TTL and CMOS compatible inputs

- No "shoot-through" current
- Thermal warning flag output at 145°C
- Thermal shutdown (outputs off) at 170°C
- Internal clamp diodes
- Shorted load protection
- Internal charge pump with external bootstrap capability

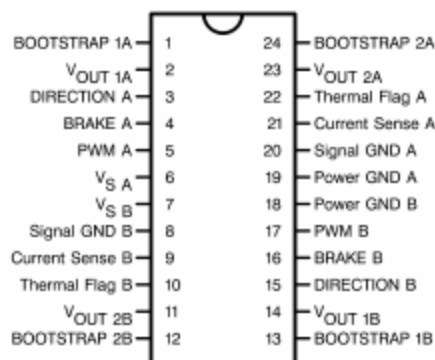
Applications

- DC and stepper motor drives
- Position and velocity servomechanisms
- Factory automation robots
- Numerically controlled machinery
- Computer printers and plotters



DS010586-2

11-Lead TO-220 Package
Top View
Order Number LMD18200T
See NS Package TA11B



APPENDIX E

POLICE DEPARTMENT SPECIFICATIONS FOR THE MOBILE ROBOTS

BOMBA İMHA ROBOTU TEKNİK ŞARTNAMESİ

1- KONUSU:

Bu teknik şartname Emniyet Genel Müdürlüğü ihtiyacı için satın alınacak "Bomba İmha Robotu"nun teknik özelliklerini, denetim, muayene ve numune alma, eğitim, garanti, ambalajlama ve ilgili diğer hususları konu alır.

2- TEKNİK ÖZELLİKLER:

2.1.Bomba imha robotu; IED/EOD kullanım amacı yanında, ayrıca NBC olaylarında da gözetleme ve görüntü alma gibi işlemlerde de kullanılacağından su ve nem geçirmez özellikte olacaktır.

2.2. Bomba imha robotunun hareket sistemi; paletli olacaktır. Ayrıca istenildiğinde kullanıcı personel tarafından robotun palet mekanizmasına tekerlek takılabilir özellikte olacaktır ve tekerlekler robotla birlikte verilecektir.

2.3. Robotun hızı, paletli durumda en az 1.8 (bir nokta sekiz) km/saat, paletlere ekstra tekerlek takıldığı durumda ise en az 2.5 (iki nokta beş) km/saat veya üstünde ve ayarlanabilir özellikte olacaktır.

2.4.Bomba imha robotu; 50 (elli) cm (±10 cm –artı- eksi on) genişlik, 50 (elli) cm (±10 cm –artı- eksi on) yükseklik, 100 (yüz) cm (±10 cm –artı- eksi on) uzunluk ebatlarında olacak, toplam ağırlığı ise 110 (yüzon)kg' dan fazla olmamalıdır.

2.5. Robot kendi eksenini etrafında dönebilmelidir.

2.6.Bomba imha robotu karşısına çıkan en az 40 (kırk) derece eğimli, düz yada yuvarlak köşe kenarlı merdiven basamaklarını devrilmeden rahatlıkla çıkabilmelidir. Robot eğim veya merdiven çıkarken durdurulduğunda herhangi bir şekilde geri kaymayacak özellikte olacaktır.

2.7.Bomba imha robotu beton, asfalt, taşlı, kumlu, çamurlu, otlu, karlı ve benzeri her türlü zor zeminde hareket edebilir özellikte olacaktır. Ayrıca robot kapalı alan içerisindeki her türlü zemin çeşitlerinde (halı, mozaik vb) üzerinde kullanılabilir olacaktır.

2.8.Bomba imha robotunda kullanılan bataryaların yedekleri, bomba imha robotu ile birlikte yedek malzeme olarak verilecektir.

2.9.Cihazlar her türlü aşırı akım ve kısa devreye karşı korumalı olacaktır.

2.10.Şebeke besleme fişi ve prizlerinde Avrupa (Türk) tipi standartlara uyulacaktır.

2.11. Her türlü fişler ve modüller yataklarına tam ve rahat oturmalı ters takılmalarına karşı önlem alınmış olmalıdır.

2.12.Her türlü hava koşullarında çalışmaya uygun olacaktır.

2.13.Robot ve kontrol paneli -10 (eksi on) derece / +50 (artı elli) derece arası çalışabilmelidir

2.2.KONTROL SİSTEMİ :

2.2.1.Robotun kontrol sistemi; radio kontrollü (Wireless control) olacaktır.

2.2.2.Açık alanda radio kontrolü en az 200 (ikiyüz) metre yayın, haberleşme mesafesine sahip olacaktır.

2.2.3.Haberleşmesi kararlı olacak ve başka frekans bandlarından etkilenmeyecektir.

2.2.4.Robottun üzerine yerleştirilecek silah sistemlerinin ateşlenme komutu, kontrol paneli üzerinden yapılacaktır. Kontrol paneli üzerinde bulunan ateşleme düğmeleri en az 2 (iki) adet ve kontrol edilebilir özellikte olacaktır. İstenildiğinde aynı anda bütün disruptorlar kontrol paneli üzerinden ateşlenebilecektir.